

Manuscript Number: STOTEN-D-18-10315R1

Title: Contribution of isotopic research techniques to characterize high-mountain-Mediterranean karst aquifers: The Port del Comte (Eastern Pyrenees) aquifer.

Article Type: Research Paper

Keywords: Stable isotopes, Seasonal isotopic amplitude, Altitudinal line, Recharge, Mean transit time, Karst

Corresponding Author: Dr. Jorge Jódar, Ph.D.

Corresponding Author's Institution: Technical University of Catalonia

First Author: Ignasi Herms, M.Sc.

Order of Authors: Ignasi Herms, M.Sc.; Jorge Jódar, Ph.D.; Albert Soler, Ph.D.; Iñaki Vadillo, Ph.D.; Luis J Lambán, Ph.D.; Sergio Martos-Rosillo, Ph.D.; Joan A Núñez, M.Sc.; Georgina Arnó, Ph.D.; Joan Jorge, Ph.D.

Abstract: Water resources in high mountain karst aquifers are usually characterized by high rainfall, recharge and discharge that lead to the sustainability of the downstream ecosystems. Nevertheless, these hydrological systems are vulnerable to the global change impact. The mean transit time (MTT) is a key parameter to describe the behavior of these hydrologic systems and also to assess their vulnerability. This work is focused on estimating MTT by using environmental tracers in the framework of high-mountain karst systems with a very thick unsaturated zone (USZ). To this end, it is adapted to alpine zones a methodology that combines a semi-distributed rainfall-runoff model to estimate recharge time series, and a lumped-parameter model to obtain MTT. The methodology has been applied to the Port del Comte Massif (PCM) hydrological system (Southeastern Pyrenees, NE Spain), a karst aquifer system with an overlying 1000 m thick USZ. Six catchment areas corresponding to most important springs of the system are considered. The obtained results show that hydrologically the behavior of the system can be described by an exponential flow model (EM), with MTT ranging between 1.9 and 2.9 years. These values are shorter than those obtained by considering a constant recharge rate along time, which is the easiest and most applied aquifer recharge hypothesis when estimating MTT through lumped-parameter models.

Response to Reviewers: COMMENTS FROM REVIEWERS: Reviewer #1

General comments

The paper by Herms et al. with title: "Contribution of isotopic research techniques to characterize high mountain-Mediterranean karst aquifers: The Port del Comte (Eastern Pyrenees) aquifer." provides an interesting study regarding the contribution of isotopic research in karst aquifers. The concept is interesting and the manuscript well written.

Thank you very much for your kind comments

However, I have a number of recommendations, which should be done before publication.

Abstract

Reviewer #1 - General comments #1: You have to include the innovative results of this study. Provide the innovation of this study:

Reply to general comment #1: Certainly, as the reviewer points, the innovative points of this study are not stated in the manuscript. In this regard, the study presents two innovations: (1) a global innovation and (2) the specific innovation with the case study.

(1) The study presents the adaptation of a procedural methodology to improve the estimation of the mean transit time (τ) in high-mountain karst aquifers. The methodology is based on the previous approach presented by Vitvar et al., 1999 to estimate groundwater residence times in pre-alpine non-karstic aquifers (tertiary and quaternary deposits in a small basin with elevation ranges between 680 to 960 m a.s.l.) by means of developing a link between distributed rainfall-runoff models to estimate recharge series, and then a lumped-parameter model using environmental tracers to solve the convolution integral. In our case the method is adapted to estimate τ in high-mountain karst systems taking into account the existing vertical gradients of precipitation and air temperature along the slope of high mountains, the role played by the snow accumulation and ablation processes in the runoff generation, and considering the hydrological system to be modelled as the whole aquifer (i.e. the unsaturated zone and saturated zones).

(2) The adapted methodology is applied to the Port del Comte high mountain karst aquifer (NE, Spain) as a practical case study. Despite the strategic role played by this hydrogeological system as water resource provider to Barcelona, the hydrological behaviour of this system is completely unknown. This is the first hydrodynamic and transit time characterization of this hydrological system. Besides, the isotopic characterization of rainfall conducted in the Port del Comte has allowed to estimate the vertical gradient of the amplitude associated to the seasonal variation of the isotopic content ($\delta^{18}O$ and δ^2H) in rainfall, an important but rarely reported parameter (only two additional references exist as reported in Table 4 of the manuscript) to correctly estimate the groundwater mean transit time when amplitude dumping method (Eq. 8 of the manuscript) is applied.

We have modified accordingly both the Abstract and the Introduction to highlight these points.

Reviewer #1 - General comment #2: Provide the future works to be implemented to generalize the results of this study.

Reply to general comment #2: Indeed. This study is the first stage in the full hydrogeological characterization of this aquifer system. The next step is to conduct the hydrogeochemical characterization of recharge and groundwater springs discharge to complement the results obtained in this

work by focusing in relevant unsolved questions like (1) the role play by the epikarst zone in the total transit time of groundwater and how this role is reflected in the hydrogeochemical evolution of the springs discharge after important rainfall events and during low-flows and (2) the use of artificial tracers and environmental isotopes (^{34}S , ^{15}N , ..) to characterize not only the mean transit time (i.e. the first moment of the transit-time distribution) but also to profile the groundwater transit-time distribution in terms of fast, intermediate and slow groundwater flows. This investigation is crucial to evaluate the aquifer vulnerability. We have included this information in the last part of the discussion a section.

Reviewer #1 - General comment #3: Compare the results of this study with similar studies.

Reply to general comment #3: A comparison in terms the mean transit time associated to the hydrological karst systems of Port del Comte and Ordesa and Monte Perdido (Jóðar et al. 2016b) was already included in the manuscript. Nevertheless, and following the reviewer suggestions, additional comparisons with the results obtained by Einsiedl et al. (2012), Garvelmann et al. (2017), and Lauber and Goldscheider (2014) for alpine karst aquifer systems with an overlying unsaturated have been included in the manuscript.

Specific comments

Introduction

Reviewer #1 - Q1: L 76-81: Including all this reference is not useful. You have to discuss this works. I suggest retaining two or three and the rest to remove them in the discussion only if you have something important to provide. Also, I suggest including information from karst systems from other Mediterranean countries (e.g. From Italy, Greece etc. see suggested literature).

Answer to Reviewer #1 - Q1: Indeed. We have rephrased the paragraph while synthetizing the cited references. Additionally, and as the reviewer suggests, the references of Allocca et al., (2015) and Kazakis et al. (2018) have been added to this paragraph to include in the storyline a link to Mediterranean karst systems

Reviewer #1 - Q2: Provide the innovation of this study. It is not clear to me. (Characterization of the hydrological behaviour of karst aquifer is not enough for an international journal)

Answer to Reviewer #1 - Q2: As it's commented in the eply to "general comment #1", the study adapts procedural approach to estimate the mean transit time in mountain karst aquifers by using a semi-distributed conceptual rainfall-runoff model and a lumped parameter model combined in a row. The first model explicitly provides the aquifer recharge time series that is used by the second model for simulating the environmental tracer transport through the hydrological system, and hence obtaining the aquifer mean transit time. Besides, the methodology has been applied in the karst aquifer system of Port del Comte (NE Spain) characterizing for

first time the hydrological behaviour of this important karst system. Moreover, this work provides an additional value of the vertical gradient of the amplitude associated to the seasonal variation of the water isotopic content ($\delta^{18}\text{O}$ and $\delta^2\text{H}$) in rainfall, an important but rarely reported parameter (only two additional references exist as reported in Table 4 of the manuscript) to correctly estimate the groundwater mean transit time when amplitude dumping method (Eq. 8 of the manuscript) is applied. We have modified accordingly both the Abstract and the Introduction to highlight these points.

Methodology

Reviewer #1 - Q3: Methodology: You can add photos of the karst spring and the cumulative precipitation gauges (maybe in supplementary materials)

Answer to Reviewer #1 - Q3: Following the reviewer suggestion photos from the main regional karst spring (S-1, S-2, S-3 and S-5) and also from the 8 cumulative precipitation gauges have been added as supplementary materials:

- Supplementary materials #1: Main regional karst springs of the Port del Comte massif (S-1, S-2, S-3 and S-5)
- Supplementary materials #2: The 8 cumulative precipitation gauges (pluviometers) used of the type CoCoRaHS RG202 Official-4

Results and discussion

Reviewer #1 - Q4: L 425-426: You plot the results in GMWL. What is the meaning of this? It provides altitude? Origin? You have to explain it. Discussion is actually missing. See also my previous comment.

Answer to Reviewer #1 - Q4: In the caption of the Figure 6 (Fig 5 in the new version) is explained the meaning of this acronym GMWL, which means the Global Meteoric Water Line. It is used to represent the isotopic variation of the rain globally. The position of the water samples isotopic composition respect to the GMWL indicates the origin of moisture generating rainfall and also indicates fractionation processes (e.g. evaporation, sublimation) affecting groundwater recharge. We have included the reference of Clarke and Fritz (1997) to help the reader if any question arise in this regard.

Conclusions

Reviewer #1 - Q5: Provide only the take home message. Avoid abbreviations in this section (e.g. The PCM.)

Answer to Reviewer #1 - Q5: Indeed. According to the reviewer suggestion we have modified the conclusions to summarize the important findings

COMMENTS FROM REVIEWERS: Reviewer #2

General comments

Reviewer #2 - General comment #1: This manuscript deals with the hydrological characterization of the karst aquifer system of the Port del Comte (NE of Spain) using stable isotopes. Specific objectives are to describe the isotopic seasonal variation of precipitation and springs to understand the groundwater flow time distribution by means of a semidistributed hydrological model and lumped parameter flow models. In my opinion, this work deserves to be published in Science of the Total Environment after a minor revision because the topic is highly relevant for the water resources management of the Barcelona city area.

The manuscript firstly presents a general introduction, describes in great detail the study area and the methodology, before showing and discussing results and finally giving a concluding section. I consider that the manuscript is well-written and presented but some sections (i.e., the methodology and study area) are extremely long and it might be a good idea to move some information to the Supplementary Material as well as some of the Figures and Tables. This might help to the better understanding of the manuscript.

Reply to general comment #1: Thank you very much for your comments. Following the reviewer suggestion, the sections "Study area" and "Materials and methods" have been restructured to make them shorter, thus facilitating the reading.

Specific comments

Reviewer #2 - Q1: Graphical Abstract: The authors might consider including some numbers such as the average isotopic composition of the precipitation and groundwater considering the elevation and the transit time distribution.

Answer to Reviewer #2- Q1: Indeed. These numbers certainly improve the understanding of the graphical abstract. According to the reviewer suggestion, we have added the mean isotopic content values corresponding to pluviometers P-02 (Bassa Clot de la Vall Z= 1946 m a.s.l), P-03 (Refugi Bages Z= 1768, m a.s.l.) and P-04 (Casa X&A Bages Z= 1657, m a.s.l.), and also the mean isotopic content of the regional spring S-05 (Fonts del Cardener).

Highlights

Reviewer #2 - Q2: The acronym PCM needs to be described in the second highlight.

Answer to Reviewer #2- Q2: Indeed. We have rephrased the sentence.

Keywords

Reviewer #2 - Q3: I suggest the term "stable" instead of "environmental" isotopes

Answer to Reviewer #2- Q3: This word has been changed. Thank you for the observation.

Abstract and introduction

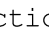
Reviewer #2 - Q4: The abstract properly summarizes the main findings of this research and the introduction content is appropriate. I do not have any major comment.

Answer to Reviewer #2- Q4: Thank you very much.

Reviewer #2 - Q5: L75: GW is not the first time that is mentioned, I think.

Answer to Reviewer #2- Q5: Thanks for catching this. We have defined the acronym the first time we mention Groundwater in the manuscript.

Reviewer #2 - Q6: Study area: Figure 1. a) The font size of the figure 1b is too small. b) Why the authors chose this geological cross section?

Answer to Reviewer #2- Q6: a) according to the reviewer suggestion, the image has been enlarged and the font size has been increased. b) The previous geological cross-section  shows the structure of the sub-basin for one of the most important springs in the zone: the spring S-05. The idea was including this section to explain how the existing faults but also the geometry of the different layer materials condition both storage capacity and flow direction inside the aquifer. Nevertheless, and from a geological point of view, it is indeed better to add at least one more geological cross-section following a perpendicular direction to the previous one, to show the structure of the massif along a N-S direction. According to this, a new geological cross-section has been added. Therefore, the first previous cross-section is now identified as A-B, and the new second one as C-D.

Reviewer #2 - Q7: L123-124: a) Is there no dry season? B) Please, indicate the period of time used to evaluate the average precipitation per month in the meteorological station MS-01.

Answer to Reviewer #2- Q7:

According to the 'Iberian Climate Atlas: Air temperature and precipitation (1971-2000)' (Agencia Estatal de Meteorología de España (AEMET) and Instituto de Meteorologia - Portugal (IMA). 2011), the Köppen Climate Classification for the study area is 'Dfb type' (defined as 'cold without dry season and temperate summer'). The reference can be consulted in the following link:
<https://www.aemet.es/documentos/es/conocermas/publicaciones/Atlas-climatologico/Atlas.pdf>

This information has been included in the manuscript.

b) Indeed. The time period to evaluate the monthly average precipitation in MS-01 is comprised between September 2005 and April 2016. This information has been included in the figure caption.

Reviewer #2 - Q8: Table 1 might be supplementary material

Answer to Reviewer #2- Q8: The information contained in Table 1 is referenced in several places along the manuscript. To facilitate the reading of the manuscript we consider that it is better to maintain this table in its original position.

Reviewer #2 - Q9: Materials and methods: This section is extremely long and the authors might consider moving some parts of the text to the Appendix or Supplementary material.

Answer to Reviewer #2- Q9: According to the reviewer comments, we have moved some parts of the manuscript at a new Appendix A. In particular, the original 'Figure 4' and 'Table 2' have been moved to an Appendix.

Reviewer #2 - Q10: L215-216: Position of "only" in the sentence: "groundwater samples were only taken with uneven frequency when it was possible".

Answer to Reviewer #2- Q10: Thanks for catching this. It has been changed.

Reviewer #2 - Q11: L233-234: I would recommend moving these lines to the supplementary material.

Answer to Reviewer #2- Q11: We suppose there is a mistake in the line numbering of this comment. In our opinion, these two lines (233-234) are necessary to following up the paragraph.

Reviewer #2 - Q12: L255: Method

Answer to Reviewer #2- Q12: Indeed. The sentence has been rephrased.

Reviewer #2 - Q13: Fig 5: might be supplementary material.

Answer to Reviewer #2- Q13: The schematic representation of the groundwater system response to a hypothetical input tracer function is a corner stone concept of this research. The authors consider that maintaining this figure in the main body of the manuscript facilitates the comprehension and reading of the text.

Reviewer #2 - Q14: L367: Might it be Eq. 5?

Answer to Reviewer #2- Q14: Indeed. Thank you for the observation. We have modified that number.

Reviewer #2 - Q15: Results and discussion: The results are discussed and presented in a detailed manner. Table 5: Might it be Supplementary material?

Answer to Reviewer #2- Q15: This table provides unpublished important data regarding the amplitude associated to the seasonal variation of the

water isotopic content ($\delta^{18}O$ and δ^2H) in rainfall, an important but rarely reported parameter (only two additional references exist as reported in this table) to correctly estimate the groundwater mean transit time when the amplitude dumping method (Eq. 8 of the manuscript) is applied. As stated in the abstract, this is one of the important findings of this work.

Reviewer #2 - Q16: L554-570: This equation and the associated text might be in the methodology.

Answer to Reviewer #2- Q16: Indeed. According to the reviewer suggestion, we have moved this part on the Methodology section inside a new sub-chapter named '3.5. Statistical analysis of the relationship between infiltration coefficient and recharge'.

Reviewer #2 - Q17: L635-658: In my opinion these lines break the flow of this section. The authors can consider include a new subsection explaining the implications of the estimation of dynamic volume stored in the aquifer for the springs in the management of water resources in Barcelona.

Answer to Reviewer #2- Q17: The authors fully agree with the reviewer's opinion. This part has been moved inside a new sub-section named "Evolution of results for groundwater management purposes".

COMMENTS FROM REVIEWERS: Reviewer #3

General Comment: The authors present the results of a groundwater modeling study of an aquifer in the Pyrenees. The topic is cogently introduced, the methodology is comprehensively explained, and the results are clearly presented and supported via high quality figures.

Overall, I think the work is well-developed and deserving of publication. I just have one major comment, and one minor comment, which I think should be addressed in revision.

Thank you very much for your kind comments

Reviewer #3 - Q1: First, a minor note: I generally disagree with the use of words like "proven" and "perfect" in research papers. In reality, these terms describe unattainable thresholds. Regardless of whether the authors might maintain they observed a "perfect mixing" in groundwater at their sites, the term rankles even the causal reader, and should be replaced.

Answer to Reviewer #3- Q1: The term 'perfect or complete mixing' is a term that can be easily found in the groundwater related bibliography when it is focussed on lumped parameter models. These models are commonly used to estimate mean transit time of hydrological systems. Despite of that, the authors fully agree with the reviewer point of view, and the terms "perfect mixing flow process" and "perfect mixing model" have been replaced by the terms "good mixing flow process" and "exponential flow model", respectively, throughout the manuscript

Reviewer #3 - Q2: As for my primary criticism, in its current form, the manuscript is a bit too close to a technical report, given the limited scope of the work and the authors' conclusions. It is obviously acceptable for a groundwater study to focus on a single aquifer. However, if the results of the work remain essentially descriptive, the work itself remains limited in applicability to a single site. Instead, I suggest the authors develop the discussion of their results to clearly note and illustrate what their work contributes to the broader discipline (other than the characterization of a single, previously uncharacterized aquifer), and how their results pertain to aquifers globally. Such discussion will increase the impact of the work and justify publication of the manuscript in an international journal.

Answer to Reviewer #3- Q2: Thank you for the sincere suggestion. Indeed, the former version of the manuscript did not focus on relevant aspects such as the applicability and usefulness of the applied methodology, which clearly improves what has been done so far when estimating groundwater transit times in high mountain karst systems with an overlying thick unsaturated zone. In this sense, the manuscript has been modified, highlighting the key innovations, and discussing the obtained results. Additionally, a deep bibliographic revision has been conducted to find studies focused on characterizing the hydrological behaviour of high mountain karst systems with an overlying not saturated zone to compare with. Unfortunately, the search has not been very successful and only four publications were found. The scarce number of publications reflects the difficulties for characterizing such hydrological systems rather than the existence of only a small number of alpine hydrological karst systems with an overlying thick unsaturated zone. In this line, we have included in the manuscript a list of sites with similar hydrogeological settings (i.e. a high mountain karst aquifer with a thick unsaturated zone) than those of the Port del Comte Massif (PCM). The location of these sites is presented in a new figure that also shows the carbonate outcrops in Europe. Looking at the figure one realizes that the number of sites analogue to PCM might be much larger.

COMMENTS FROM REVIEWERS: Reviewer #4

General Comment: I think that this research has very interesting results, the methodology is well described and the study area description is of a good quality. The figures also are of a good quality. The conclusions are well sustained by data. There are some general concerns that I suggest to the authors in order to improve the manuscript, being the first one critical:

Thank you very much for your kind comments

Reviewer #4 - Q1: I feel that the results are too localized to the study site being investigated or some other areas that some of the authors have already published in Spain and a more general setting is needed, comparing the results and the methodological approach in other climates regimes. To declare what is the novelty of the work and why is so an important contribution to scientific knowledge.

Answer to Reviewer #4- Q1: The authors fully agree with the reviewer. The original work did not focus on the key aspects from a global perspective, including the applicability and usefulness of the applied methodology. In

this sense, the introduction has been modified to highlight the novelty and importance of this work. Additionally, a deep bibliographic revision has been conducted to find studies focused on characterizing the hydrological behaviour of high mountain karst systems with an overlying not saturated zone to compare with. Unfortunately, the search has not been very successful and only five publications were found. Despite of that, the results of these studies are compared with the obtained in our manuscript. The scarce number of publications reflects the difficulties for characterizing such hydrological systems rather than the existence of only a small number of alpine hydrological karst systems with an overlying thick unsaturated zone. In this line, we have included in the manuscript a list of sites with similar hydrogeological settings (i.e. a high mountain karst aquifer with a thick unsaturated zone) than those of the Port del Comte Massif (PCM). The location of these sites is presented in a new figure that also shows the carbonate outcrops in Europe. Looking at the figure one realizes that the number of sites analogue to PCM might be much larger.

Reviewer #4 - Q2: The second issue is that more schematic geological profiles are needed to fully understand the aquifer geometry.

Answer to Reviewer #4- Q2: Indeed. A new geological cross-section has been included in Figure 1. The new section is orthogonal to the previous one and improves the understanding of the whole geometry of the Port del Comte Massif.

Reviewer #4 - Q3: The third and final issue is the abstract. Its need some rewriting will improve its quality, because some ideas are repeated, like the realization of the isotopic study.

Answer to Reviewer #4- Q3: Thanks for catching this. The abstract has been changed accordingly.

To whom concern:

The Port del Comte karst aquifer system discharges into the Cardener River, the most important tributary of the populated Llobregat River basin that provides drinking water to the city of Barcelona (NE Spain), where the population is larger than 2 million people, and where more than 70% of the water supply derives from surface waters. These waters also feed one of the major groundwater reservoirs for the Barcelona area, the aquifers of the Llobregat Delta (Otero et al., 2008). Surprisingly, the hydrological behavior of this important mountain karst system is still unknown.

In addition, high mountain environments are very sensitive to water driving vectors such the hydro-climatic forcing expected to be generated by climate change. Management and preservation of these water dependent systems requires a thorough understanding of the processes governing the hydrologic behavior of these systems. Furthermore, it is extremely important to characterize the hydrological behavior of the hydrological systems located in the mountain zones since they can be used as early warning system of water shortage events to minimize the impact of such events in the low valley zones.

Processes such as precipitation, evapotranspiration, aquifer recharge and runoff generation which force and describe the hydrological systems response also belong to the main knowledge areas considered by Science of the Total Environment, by including the atmosphere, hydrosphere, biosphere, lithosphere, and anthroposphere.

Barcelona, 20/09/2018

The authors: Ignasi Herms, Jorge Jódar, Albert Soler, Iñaki Vadillo, Luis Javier Lambán, Sergio Martos-Rosillo, Joan Agustí Núñez, Georgina Arnó, and Joan Jorge

1
2
3
4
5
6
7
8
9
10
11
12
13
14
15
16
17
18
19
20
21
22
23
24
25
26
27
28
29
30
31
32
33
34
35
36
37
38
39
40
41
42
43
44
45
46
47
48
49
50
51
52
53
54
55
56
57
58
59
60
61
62
63
64
65

Contribution of isotopic research techniques to characterize high-mountain-Mediterranean karst aquifers: The Port del Comte (Eastern Pyrenees) aquifer.

Herms, I.^a, Jódar, J.^{b,*}, Soler, A.^c, Vadillo, I.^d, Lambán, L.J.^e, Martos-
Rosillo, S.^e, Núñez, J.A.^a, Arnó, G.^a, Jorge, J.^f

(a) Àrea de Recursos Geològics. Institut Cartogràfic i Geològic de Catalunya (ICGC), Barcelona, Spain

(b) Groundwater Hydrology Group. Dept. Civil Engineering and Environment, Technical University of
Catalonia (UPC), Barcelona, Spain & Aquageo Proyectos S.L., Spain

(c) Grup de Mineralogia Aplicada i Geoquímica i Geomicrobiologia, Departament de Mineralogia,
Petrologia i Geologia Aplicada, Facultat de Ciències de la Terra, Universitat de Barcelona (UB),
Barcelona, Spain

(d) Centro de Hidrogeología, Universidad de Málaga (UMA), Málaga, Spain

(e) Instituto Geológico Minero de España (IGME), Spain

(f) Departament d'Enginyeria Minera, Industrial i TIC. Universitat Politècnica de Catalunya (UPC),
Manresa, Spain

* Corresponding author: Jorge Jódar (jorge.jodar@hydromodelhost.com). Telf:(+34)

619712122

Dear Professor Damià Barcelo, Co-Editor in Chief of Science of the Total Environment

Manuscript. No.: STOTEN-D-18-10315

Title: **“Contribution of isotopic research techniques to characterize high-mountain-Mediterranean karst aquifers: The Port del Comte (Eastern Pyrenees) aquifer.”**

First of all we want to thank you and the reviewers for the effort of reviewing the manuscript.

We have corrected the manuscript by accounting the reviewer’s suggestions.

Sincerely,

Ignasi Herms Canellas, M.Sc.

Jorge Jódar Bermúdez, Ph.D.

Albert Soler Gil, Ph.D.

Iñaki Vadillo Pérez, Ph.D.

Luis Javier Lambán Jiménez, Ph.D.

Sergio Martos Rosillo, Ph.D.

Joan Agustí Núñez, M.Sc.

Georgina Arnó Pons, B.Sc.

Joan Jorge Sánchez, Ph.D.

COMMENTS FROM REVIEWERS: Reviewer #1

General comments

The paper by Herms et al. with title: "Contribution of isotopic research techniques to characterize high mountain-Mediterranean karst aquifers: The Port del Comte (Eastern Pyrenees) aquifer." provides an interesting study regarding the contribution of isotopic research in karst aquifers. The concept is interesting and the manuscript well written.

Thank you very much for your kind comments

However, I have a number of recommendations, which should be done before publication.

Abstract

Reviewer #1 - General comments #1: You have to include the innovative results of this study. Provide the innovation of this study:

Reply to general comment #1: Certainly, as the reviewer points, the innovative points of this study are not stated in the manuscript. In this regard, the study presents two innovations: (1) a global innovation and (2) the specific innovation with the case study.

(1) The study presents the adaptation of a procedural methodology to improve the estimation of the mean transit time (τ) in high-mountain karst aquifers. The methodology is based on the previous approach presented by Vitvar et al., 1999 to estimate groundwater residence times in pre-alpine non-karstic aquifers (tertiary and quaternary deposits in a small basin with elevation ranges between 680 to 960 m a.s.l.) by means of developing a link between distributed rainfall-runoff models to estimate recharge series, and then a lumped-parameter model using environmental tracers to solve the convolution integral. In our case the method is adapted to estimate τ in high-mountain karst systems taking into account the existing vertical gradients of precipitation and air temperature along the slope of high mountains, the role played by the snow accumulation and ablation processes in the runoff generation, and considering the hydrological system to be modelled as the whole aquifer (i.e. the unsaturated zone and saturated zones).

(2) The adapted methodology is applied to the Port del Comte high mountain karst aquifer (NE, Spain) as a practical case study. Despite the strategic role played by this hydrogeological system as water resource provider to Barcelona, the hydrological behaviour of this system is completely unknown. This is the first hydrodynamic and transit time characterization of this hydrological system. Besides, the isotopic characterization of rainfall conducted in the Port del Comte has allowed to estimate the vertical gradient of the amplitude associated to the seasonal variation of the isotopic content ($\delta^{18}\text{O}$ and $\delta^2\text{H}$) in rainfall, an important but rarely reported parameter (only two additional references exist as reported in Table 4 of the manuscript) to correctly estimate the groundwater mean transit time when amplitude dumping method (Eq. 8 of the manuscript) is applied.

We have modified accordingly both the Abstract and the Introduction to highlight these points.

Reviewer #1 - General comment #2: Provide the future works to be implemented to generalize the results of this study.

Reply to general comment #2: Indeed. This study is the first stage in the full hydrogeological characterization of this aquifer system. The next step is to conduct the hydrogeochemical characterization of recharge and groundwater springs discharge to complement the results obtained in this work by focusing in relevant unsolved questions like (1) the role play by the epikarst zone in the total transit time of groundwater and how this role is reflected in the hydrogeochemical evolution of the springs discharge after important rainfall events and during low-flows and (2) the use of artificial tracers and environmental isotopes (^{34}S , ^{15}N , ..) to characterize not only the mean transit time (i.e. the first moment of the transit-time distribution) but also to profile the groundwater transit-time distribution in terms of fast, intermediate and slow groundwater flows. This investigation is crucial to evaluate the aquifer vulnerability. We have included this information in the last part of the discussion a section.

Reviewer #1 - General comment #3: Compare the results of this study with similar studies.

Reply to general comment #3: A comparison in terms the mean transit time associated to the hydrological karst systems of Port del Comte and Ordesa and Monte Perdido (Jódar et al. 2016b) was already included in the manuscript. Nevertheless, and following the reviewer suggestions, additional comparisons with the results obtained by Einsiedl et al. (2012), Garvelmann et al. (2017), and Lauber and Goldscheider (2014) for alpine karst aquifer systems with an overlying unsaturated have been included in the manuscript.

Specific comments

Introduction

Reviewer #1 – Q1: L 76-81: Including all this reference is not useful. You have to discuss this works. I suggest retaining two or three and the rest to remove them in the discussion only if you have something important to provide. Also, I suggest including information from karst systems from other Mediterranean countries (e.g. From Italy, Greece etc. see suggested literature).

Answer to Reviewer #1 – Q1: Indeed. We have rephrased the paragraph while synthetizing the cited references. Additionally, and as the reviewer suggests, the references of Allocca et al., (2015) and Kazakis et al. (2018) have been added to this paragraph to include in the storyline a link to Mediterranean karst systems

Reviewer #1 – Q2: Provide the innovation of this study. It is not clear to me. (Characterization of the hydrological behaviour of karst aquifer is not enough for an international journal)

Answer to Reviewer #1 – Q2: As it's commented in the reply to "general comment #1", the study adapts procedural approach to estimate the mean transit time in mountain karst aquifers by using a semi-distributed conceptual rainfall-runoff model and a lumped parameter model combined in a row. The first model explicitly provides the aquifer recharge time series that is used by the second model for simulating the environmental tracer transport through the hydrological system, and hence obtaining the aquifer mean transit time. Besides, the methodology has been applied in the karst aquifer system of Port del Comte (NE Spain) characterizing for first time the hydrological behaviour of this important karst system. Moreover, this work provides an additional value of the vertical gradient of the amplitude associated to the seasonal variation of the water isotopic content ($\delta^{18}\text{O}$ and $\delta^2\text{H}$) in rainfall, an important but rarely reported parameter (only two additional references exist as reported in Table 4 of the manuscript) to correctly estimate the groundwater mean transit time when amplitude dumping method (Eq. 8 of the manuscript) is applied. We have modified accordingly both the Abstract and the Introduction to highlight these points.

Methodology

Reviewer #1 – Q3: Methodology: You can add photos of the karst spring and the cumulative precipitation gauges (maybe in supplementary materials)

Answer to Reviewer #1 – Q3: Following the reviewer suggestion photos from the main regional karst spring (S-1, S-2, S-3 and S-5) and also from the 8 cumulative precipitation gauges have been added as supplementary materials:

- Supplementary materials #1: Main regional karst springs of the Port del Comte massif (S-1, S-2, S-3 and S-5)
- Supplementary materials #2: The 8 cumulative precipitation gauges (pluviometers) used of the type CoCoRaHS RG202 Official-4

Results and discussion

Reviewer #1 – Q4: L 425-426: You plot the results in GMWL. What is the meaning of this? It provides altitude? Origin? You have to explain it. Discussion is actually missing. See also my previous comment.

Answer to Reviewer #1 – Q4: In the caption of the Figure 6 (Fig 5 in the new version) is explained the meaning of this acronym GMWL, which means the Global Meteoric Water Line. It is used to represent the isotopic variation of the rain globally. The position of the water samples isotopic composition respect to the GMWL indicates the origin of moisture generating rainfall and also indicates fractionation processes (e.g. evaporation, sublimation) affecting groundwater recharge. We have included the reference of Clarke and Fritz (1997) to help the reader if any question arise in this regard.

Conclusions

Reviewer #1 – Q5: Provide only the take home message. Avoid abbreviations in this section (e.g. The PCM.)

Answer to Reviewer #1 – Q5: Indeed. According to the reviewer suggestion we have modified the conclusions to summarize the important findings

COMMENTS FROM REVIEWERS: Reviewer #2

General comments

Reviewer #2 - General comment #1: This manuscript deals with the hydrological characterization of the karst aquifer system of the Port del Comte (NE of Spain) using stable isotopes. Specific objectives are to describe the isotopic seasonal variation of precipitation and springs to understand the groundwater flow time distribution by means of a semidistributed hydrological model and lumped parameter flow models. In my opinion, this work deserves to be published in Science of the Total Environment after a minor revision because the topic is highly relevant for the water resources management of the Barcelona city area.

The manuscript firstly presents a general introduction, describes in great detail the study area and the methodology, before showing and discussing results and finally giving a concluding section. I consider that the manuscript is well-written and presented but some sections (i.e., the methodology and study area) are extremely long and it might be a good idea to move some information to the Supplementary Material as well as some of the Figures and Tables. This might help to the better understanding of the manuscript.

Reply to general comment #1: Thank you very much for your comments. Following the reviewer suggestion, the sections "Study area" and "Materials and methods" have been restructured to make them shorter, thus facilitating the reading.

Specific comments

Reviewer #2 – Q1: Graphical Abstract: The authors might consider including some numbers such as the average isotopic composition of the precipitation and groundwater considering the elevation and the transit time distribution.

Answer to Reviewer #2– Q1: Indeed. These numbers certainly improve the understanding of the graphical abstract. According to the reviewer suggestion, we have added the mean isotopic content values corresponding to pluviometers P-02 (Bassa Clot de la Vall Z= 1946 m a.s.l), P-03 (Refugi Bages Z= 1768, m a.s.l.) and P-04 (Casa X&A Bages Z= 1657, m a.s.l.), and also the mean isotopic content of the regional spring S-05 (Fonts del Cardener).

Highlights

Reviewer #2 – Q2: The acronym PCM needs to be described in the second highlight.

Answer to Reviewer #2– Q2: Indeed. We have rephrased the sentence.

Keywords

Reviewer #2 – Q3: I suggest the term "stable" instead of "environmental" isotopes

Answer to Reviewer #2– Q3: This word has been changed. Thank you for the observation.

Abstract and introduction

Reviewer #2 – Q4: The abstract properly summarizes the main findings of this research and the introduction content is appropriate. I do not have any major comment.

Answer to Reviewer #2– Q4: Thank you very much.

Reviewer #2 – Q5: L75: GW is not the first time that is mentioned, I think.

Answer to Reviewer #2– Q5: Thanks for catching this. We have defined the acronym the first time we mention Groundwater in the manuscript.

Reviewer #2 – Q6: Study area: Figure 1. a) The font size of the figure 1b is too small. b) Why the authors chose this geological cross section?

Answer to Reviewer #2– Q6: a) according to the reviewer suggestion, the image has been enlarged and the font size has been increased. b) The previous geological cross-section α - β shows the structure of the sub-basin for one of the most important springs in the zone: the spring S-05. The idea was including this section to explain how the existing faults but also the geometry of the different layer materials condition both storage capacity and flow direction inside the aquifer. Nevertheless, and from a geological point of view, it is indeed better to add at least one more geological cross-section following a perpendicular direction to the previous one, to show the structure of the massif along a N-S direction. According to this, a new geological cross-section has been added. Therefore, the first previous cross-section is now identified as A-B, and the new second one as C-D.

Reviewer #2 – Q7: L123-124: a) Is there no dry season? B) Please, indicate the period of time used to evaluate the average precipitation per month in the meteorological station MS-01.

Answer to Reviewer #2– Q7:

According to the ‘Iberian Climate Atlas: Air temperature and precipitation (1971-2000)’ (Agencia Estatal de Meteorología de España (AEMET) and Instituto de Meteorología – Portugal (IMA). 2011), the Köppen Climate Classification for the study area is ‘Dfb type’ (defined as ‘cold without dry season and temperate summer’). The reference can be consulted in the following link:

<https://www.aemet.es/documentos/es/conocermas/publicaciones/Atlas-climatologico/Atlas.pdf>

This information has been included in the manuscript.

b) Indeed. The time period to evaluate the monthly average precipitation in MS-01 is comprised between September 2005 and April 2016. This information has been included in the figure caption.

Reviewer #2 – Q8: Table 1 might be supplementary material

Answer to Reviewer #2– Q8: The information contained in Table 1 is referenced in several places along the manuscript. To facilitate the reading of the manuscript we consider that it is better to maintain this table in its original position.

Reviewer #2 – Q9: Materials and methods: This section is extremely long and the authors might consider moving some parts of the text to the Appendix or Supplementary material.

Answer to Reviewer #2– Q9: According to the reviewer comments, we have moved some parts of the manuscript at a new Appendix A. In particular, the original ‘**Figure 4**’ and ‘**Table 2**’ have been moved to an Appendix.

Reviewer #2 – Q10: L215-216: Position of "only" in the sentence: "groundwater samples were only taken with uneven frequency when it was possible".

Answer to Reviewer #2– Q10: Thanks for catching this. It has been changed.

Reviewer #2 – Q11: L233-234: I would recommend moving these lines to the supplementary material.

Answer to Reviewer #2– Q11: We suppose there is a mistake in the line numbering of this comment. In our opinion, these two lines (233-234) are necessary to following up the paragraph.

Reviewer #2 – Q12: L255: Method

Answer to Reviewer #2– Q12: Indeed. The sentence has been rephrased.

Reviewer #2 – Q13: Fig 5: might be supplementary material.

Answer to Reviewer #2– Q13: The schematic representation of the groundwater system response to a hypothetical input tracer function is a corner stone concept of this research. The authors consider that maintaining this figure in the main body of the manuscript facilitates the comprehension and reading of the text.

Reviewer #2 – Q14: L367: Might it be Eq. 5?

Answer to Reviewer #2– Q14: Indeed. Thank you for the observation. We have modified that number.

Reviewer #2 – Q15: Results and discussion: The results are discussed and presented in a detailed manner. Table 5: Might it be Supplementary material?

Answer to Reviewer #2– Q15: This table provides unpublished important data regarding the amplitude associated to the seasonal variation of the water isotopic content ($\delta^{18}O$ and δ^2H) in rainfall, an important but rarely reported parameter (only two additional references exist as reported in this table) to correctly estimate the groundwater mean transit time when the amplitude dumping method (Eq. 8 of the manuscript) is applied. As stated in the abstract, this is one of the important findings of this work.

Reviewer #2 – Q16: L554-570: This equation and the associated text might be in the methodology.

Answer to Reviewer #2– Q16: Indeed. According to the reviewer suggestion, we have moved this part on the Methodology section inside a new sub-chapter named ‘3.5. Statistical analysis of the relationship between infiltration coefficient and recharge’.

Reviewer #2 – Q17: L635-658: In my opinion these lines break the flow of this section. The authors can consider include a new subsection explaining the implications of the estimation of dynamic volume stored in the aquifer for the springs in the management of water resources in Barcelona.

Answer to Reviewer #2– Q17: The authors fully agree with the reviewer’s opinion. This part has been moved inside a new sub-section named “Evolution of results for groundwater management purposes”.

COMMENTS FROM REVIEWERS: Reviewer #3

General Comment: The authors present the results of a groundwater modeling study of an aquifer in the Pyrenees. The topic is cogently introduced, the methodology is comprehensively explained, and the results are clearly presented and supported via high quality figures.

Overall, I think the work is well-developed and deserving of publication. I just have one major comment, and one minor comment, which I think should be addressed in revision.

Thank you very much for your kind comments

Reviewer #3 – Q1: First, a minor note: I generally disagree with the use of words like "proven" and "perfect" in research papers. In reality, these terms describe unattainable thresholds. Regardless of whether the authors might maintain they observed a "perfect mixing" in groundwater at their sites, the term rankles even the causal reader, and should be replaced.

Answer to Reviewer #3– Q1: The term 'perfect or complete mixing' is a term that can be easily found in the groundwater related bibliography when it is focussed on lumped parameter models. These models are commonly used to estimate mean transit time of hydrological systems. Despite of that, the authors fully agree with the reviewer point of view, and the terms "perfect mixing flow process" and "perfect mixing model" have been replaced by the terms "good mixing flow process" and "exponential flow model", respectively, throughout the manuscript

Reviewer #3 – Q2: As for my primary criticism, in its current form, the manuscript is a bit too close to a technical report, given the limited scope of the work and the authors' conclusions. It is obviously acceptable for a groundwater study to focus on a single aquifer. However, if the results of the work remain essentially descriptive, the work itself remains limited in applicability to a single site. Instead, I suggest the authors develop the discussion of their results to clearly note and illustrate what their work contributes to the broader discipline (other than the characterization of a single, previously uncharacterized aquifer), and how their results pertain to aquifers globally. Such discussion will increase the impact of the work and justify publication of the manuscript in an international journal.

Answer to Reviewer #3– Q2: Thank you for the sincere suggestion. Indeed, the former version of the manuscript did not focus on relevant aspects such as the applicability and usefulness of the applied methodology, which clearly improves what has been done so far when estimating groundwater transit times in high mountain karst systems with an overlaying thick unsaturated zone. In this sense, the manuscript has been modified, highlighting the key innovations, and discussing the obtained results. Additionally, a deep bibliographic revision has been conducted to find studies focused on characterizing the hydrological behaviour of high mountain karst systems with an overlying not saturated zone to compare with. Unfortunately, the search has not been very successful and only four publications were found. The scarce number of

publications reflects the difficulties for characterizing such hydrological systems rather than the existence of only a small number of alpine hydrological karst systems with an overlying thick unsaturated zone. In this line, we have included in the manuscript a list of sites with similar hydrogeological settings (i.e. a high mountain karst aquifer with a thick unsaturated zone) than those of the Port del Comte Massif (PCM). The location of these sites is presented in a new figure that also shows the carbonate outcrops in Europe. Looking at the figure one realizes that the number of sites analogue to PCM might be much larger.

COMMENTS FROM REVIEWERS: Reviewer #4

General Comment: I think that this research has very interesting results, the methodology is well described and the study area description is of a good quality. The figures also are of a good quality. The conclusions are well sustained by data. There are some general concerns that I suggest to the authors in order to improve the manuscript, being the first one critical:

Thank you very much for your kind comments

Reviewer #4 – Q1: I feel that the results are too localized to the study site being investigated or some other areas that some of the authors have already published in Spain and a more general setting is needed, comparing the results and the methodological approach in other climates regimes. To declare what is the novelty of the work and why is so an important contribution to scientific knowledge.

Answer to Reviewer #4– Q1: The authors fully agree with the reviewer. The original work did not focus on the key aspects from a global perspective, including the applicability and usefulness of the applied methodology. In this sense, the introduction has been modified to highlight the novelty and importance of this work. Additionally, a deep bibliographic revision has been conducted to find studies focused on characterizing the hydrological behaviour of high mountain karst systems with an overlying not saturated zone to compare with. Unfortunately, the search has not been very successful and only five publications were found. Despite of that, the results of these studies are compared with the obtained in our manuscript. The scarce number of publications reflects the difficulties for characterizing such hydrological systems rather than the existence of only a small number of alpine hydrological karst systems with an overlying thick unsaturated zone. In this line, we have included in the manuscript a list of sites with similar hydrogeological settings (i.e. a high mountain karst aquifer with a thick unsaturated zone) than those of the Port del Comte Massif (PCM). The location of these sites is presented in a new figure that also shows the carbonate outcrops in Europe. Looking at the figure one realizes that the number of sites analogue to PCM might be much larger.

Reviewer #4 – Q2: The second issue is that more schematic geological profiles are needed to fully understand the aquifer geometry.

Answer to Reviewer #4– Q2: Indeed. A new geological cross-section has been included in Figure 1. The new section is orthogonal to the previous one and improves the understanding of the whole geometry of the Port del Comte Massif.

Reviewer #4 – Q3: The third and final issue is the abstract. Its need some rewriting will improve its quality, because some ideas are repeated, like the realization of the isotopic study.

Answer to Reviewer #4– Q3: Thanks for catching this. The abstract has been changed accordingly.

1 Contribution of isotopic research techniques to characterize
2 high-mountain-Mediterranean karst aquifers: The Port del
3 Comte (Eastern Pyrenees) aquifer.

4

5 Herms, I.^a, Jódar, J.^{b,*}, Soler, A.^c, Vadillo, I.^d, Lambán, L.J.^e, Martos-
6 Rosillo, S.^e, Núñez, J.A.^a, Arnó, G.^a, Jorge, J.^f

7

8 (a) Àrea de Recursos Geològics. Institut Cartogràfic i Geològic de Catalunya (ICGC), Barcelona, Spain

9 (b) Groundwater Hydrology Group. Dept. Civil Engineering and Environment, Technical University of
10 Catalonia (UPC), Barcelona, Spain & Aquageo Proyectos S.L., Spain

11 (c) Grup de Mineralogia Aplicada i Geoquímica i Geomicrobiologia, Departament de Mineralogia,
12 Petrologia i Geologia Aplicada, Facultat de Ciències de la Terra, Universitat de Barcelona (UB),
13 Barcelona, Spain

14 (d) Centro de Hidrogeología, Universidad de Málaga (UMA), Málaga, Spain

15 (e) Instituto Geológico Minero de España (IGME), Spain

16 (f) Departament d'Enginyeria Minera, Industrial i TIC. Universitat Politècnica de Catalunya (UPC),
17 Manresa, Spain

18 * Corresponding author: Jorge Jódar (jorge.jodar@hydromodelhost.com). Telf:(+34)
19 619712122

20

21

22 **Abstract**

23 [Water resources in high mountain karst aquifers are usually characterized by high](#)
24 [rainfall, recharge and discharge that lead to the sustainability of the downstream](#)
25 [ecosystems. Nevertheless, these hydrological systems are vulnerable to the global](#)
26 [change impact. The mean transit time \(MTT\) is a key parameter to describe the behavior](#)

27 of these hydrologic systems and also to assess their vulnerability. This work is focused
28 on estimating MTT by using environmental tracers in the framework of high-mountain
29 karst systems with a very thick unsaturated zone (USZ). To this end, it is adapted to
30 alpine zones a methodology that combines a semi-distributed rainfall-runoff model to
31 estimate recharge time series, and a lumped-parameter model to obtain MTT. The
32 methodology has been applied to the Port del Comte Massif (PCM) hydrological system
33 (Southeastern Pyrenees, NE Spain), a karst aquifer system with an overlying 1000 m
34 thick USZ. Six catchment areas corresponding to most important springs of the system
35 are considered. The obtained results show that hydrologically the behavior of the system
36 can be described by an exponential flow model (EM), with MTT ranging between 1.9
37 and 2.9 years. These MTT values are shorter than those obtained by considering a
38 constant recharge rate along time, which is the easiest and most applied aquifer recharge
39 hypothesis when estimating MTT through lumped-parameter models.

Comment [JJ1]: Answer to Reviewer #1 –
General comment 1
Answer to Reviewer #1 – Q2
Answer to Reviewer #4– Q3

41 **Keywords:** Stable isotopes; Seasonal isotopic amplitude; Altitudinal line; Recharge;
42 Mean transit time; Karst.

Comment [JJ2]: Answer to Reviewer #2 –
Q3

43

44 1. Introduction

45 High mountain zones are known as "water towers" because they generate the main
46 water resources feeding the most important rivers in the world (Viviroli et al., 2007).
47 This phenomenon is especially important in the drought-prone Mediterranean area
48 (Vicente-Serrano et al 2014), where water availability is scarce and greatly dependent
49 on runoff from headwater basins (De Jong et al., 2009). Moreover, water discharge from
50 mountain areas is critical to ensure water supply in the lowland and coastal fringe

51 (Viviroli and Weingartner, 2004; García-Ruiz et al 2011), where human activity
52 (agriculture, industry, tourism) concentrates.

53

54 Future scenarios for climate change in the whole Mediterranean region forecast an
55 increase in temperature and a decrease in precipitation at the end of the 21st century
56 (Giorgi and Lionello, 2008). These effects may well impact the Mediterranean high
57 mountain zones (Nogués-Bravo et al., 2008; Lopez-Moreno et al., 2009; Ribalaygua et
58 al., 2013), modifying the hydrological behavior of their headwater basins (Barnett et al.,
59 2005; García-Ruiz et al. 2011, and references therein). Nevertheless, the first evidence
60 of such changes has already been reported in the Pyrenees, the southernmost European
61 range where glaciers can be found (Grunewald and Scheithauer, 2010). Pyrenean
62 glaciers have undergone an intense retreat since the middle of the last century, causing
63 most of them to face a certain close extinction (Chueca et al., 2007; René 2013; Marti et
64 al., 2015; López-Moreno et al., 2016). In addition, during this period, both mean annual
65 precipitation and number of rainy days have shown a clear decreasing trend in this zone
66 (Lopez-Moreno et al., 2010), along with a lesser snowfall and snow accumulation
67 (López-Moreno, 2005). These effects directly impact the water storage capacity of the
68 associated headwater systems (Seibert et al., 2015), as well as their associated
69 hydrological response in terms of both river discharge flowrates and timing of
70 maximum discharges (López-Moreno and García-Ruiz, 2004; Gremaud et al., 2009).
71 These changes will directly impact the downstream zones by complicating the current
72 water stress situation in the Mediterranean zone (Milano et al., 2013; Hernández-Mora
73 et al., 2014, Molina and Melgarejo, 2016). Because of the hydrological outlook that is
74 not so promising, it is essential to understand the functioning of the mountain
75 hydrological systems of the Mediterranean area, especially those scenarios in which

Comment [JJ3]: Answer to Reviewer #21 – Q5

76 groundwater (GW) plays a major role in the headwater discharge, because mountain
77 aquifers maintain base flows to rivers during the recurrent Mediterranean dry periods
78 (Hoerling et al 2012; Vicente-Serrano et al., 2014).

79

80 Despite playing a strategic role, most high mountain hydrogeological systems are still
81 insufficiently understood (Goldscheider, 2011). Conventional hydrogeological
82 investigation techniques (Bakalowicz, 2005; Goldscheider and Drew, 2007) are often
83 difficult to apply in alpine regions because of the difficult access and the harsh working
84 conditions, along with the types of instruments needed for conducting research in high
85 mountain zones (Lauber et al., 2014; Hood and Hayashi, 2010). However, a growing
86 number of publications are focusing on the importance of groundwater in the
87 functioning of high-mountain watershed rivers in different geological settings, including
88 alluvial/rockfall/talus aquifers (Lauber and Goldscheider, 2014; Kurylyk and Hayashi,
89 2017), fractured aquifers (Jódar et al., 2017; Barberá et al., 2018a) and karst systems
90 (Wetzel, 2004; Goldscheider, 2005; Gremaud et al., 2009; Mudarra et al., 2014; Allocca
91 et al., 2015; Lambán et al., 2015; Chen, 2017; Barberá et al., 2018b; Kazakis et al.,
92 2018). Determining the magnitude of groundwater recharge and aquifer Mean Transit

Comment [JJ4]: Answer to Reviewer #1 – Q1

93 Time (MTT) are key issues for understanding and managing alpine groundwater
94 systems. Spring hydrograph analysis and environmental tracer methods allow for
95 characterizing aquifer recharge and discharge processes, estimating recharge zone
96 elevation and transit times, determining drainage structures, and assessing spring
97 vulnerability, as well as calculating water resources in headwater aquifers (Wetzel,
98 2004; Rodgers et al., 2005; Einsiedl, 2005; Farlin and Maloszewski, 2013; Jódar et al.,
99 2016b; Malard et al., 2016; Epting et al., 2018).

100

101 In high-altitude alpine karst aquifers, groundwater recharge processes highly depend on
102 temporal and spatial distribution of precipitation and snowmelt (Lauber and
103 Goldscheider, 2014). The estimation of MTT in karst systems is conditioned by the
104 existence of variable flow conditions. These systems normally show triple-porosity and
105 different connected parts: the karstic conduits that allows rapid flow, and the fissured-
106 porous matrix that shows intermediate to slow flow. Artificial tracer test normally
107 injected in preferential flow paths (i.e. the channels) doesn't consider the fissured-
108 porous matrix of the aquifer, which can be important as far as the total karst water
109 volumes (Maloszewski et al., 2002). In this respect, the use of artificial tracers to
110 characterize such hydrological systems is not enough since it doesn't allow
111 characterizing all the components of the flow. Others important factors that govern the
112 suitability of injection test for MTT estimations is the existence of a thick unsaturated
113 zones (USZ): conducting tracer tests by injecting it at the surface of the thick USZ is
114 likely a failing tracer test given the large uncertainties regarding the likelihood of
115 hydraulic connection between the tracer injection point and the sampled system
116 discharge point (Lauber and Goldscheider, 2014). Additionally, the adverse working
117 conditions and the type of material of the instruments necessary to correctly perform the
118 tracer test (Goldscheider et al., 2008) in high-mountain areas make it difficult to execute
119 them.

120

121 As a result, the hydrogeological behavior of most of the mountain karst systems with an
122 associated thick USZ remain uncharacterized, despite of being the exploration of these
123 systems on the focus of speleogenetic research since the last decades (Ballesteros et al.,
124 2015a, and references therein).

125

126 Lumped parameter models (LPMs) are useful to simulate the behavior of such complex
127 mountain karst systems, even when they are poorly characterized. These models do not
128 require a detailed hydrological knowledge of the physical system. Moreover, LPMs
129 naturally integrate the USZ of the aquifer as a part of the whole hydrological system to
130 be modeled (Turnadge and Smerdon, 2014). Additionally, the stable isotopes of water
131 ($\delta^{18}\text{O}$ and $\delta^2\text{H}$) in rainfall have proved to be good environmental tracers for
132 investigating the dynamics of such hydrological systems karst systems (Andreo et al.,
133 2004). These tracers enter the system as recharge, migrate downgradient exploring the
134 whole hydrological system, and leave the karst aquifer with spring discharge or by
135 lateral mass transfer to other hydrogeologically connected aquifer units. In this line, this
136 work is devoted to estimate MTT of a high-mountain karst aquifer with a thick
137 unsaturated zone by using ^{18}O and ^2H as environmental tracers along with LPMs. To this
138 end, it is considered the approach presented by Vitvar et al. (1999) to estimate MTT in a
139 small Swiss pre-alpine aquifer. The original approach is adapted to high mountain zones
140 by considering the existing vertical gradients of precipitation and air temperature along
141 the slope of high mountains, but also the role played by the snow accumulation and
142 ablation processes in the runoff generation. The resulting method combines in series
143 two LPMs: (1) a semi-distributed rainfall-runoff HBV model (Bergström, 1976; Seibert,
144 2005) that simulates the observed hydrodynamical system response while taking into
145 account the elevation dependences of the different hydrometeorological variables (i.e.
146 Precipitation and temperature) and associated processes (e.g. snow accumulation and
147 ablation), and (2) a FlowPC model (Małozzewski and Zuber, 1996) that estimates the
148 mean transit time of the hydrological system while simulating the environmental tracer
149 content evolution in the system discharge. This is done by numerically integrating a
150 convolution integral (Malozzewski et al., 1983; Jódar et al., 2014). In our case, the

151 FlowPC model uses as input data: a) the recharge time series of the aquifer obtained
152 with the HBV model, and b) the time series isotope content ($\delta^{18}\text{O}$ and $\delta^2\text{H}$) in recharge,
153 which is obtained through a spatiotemporal characterization of the isotope contained of
154 precipitation.

155

156 The methodology is applied to the hydrological system of Port del Comte Massif (PCM;
157 NE Spain), a karst aquifer with a 1000 m thick USZ. The hydrological system mainly
158 discharges through the Cardener springs into the homonym river, which is the main
159 tributary of the Llobregat River, the first water resources provider to the city of
160 Barcelona (NE Spain). Despite the strategic role of Cardener springs the hydrologic
161 behavior of the karst system remains unknown. This study contributes to a better
162 hydrological characterization of PCM hydrological system. Moreover, the proposed
163 methodology can be applied to characterize other high mountain karst aquifers with an
164 overlying thick USZ that are common in many alpine zones elsewhere the globe.

165

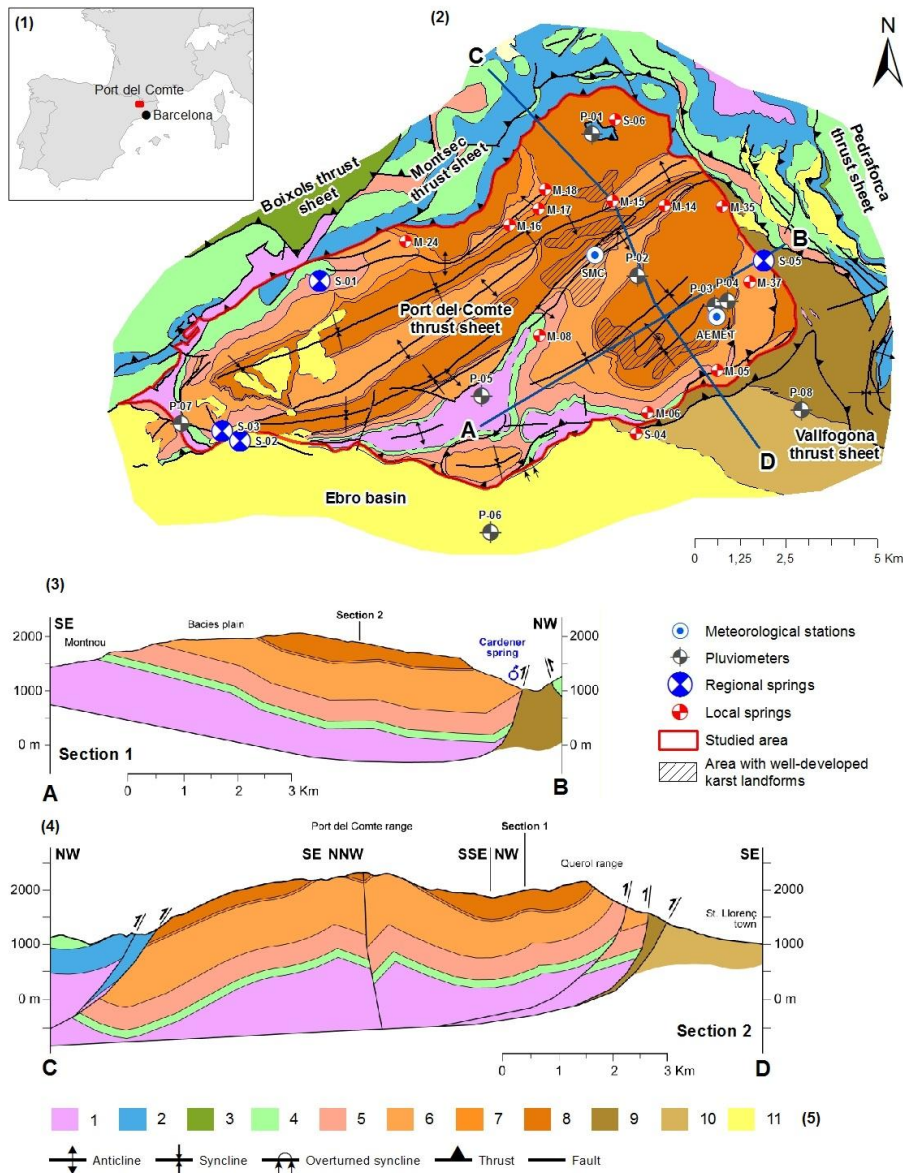
166

167 2. Study area

168 The study area is located at the Port del Comte Massif (PCM), which is situated in the
169 eastern part of the Pyrenees, NE Spain (Fig. 1). The elevation of the watershed ranges
170 from approximately 900 m a.s.l., up to 2387 m a.s.l., at the 'Pedró dels Quatre Batlles'
171 peak. With approximately 110 km², it contains one of the main mountain karst aquifers
172 of the Catalan Pyrenees. The watershed of the massif divides the river basin of the
173 Cardener River at the E and S and the river basin of the Segre River at the NW and SW.
174 The massif constitutes an independent structural and hydrogeological unit.

175

Comment [JJ5]: Answer to Reviewer #1 -
Geeneral comment 1
Answer to Reviewer #1 – Q2



176

177 Fig. 1. (1) Location map of the study zone. (2) Geological map (geological map modified from
 178 ICGC, 2007). (3) Geological cross-section A-B. (4) Geological cross-section C-D. (5)
 179 Geological legend: [1] Triassic – shales, limestones, dolomites and evaporates; [2] Jurassic –
 180 marls, bioclastic limestones and dolomites; [3] Lower Cretaceous – mudstones, ammonite
 181 limestones and marl; [4] Upper Cretaceous – limestones, marls, calcarenites and terrigenous

182 deposit; [5] Garumnian – red shales and limestones; [6] Lower Eocene – fissured and karstified
183 alveoline limestones and dolomites; [7] Lower Eocene – marls, sandstones and limestone; [8]
184 Lower Eocene – fissured and karstified micritic and bioclastic limestones; [9] Middle Eocene –
185 sandstones, marls, conglomerates, limestones and evaporates; [10] Upper Eocene – continental
186 alluvial systems: conglomerates and sandstones; [11] Oligocene – continental alluvial systems:
187 conglomerates, breccias and sandstones.

188

189 **2.1 Meteorological setting**

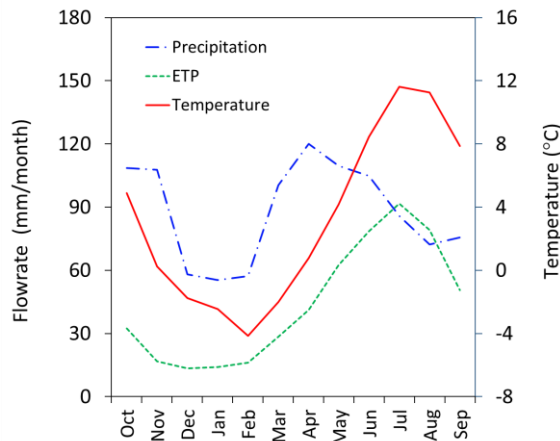
190 From a climatic point of view, and according to the Köppen-Geiger classification (Peel
191 et al., 2007), the study zone has a cold climate without dry season and temperate
192 summer (defined as ‘Dfb’ type; accordingly to AEMET and IMA, 2011). At the
193 meteorological station MS-01 (Fig. 1), which is located at 2315 m a.s.l., the average
194 values of precipitation (P), temperature (T) and potential evapotranspiration (ETP)
195 calculated with the Hargreaves and Samani (1982) equation are 1055 mm/yr, 3,24 °C
196 and 525 mm/yr, respectively. These three variables show a seasonal variation (Fig. 2)
197 and an elevation dependence. The measured vertical gradients (lapse rate) of
198 precipitation ($\nabla_z P$), atmospheric temperature ($\nabla_z T$) and potential evapotranspiration
199 ($\nabla_z ETP$) are 8,9 mm/yr/100 m, -0,74 °C/100 m and -32,3 mm/yr/100 m, respectively.
200 The snow cap is present in the upper zones of the basin in winter and spring, maintained
201 annually for 3 to 4 months since 1800 m a.s.l., meaning that precipitation is partly
202 produced as snow.

203

204 Despite the high average rainfall above 1000 mm/year, in most of the study area the
205 surface runoff is almost nonexistent, and it is not observed until reaching lower
206 altitudes.

207

Comment [JJ7]: Answer to Reviewer #2-Q7:



208

209 Fig. 2. Seasonal variation of precipitation, potential evapotranspiration and temperature
 210 measured at the meteorological station MS-01 (see Table 1) located at 2315 m a.s.l. [for the](#)
 211 [period Sep 2005- Apr 2016](#).

212

213 **2.2 General settings of the study zone**

214 From a geological perspective, the massif belongs to the PCM thrust sheet that presents
 215 complex structural relationships in its contours (Fig. 1). On the E, the PCM mantle
 216 borders on the mantle of Cadí, coinciding with the point of origin for the Cardener
 217 River (spring S-05; Fig. 1). To the NE and NW, the PCM is limited by the tectonic
 218 plates of the mantles of Sierras Marginales, Montsec and Boixols. To the S, the PCM
 219 mantle overlaps with the conglomeratic materials of the Ebro Basin, the southern
 220 foreland basin of the Pyrenees. The internal structure of the PCM mantle is formed by a
 221 set of folds and thrusts detached above the Triassic. These folds have a constant
 222 direction NE-SW parallel to the NW limit of the mantle (Vergés, 1999). The
 223 stratigraphic series contains materials from the Triassic, Jurassic, Cretaceous and
 224 Paleogene with a total of approximately 1000 m thickness. The main karst aquifer
 225 inside PCM massif is in the Paleocene - Eocene carbonate rocks. The geologic structure
 226 and stratigraphy of the PCM thrust strongly influence the location of the existing karst

Comment [JJ8]: Answer to Reviewer #2-Q7

227 springs, their groundwater geochemistry and their hydrologic behavior. The lower
228 Upper Cretaceous/Paleocene (Garumnian facies) substrate materials underlying the
229 Palaeocene aquifer are composed of sandstone, siltstone and shale. These materials
230 constitute an impervious layer for the overlaying aquifer system.

231

232 From the geomorphological point of view, the PCM has a characteristic triangular
233 geometry. The PCM has a smooth rounded landscape with a plain in the highest part
234 without vegetation cover and with almost no soil, which corresponds to approximately
235 10% of the total area. The rest of the massif is covered by mountain meadows (29%)
236 and forest (61%) with scarce soil depth up to medium developed soil cover. Different
237 karstic forms progressively appear from 1950 m a.s.l. upwards, being well developed at
238 2050 m a.s.l., with sinkholes, dry caves, dolines and karren fields, generating a
239 heterogeneous karstified hydrogeological system.

240

241 The hydrogeological conceptual model of the PCM aquifer system considers that
242 recharge is produced by infiltration of precipitation as rainfall and snowmelt. The
243 magnitude and distribution of infiltration is conditioned by the development of the karst
244 landforms. The infiltration is produced (1) in a concentrated way through the local
245 karstic elements such as dolines and (2) in a diffuse way by rain and snowmelt along the
246 whole PCM area. The epikarst unsaturated zone (NSZ) presents a thickness close to
247 1000 m in the highest zones of the PCM. The infiltrated water flows vertically through
248 the NSZ towards the saturated zone.

249

250 The hydrogeological system naturally discharges through the large number of existing
251 springs. Approximately 100 springs have been found in the PCM showing large

252 discrepancies in their mean discharge flow rate, ranging from values $\ll 1$ L/s up to
 253 values > 100 L/s. Most of these springs discharge a local subhorizontal interflow
 254 characteristic of a small entity (i.e., Local springs, Table 1). However, in terms of
 255 groundwater discharge, there are six important springs in the PCM (i.e., Regional
 256 springs, Table 1). These springs have been monitored regularly for this research,
 257 showing that all of them have a highly variable discharge flow rate (Fig. 3). Four of
 258 these regional springs (S-01, S-02, S-03 and S-05) are the principals discharging points
 259 of the whole hydrogeological system. The four springs are located at elevations between
 260 944 and 1098 m a.s.l. (see Table 1). Through these main springs, the hydrogeological
 261 system discharges at two principal watersheds: the Cardener River watershed to the east
 262 and the Segre River watershed to the northwest. Groundwater flow direction is
 263 conditioned by the geological structure of PCM. Nevertheless, the exact position of the
 264 regional groundwater table is poorly known.

265

266 Table 1. Meteorological stations, pluviometers and springs in the study zone sampled during the
 267 period July 2013 – October 2015.

Code	Type	Name	Elevation (m a.s.l.)	Num. water samples (-)	Discharge rate (L/s)
MS-01	Met. Station	SMC-Z8	2315	-	-
MS-02	Met. Station	AEMET-01270	1800	-	-
P-01	Pluviometer	Refugi de l'Arp	1936	7	-
P-02	Pluviometer	Bassa Clot de la Vall	1946	8	-
P-03	Pluviometer	Refugi Bages	1768	8	-
P-04	Pluviometer	Casa X&A	1657	8	-
P-05	Pluviometer	Casa Ramonet	1450	8	-
P-06	Pluviometer	Casa Cavallera	1216	7	-
P-07	Pluviometer	Camp. La Comella	1062	8	-

P-08	Pluviometer	Camp. Morunys	896	9	-
S-01	Regional Spring	Font Aiguaneix	1098	25	8 - 73
S-02	Regional Spring	Font Sant Quintí	944	25	70 – 575
S-03	Regional Spring	Font Can Sala	1062	25	0,25 – 148
S-04	Local Spring	Font Coll de Jou	1464	25	0,07 - 0,59
S-05	Regional Spring	Fonts del Cardener	1032	25	57 – 904
S-06	Local Spring	Font carretera Refugi Arp	1858	25	0,04 – 7
M-05	Local Spring	Font del Ginebró	1730	4	<0,001
M-06	Local Spring	Font de la Garganta	1657	4	0,02-0,49
M-08	Local Spring	Font Orris 02	1871	4	0,1 – 0,7
M-14	Local Spring	Font Estivella	2053	4	0,07 – 5
M-15	Local Spring	Font Arderic	2158	3	0,03 – 2,8
M-16	Local Spring	Font del Casalí	2077	1	<0,001
M-17	Local Spring	Font del Diumenge	1989	2	0,004 – 0,026
M-18	Local Spring	Font barraca Sangonella	1940	1	0,001 - 0,01
M-24	Local Spring	Font dels Acens	1550	4	0,06 – 0,23
M-35	Local Spring	Font Ca l'Arreplagant	1330	4	<0,001 – 0,02
M-37	Local Spring	Font La Part (esllav.)	1315	4	0,5 – 1

268

269

270 3. Materials and methods

271 3.1 Field work

272 To collect precipitation samples, a network of 8 cumulative precipitation gauges
 273 (pluviometers) of the type CoCoRaHS RG202 Official-4 was installed at elevations
 274 between 896 and 1935 m a.s.l. (P-01 a P-08; Fig. 1). The pluviometers consist of a
 275 polycarbonate cylindrical deposit with a diameter of 10,8 cm. The pluviometers include
 276 a top funnel that captures and guides precipitation into the storing deposit, where

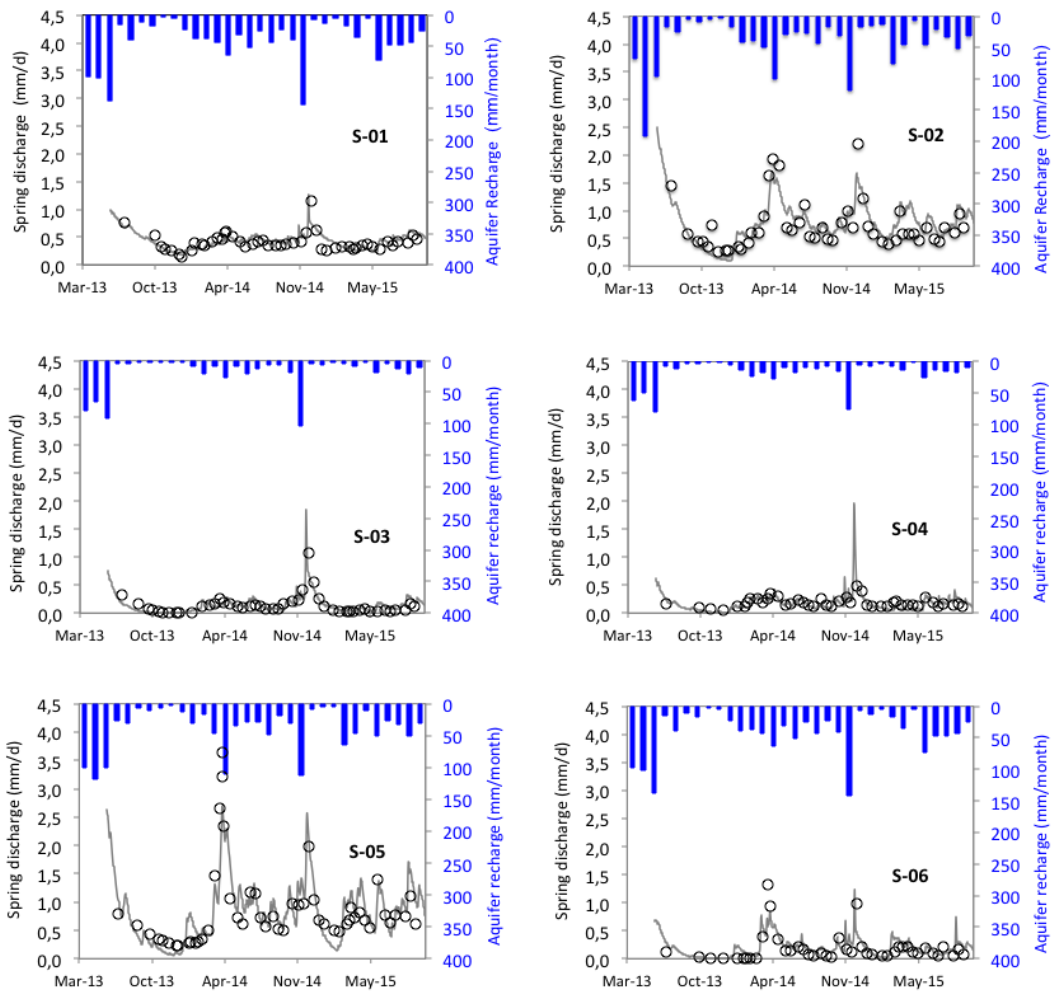
277 according to the technical procedure for the stations of the Global Network of Isotopes
278 in Precipitation (GNIP) of the International Atomic Energy Agency (IAEA), a 0,5 cm
279 paraffin oil floating layer is added to avoid evaporation. The pluviometers were sampled
280 seasonally (except the first winter with two campaigns), a total of 9 campaigns from
281 Dec. 2013 to Dec. 2015. Additionally, one snow sampling survey was conducted in
282 December 2003. The snow samples were obtained by drilling through the entire snow
283 depth (Lambán et al., 2015) and were taken at different locations with elevations
284 ranging from 1935 to 2150 m a.s.l.

285

286 Groundwater samples were collected under different hydrodynamic conditions between
287 Oct. 2013 and Dec. 2015. In this period, the springs S-01 to S-06 were sampled
288 approximately monthly, for a total of 25 sampling campaigns. Groundwater samples
289 were taken before the snow arrival in autumn (Oct. 2013 and Oct. 2014), and after the
290 snow-melting season (Apr. 2014 and Apr. 2015). In these springs, groundwater
291 discharge was measured once every two weeks from Jul. 2013 to Oct. 2015 (Fig. 3). In
292 springs S-01, S-02, S-03 and S-05 the discharge flow rate was measured by conducting
293 slug-injection salt dilution tests (Cervi et al., 2014), whereas the volumetric method was
294 used for the precision discharge measurement in springs S-04 and S-06. The M-##
295 springs (Table 1) showed a tiny and intermittent discharge. Therefore, groundwater
296 samples were **only** taken with uneven frequency when it was possible.

297

Comment [JJ9]: Answer to Reviewer #2-Q10



298

299 Fig. 3. Measured spring discharge (circles) in the six monitored springs (S-01 to S-06, Table 1)
 300 of the PCM hydrogeological system. Gray lines indicate the spring discharge numerically
 301 simulated with the HBV model (Seibert and Vis, 2012). For each spring, blue columns
 302 indicate the recharge values time series used as input data to the corresponding HBV model.

303

304 The isotopic composition ($\delta^2\text{H}$ and $\delta^{18}\text{O}$) of all low salinity water samples was
 305 determined in the Center of Hydrogeology of the University of Málaga (CEHIUMA),
 306 where a Picarro® “L2130-I” isotopic water analyzer was used. The analytical

307 uncertainties for $\delta^{18}\text{O}$ and $\delta^2\text{H}$ are ± 0.2 ‰ and ± 1.0 ‰, respectively. According to
308 Coplen et al., (2011) several international and laboratory standards have been
309 interspersed for normalization of analyses. The standards used (WICO-13, WICO-14,
310 WICO-15) were calibrated in an interlaboratory comparison (Wassenaar et al., 2012).
311 All results are given relative to the V-SMOW standard.

312

313 **3.2 Approach for spring catchment delineation**

314 A critical aspect to understand the behavior of karst hydrogeological flow systems is the
315 delineation of the spring capture zones (i.e., recharge areas) and their boundaries
316 (Goldscheider and Drew, 2007). Ideally, the delineation should be based on the proven
317 information of connection between recharge areas and the discharge points. In high
318 mountain zones, this connection may be confirmed by conducting tracer tests
319 (Goldscheider et al., 2008; Mudarra et al., 2014; Barberá et al., 2018b). When this
320 information is not available, the spring capture zone can be indirectly inferred by
321 considering inputs from other classical information sources such as geophysics,
322 structural geology and geomorphology data interpretation. However, 3D conceptual
323 modeling techniques are currently being used to delineate the spring capture zones:
324 Malard et al. (2015) analyze spring discharge hydrographs based on geological three-
325 dimensional (3D) conceptual modeling (Butscher and Huggenberger, 2007, 2008;
326 Martos-Rosillo et al., 2014; Ruiz-Costán et al., 2015; Malard et al., 2015; Ballesteros et
327 al., 2015b; Epting et al., 2018).

328

329 In this work, a combined 3D conceptual methodology has been used to delineate the
330 catchment areas associated with each spring. The delineating criteria are based on the

331 information provided by three complementary methods: (1) the interpretation of the
332 geological structure and the subsurface catchments relative to each spring location. To
333 this end, a 3D geological model has been developed in the 3DMove software platform
334 (Midland Valley Exploration Ltd.); (2) the analysis of the disposition and location of the
335 karst landforms over the area, and (3) the analysis through GIS spatial analysis tools of
336 the ground surface structure, including type of soils (CREAF, 2009) and vegetation
337 (Appendix A) at the spring recharge elevation zones. In the case of the regional springs
338 S-01, S-02, S-03 and S-05, the three listed methods have been applied to delineate their
339 catchment zone, whereas in the case of the perched springs S-04 and S-06, **only the**
340 **previous methods (2) and (3) could be applied.** Fig. A1 (Appendix A) shows the
341 catchment zones (i.e., aquifer units) obtained for the selected springs.

342

343 The delineated catchment zones associated with the regional springs divide PCM into
344 two main blocks: (1) a southwestern block that includes only the catchment zone
345 associated with S-05. This catchment zone is characterized by a syncline dipping NW
346 structure (Fig. 1). From a functional point of view, this zone is hydrodynamically
347 independent of the rest of PCM given the existence of an anticline and a main NE-SW
348 fault that prevents lateral flows. (2) The northeastern block formed by the catchment
349 zone associated with springs S-01, S-02 and S-03. The geological structure of this block
350 regulates the regional groundwater flows, so as the Alinyà anticline controls the
351 discharge of spring S-01, and the main syncline-anticline system dips SW along with
352 the minor faults and synclines dipping south conditions the discharge of springs S-02
353 and S-03. Table A1 (Appendix A) provides the geographical details of the delineated
354 groundwater catchment zones.

355

Comment [JJ10]: Answer to Reviewer #2- Q12:

3.3 Characterizing the seasonal variation of environmental tracers

The evolution of some environmental variables is linked to the atmospheric temperature variation. As a result, these variables often show a similar seasonal pattern that can be characterized with a general sinusoidal function $\delta(t)$ (Jódar et al., 2014). This function consists of two additive terms, a sine-wave function [Eq. 1] plus a temporal linear trend for the mean [Eq. 2].

$$\delta(t) = A \sin(\omega(t - t_0) + \varphi) + \bar{\delta} \quad (1)$$

$$\bar{\delta} = \alpha(t - t_0) + \bar{\delta}_0 \quad (2)$$

where A is the amplitude of the sinusoidal function, ω is the angular frequency, φ is the angular initial at time t_0 , α is the slope of the linear trend, and $\bar{\delta}_0$ is the linear trend value at time t_0 . The parameters A , α and $\bar{\delta}_0$ can be estimated by using the solution of any of the commonly available spreadsheet software's or manually. In this work, the root-mean-squared error (RMSE) is used as the selection criterion for the best fit to the measured isotope content time series.

In the case time series with a short amount of data (e.g., associated with the M-## springs in Table 1), it is not possible to obtain reliable estimates for, α , A , and $\bar{\delta}_0$ by using the method proposed above. In this case, no linear trend in the mean value is assumed ($\alpha = 0$), and $\bar{\delta}_0$ and A are estimated as:

$$\bar{\delta}_0 = \frac{1}{N} \sum_{i=1}^N \delta_i \quad (3)$$

$$A = \max(\text{Abs}(\bar{\delta}_0 - \delta_i)); \forall i = 1 \div N \quad (4)$$

375

376 where N is the number of the isotopic content value of the time series.

377

378 Hydrogeological systems transfer the isotopic input signal of recharge. The tracer input
379 seasonal signal is buffered and delayed as it propagates through the aquifer towards the
380 discharging point (Fig. 4). This tracer transport process through the hydrological system
381 can be described by the convolution integral that relates the tracer input content in
382 recharge δ_{in} to the tracer input content in the spring discharge δ_{out} as shown below.

383

$$\delta_{out}(t) = \int_{-\infty}^t \delta_{in}(t')g(t-t')dt' \quad (5)$$

384

385 where t is the time of tracer entry as recharge, t' is the integration variable and $g(t')$ is a
386 weighting function describing the Transit Time Distribution (TTD) exit of tracer content
387 that entered the aquifer at different times in the past. The differences between the input
388 and the output tracer signals are related to the aquifer system MTT (τ) which is the first
389 moment of the system TTD and is given by

$$\tau = \int_0^{\infty} tg(t)dt \quad (6)$$

390

391 where V is the volume of mobile water in the system (Małozzewski et al., 1983), and Q
392 is the volumetric flow rate through the system. In the case of natural gradient
393 hydrogeological systems, MTT corresponds to the mean amount of time for
394 groundwater to travel from the recharge zone to the discharging spring. In this situation,
395 MTT is related to the spring discharge flow rate Q , and the aquifer storage V as follows
396 (Custodio and Llamas, 1976):

$$\tau = \frac{V}{Q} \quad (7)$$

397

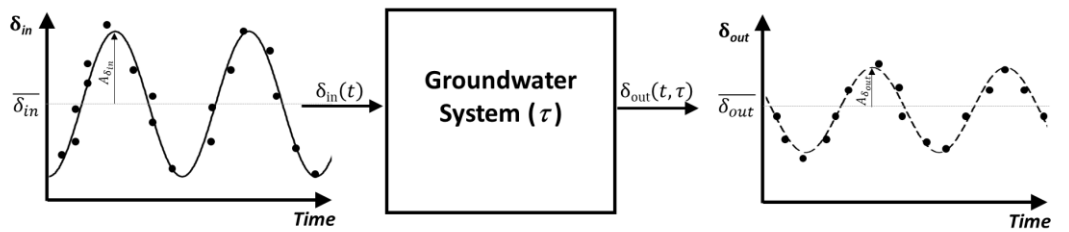
398 Additionally, in natural gradient hydrogeological systems with a seasonal varying input
 399 tracer function, MTT can be estimated as (Małozzewski et al., 1983):

$$\tau = \frac{1}{\omega} \sqrt{\left(\frac{A_{\delta_{in}}}{A_{\delta_{out}}}\right)^2 - 1} \quad (8)$$

400

401 where $A_{\delta_{in}}$ and $A_{\delta_{out}}$ are the amplitudes of the seasonal variation of the isotopic content
 402 in the aquifer recharge and the spring discharge, respectively. As can be shown, the
 403 above equation compares $A_{\delta_{in}}$ with respect to $A_{\delta_{out}}$, so the larger the amplitude
 404 dampening is, the longer the transit time.

405



406

407 Fig. 4. Schematic representation of the groundwater system response $\delta_{out}(t, \tau)$ to a
 408 hypothetical input tracer function $\delta_{in}(t)$ (modified from Jódar et al., 2016b), where τ
 409 means MTT.

410

411 3.4 Numerical approach for simulating the aquifer behavior

412 To reproduce the observed spring discharge flow rates and the associated isotopic
 413 content, a two-step methodology has been used:

414

415 (1) Simulation of the hydrodynamic behavior of the hydrogeological system. To this
416 end, the freely available version of the semi-distributed conceptual
417 precipitation–runoff model HBV-Light (Seibert and Vis, 2012) is used. HBV is
418 a conceptual rainfall-runoff model for catchment hydrology modeling that solves
419 a general water balance equation. HBV has been used in different alpine
420 mountain hydrologic research studies (Braun and Renner, 1992; Hottelet, et al.,
421 1993; Uhlenbrook et al., 1999; Merz and Blöschl, 2004; Konz and Seibert, 2010;
422 Staudinger et al., 2017; Epting, et al., 2018; Jódar et al., 2018). This model has
423 become a standard tool for simulating high mountain snow-dominated
424 hydrological systems. This code requires as input data some hydroclimatic
425 catchment information such as the relative weight with respect to the total area
426 of the different altitude and associated vegetation zones in the catchment, the
427 vertical lapse rates $\nabla_z P$ and $\nabla_z T$, as well as the time series of daily P, T, and
428 ETP. The hydrological catchment can be separated into numerous elevation
429 zones, depending on the elevation gap between the lowest and the highest points
430 of the catchment. In this work, every zone has been divided into three elevation
431 zones (Table A1 in Appendix A). Additionally, every elevation zone can be
432 divided into different vegetation zones. Based on the Land Cover Map of
433 Catalonia (CREAF, 2009), three vegetation zones are considered: (1) open areas
434 corresponding to zones of both poor or no soils where karst landforms are very
435 well-developed (karren fields, sinkholes, dolines, etc.), (2) areas with mountain
436 meadows and soil moderately developed, and (3) alpine forest zones with
437 moderate to well-developed soils. A two stacked linear reservoir is used to
438 simulate the hydrological system dynamics. The upper reservoir is used to
439 generate surface and subsurface runoff whereas the lower reservoir generates

440 groundwater runoff. The model considers vegetation zones parameters and
441 catchment zone parameterer (Tables C1 and C2 of Appendix C, respectively).
442 They are can be automatically calibrated by minimizing an efficiency objective
443 function (R_{eff} ; Table C3, Appendix C), which is already implemented in HBV.
444 The model output includes the daily time series of aquifer recharge Q_R , which is
445 used in the following step.

446

447 (2) Simulation of the transient isotopic content variation in the groundwater
448 discharge. The temporal variation of the isotopic content in the spring discharge
449 is simulated with FlowPC (Małozzewski and Zuber, 1996, 2002), a lumped
450 parameter model typically used to estimate groundwater MTTs with the aid of
451 observed environmental tracer data (Viville et al., 2006; Einsiedl et al., 2009;
452 Katsuyama et al., 2010; Lauber and Goldscheider, 2014; Sánchez-Murillo et al.,
453 2015; Mađrala et al., 2017). The program solves the convolution integral [Eq. 5]
454 and transforms the isotopic input tracer signal $\delta_{\text{in}}(t)$ entering the hydrogeological
455 system as recharge into the isotopic output tracer signal $\delta_{\text{out}}(t)$ leaving the
456 system through the spring discharge. To this end, FlowPC includes among
457 others two parametric TTDs which are especially well suited for simulating karst
458 aquifer systems: (A) The exponential model (EM), also known as a “good
459 mixing model”, is typically applied in systems where the groundwater flow lines
460 tend to converge towards the water sampling points (Zuber, 1986; Amin and
461 Campana, 1996). (B) The Exponential-Piston model (EPM) or “real system
462 model”, which combines two parts in line, an unconfined upstream part where
463 recharge enters the system and an exponential distribution of transit times is
464 assumed, and a confined downstream part where the flow scheme is

Comment [JJ11]: Answer to Reviewer
#2- Q14

Comment [JJ12]: Answer to Reviewer
#3- Q1

465 approximated like the piston flow model (Zuber, 1986). The weighting function
 466 for EPM is described by the following equation.

467

$$g(t) = \begin{cases} 0 & t < \tau \left(1 - \frac{1}{\eta}\right) \equiv t_\tau \\ \frac{1}{\tau} \eta e^{-\frac{\eta}{\tau} + \eta - 1} & t \geq t_\tau \end{cases} \quad (9)$$

468

469 where η is the ratio of total volume of the hydrogeological system to the volume
 470 of the system in which the exponential TDD exists, and τ is MTT. [Eq. 9] also
 471 describes the EM weighting functions when $\eta = 1$, which is the lowest bound of
 472 this parameter. The model parameters (η and τ) are calibrated by minimizing the
 473 RMSE function.

474

475 FlowPC requires the time series of (1) monthly aquifer recharge \widehat{Q}_R (hereinafter,
 476 a circumflex accent over a flow or an isotopic content variable indicates that the
 477 variable is cumulated monthly or averaged, respectively), which is obtained
 478 from the HBV model outputs for each simulation, and (2) the corresponding
 479 monthly averaged isotopic content of the recharge $\widehat{\delta}_R$. Given the karstic nature of
 480 the hydrogeological system, we assume that the isotopic content of local
 481 recharge and its seasonal characteristics (i.e., $\bar{\delta}_{in}, A_{\delta_{in}}$) are the same as the
 482 isotopic content and seasonal characteristics of local precipitation ($\bar{\delta}_P, A_{\delta_P}$).
 483 Since $\bar{\delta}_P$ and A_{δ_P} are known, then $\delta_P(t)$ is analytically obtained through [Eq.1].
 484 As $\delta_P(t)$ is a daily time function, it is necessary to transform it into $\widehat{\delta}_P$. For the

485 j^{th} month, $\widehat{\delta}_{P_j}$ is obtained by weighting the daily values of recharge isotopic
 486 content $\delta_{P_{ij}}$ by the corresponding daily recharge rate $Q_{R_{ij}}$ as

$$\widehat{\delta}_{R_j} \sim \widehat{\delta}_{P_j} = \frac{\sum_{i=1}^N \delta_{P_{ij}} Q_{R_{ij}}}{\sum_{i=1}^N Q_{R_{ij}}} \quad (10)$$

487 where N is the number of days of the j^{th} month. The Appendix D includes all the
 488 technical details corresponding to the different FlowPC models used in this work

489

490 **3.5 Statistical analysis of the relationship between the infiltration coefficient** 491 **and recharge**

492 To analyze the factors that controls the mean calculated infiltration coefficient (ξ) in the
 493 PCM, a linear regression model has been built, expressing the dependent variable ξ as a
 494 linear function of N explanatory variables Ψ_i as

$$\xi = \lambda_0 + \sum_{i=1}^N \lambda_i \Psi_i \quad (11)$$

495 where λ_0 is the intercept (constant) term, and λ_i ($i \geq 1 \div N$) are the regression coefficients
 496 associated with the predictors Ψ_i . In this study, the predictor variables of the linear
 497 regression model of the [Eq.11] are the elevation of the spring recharge zone Z_R (Table
 498 3), the mean precipitation at the spring recharge zone P_{ZR} (Table 6), and the percentages
 499 of open areas, mountain meadows and forest in the spring catchment zones (VZ_1 , VZ_2
 500 and VZ_3 , respectively; Table A1 in Appendix A). The coefficient of determination of
 501 the regression is one, so the model reproduces the whole variance of ξ . Table 7 shows
 502 the intercept value λ_0 , the regression coefficients λ_i , and their corresponding
 503 standardized value β_i ($i \geq 1 \div N$). The standardized value β_i measures the expected
 504 change in ξ , in standard deviation units, for a one standard deviation change in Ψ_i ,

505 provided that other explanatory variables in the model ($\Psi_j, \forall i \neq j$) are fixed (Nimon and
506 Oswald, 2013). The larger the absolute value of β_i , the more important the
507 corresponding predictor Ψ_j is.

Comment [JJ13]: Answer to Reviewer
#2- Q16

508

509

510 4. Results and discussion

511 4.1 Results from observed data

512 The isotopic content of the precipitation corresponding to the water samples taken is
513 shown in Fig. 5A. The mean isotopic content of precipitation is lighter in winter and
514 autumn than that in spring and summer, as one would expect given the dependence
515 between the isotopic content in rainfall and temperature (Mook and De Vries, 2000).
516 The obtained values are aligned between the Global Meteoric Water Line (GMWL) and
517 the West Mediterranean Meteoric Water Line (WMMWL) (Fig. 5A). The local water
518 meteoric water line (LMWL) that is obtained by linear regression ($N= 76; R^2= 0,97$) is
519 defined as $\delta^2\text{H} = 8,05 \cdot \delta^{18}\text{O} + 12,74$. From a seasonal point of view, the isotopic content
520 of precipitation in autumn and winter presents a larger variability than the isotopic
521 content of precipitation in spring and summer, as shown in Fig. 5B by the error bars
522 indicating the standard deviation associated with every seasonal value. The isotopic
523 content in groundwater changes seasonally much less, than the isotopic content in
524 precipitation (Fig. 5B), pointing out the existence of a **good** mixing flow process in the
525 discharging points of the aquifer.

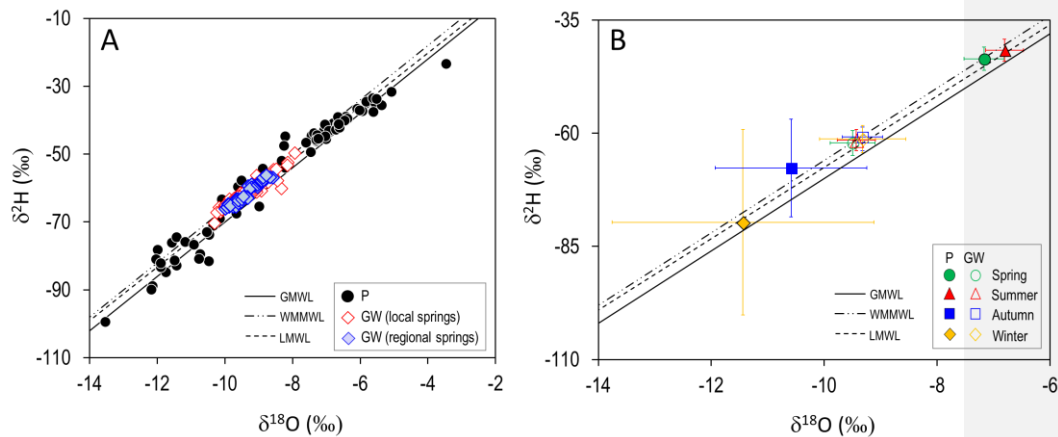
Comment [JJ14]: Answer to Reviewer
#3- Q1

526

527 The geographical location of the study zone postulates the Mediterranean as the most
528 important source of precipitation. This assumption is supported by the overall mean
529 deuterium excess ($dex= \delta^2\text{H} - 8 \cdot \delta^{18}\text{O}$) value of $12,03 \pm 3,37$ ‰ obtained for all the

530 precipitation samples analyzed (Celle-jeanton et al., 2001; Jiménez-Martínez and
 531 Custodio, 2008). Nevertheless, the Atlantic fingerprint in rainfall can be observed in the
 532 above *dex* value through its variation interval, which provides a minimum *dex* value of
 533 8,66 ‰ (Froehlich et al., 2001; Araguás-Araguás and Díaz-Teijeiro, 2005).

534



535

536

537 Fig. 5. (A) Values of $\delta^{18}\text{O}$ and $\delta^2\text{H}$ in precipitation (P; solid circles) and groundwater (GW)
 538 from local springs (empty red diamonds) and from regional springs (solid blue diamonds) for
 539 the period Oct. 2013 – Dec. 2015. (B) Seasonal overall averages of $\delta^{18}\text{O}$ and $\delta^2\text{H}$ for
 540 precipitation (P; solid symbols) and groundwater (GW; empty symbols). The spring, summer
 541 autumn and winter values are indicated by green circles, red triangles, blue squares and orange
 542 diamonds, respectively. GMWL (Clarke and Fritz, 1997) is the Global Meteoric Water Line
 543 (slope 8 and *dex*=10‰), WMMWL is the Western Mediterranean Meteoric Water Line (slope 8
 544 and *dex*=14‰) and LMWL is the Local Meteoric water Line (slope 8,05 and *dex*=12,74‰).

545

546 The isotopic composition of precipitation and spring discharge show a seasonal
 547 variation, which is not reflected in the deuterium excess. A seasonal variation in *dex*
 548 would indicate the existence of different moisture sources generating rainfall in the

Comment [JJ15]: Answer to Reviewer #1
 - Q4

549 study zone by following a certain seasonal pattern (Schotterer et al 1993; Liu et al 2008;
 550 Froehlich et al 2008). The lack of such seasonal pattern supports the Mediterranean as
 551 the main rainfall source.

552

553 A sine-wave function [Eq.1] is used to characterize every one of the measured seasonal
 554 time series of isotopic content in water from the sampling points (Fig. B1 in Appendix
 555 B). Tables 2 and 3 show the calibrated mean isotopic content ($\bar{\delta}$) and amplitude (A)
 556 corresponding to the time series of isotopic content of precipitation and spring
 557 discharge, respectively.

558

559 Table 2. Mean value $\bar{\delta}_{in}$ and amplitude $A_{\delta_{in}}$ of the seasonal variation in the isotopic content of
 560 precipitation for the sampled pluviometers.

Pluviometer	$\bar{\delta}_{in}$ (‰)			$A_{\delta_{in}}$ (‰)	
	$\delta^{18}\text{O}$	$\delta^2\text{H}$	dex	$\delta^{18}\text{O}$	$\delta^2\text{H}$
P-01	-9.20	-59.91	14.56	3.34	26.89
P-02	-9.50	-62.29	13.88	2.87	23.23
P-03	-9.20	-60.25	12.94	3.29	27.92
P-04	-8.60	-56.11	12.87	3.02	26.05
P-05	-8.60	-55.65	12.37	3.05	23.31
P-06	-7.80	-51.10	9.53	2.76	23.96
P-07	-7.50	-49.06	10.24	2.59	20.92
P-08	-7.50	-50.22	9.40	2.55	19.53

561

562

563 Table 3. Mean value $\bar{\delta}_{out}$ and amplitude $A_{\delta_{out}}$ of the seasonal variation in the isotopic content of
 564 groundwater for the springs sampled. For every spring, the elevation of the corresponding
 565 recharge zone Z_R is included. For this elevation, the associated amplitude $A_{\delta_{ZR}}$ of the seasonal
 566 variation in isotopic content of precipitation is shown.

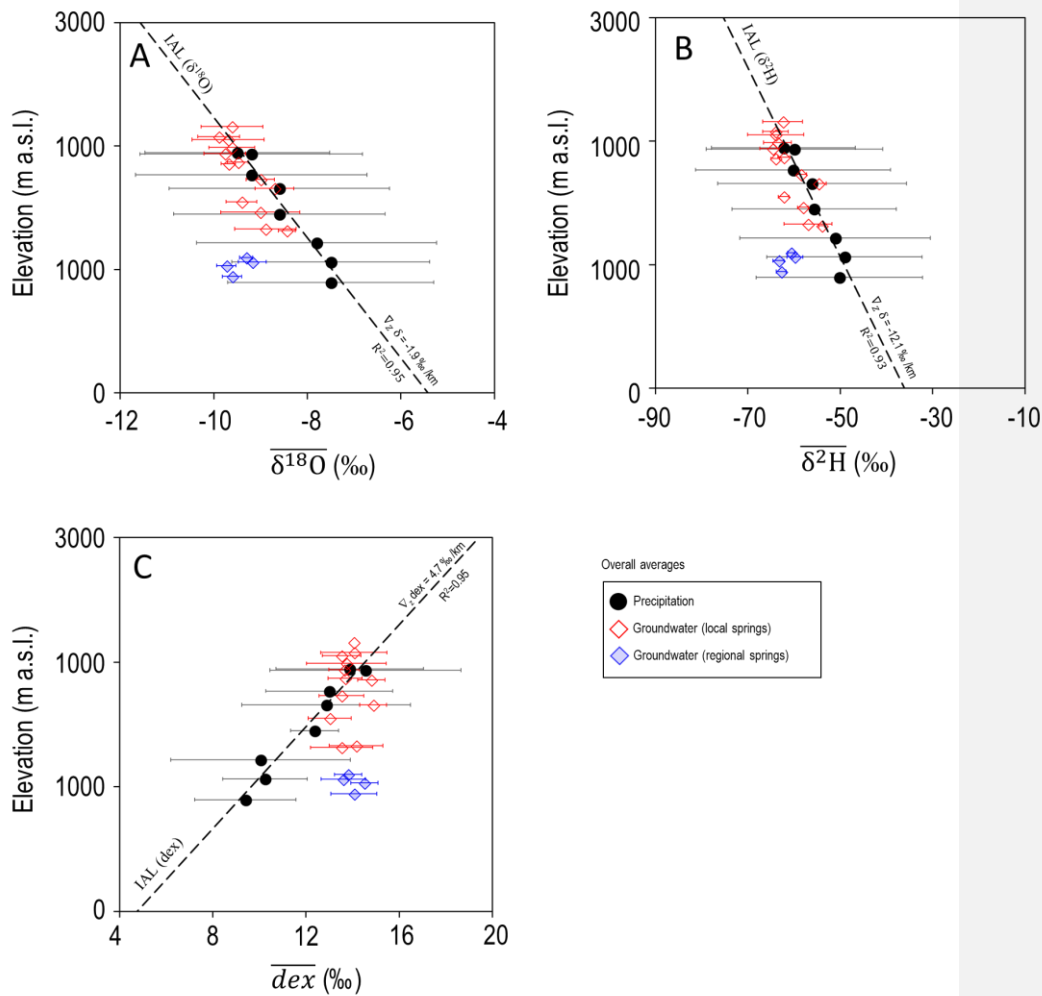
$\bar{\delta}_{out}$ (‰)	$A_{\delta_{out}}$ (‰)	Z_R (m a.s.l)	$A_{\delta_{ZR}}$ (‰)
--------------------------	------------------------	-----------------	-----------------------

Spring	$\delta^{18}\text{O}$	$\delta^2\text{H}$	dex	$\delta^{18}\text{O}$	$\delta^2\text{H}$	$\delta^{18}\text{O}$	$\delta^2\text{H}$	dex	$\delta^{18}\text{O}$	$\delta^2\text{H}$
S-01	-9,31	-60,65	13,81	0,12	1,10	1892	1881	1852	3,16	26,23
S-02	-9,61	-62,82	14,06	0,25	1,93	2038	2046	1902	3,24	27,18
S-03	-9,18	-59,85	13,60	0,11	1,07	1830	1819	1702	3,12	25,88
S-04	-9,01	-58,11	13,95	0,10	0,67	1745	1686	1881	3,07	25,12
S-05	-9,73	-63,36	14,50	0,14	0,88	2099	2088	1994	3,28	27,41
S-06	-9,69	-64,03	14,80	0,15	0,90	2078	2140	1798	3,27	27,71
M-05	-9,01	-58,53	13,52	0,44	1,81	1744	1718	1793	3,07	25,31
M-06	-8,70	-54,75	14,88	0,54	2,51	1597	1428	2071	2,98	23,65
M-08	-9,49	-62,22	13,68	0,27	1,84	1979	2001	1826	3,21	26,92
M-14	-9,69	-64,01	13,53	1,08	8,01	2079	2138	1795	3,27	27,70
M-15	-9,73	-63,81	14,05	0,87	6,24	2099	2123	1901	3,28	27,61
M-16	-9,77	-64,13	14,05	0,65	4,00	2118	2147	1902	3,29	27,75
M-17	-9,76	-64,32	13,73	0,49	2,86	2110	2161	1836	3,29	27,83
M-18	-9,59	-63,12	13,64	0,62	4,12	2031	2070	1817	3,24	27,31
M-24	-9,41	-62,26	13,02	0,47	1,64	1941	2004	1690	3,19	26,93
M-35	-8,90	-57,02	14,14	0,94	7,54	1690	1602	1920	3,04	24,65
M-37	-8,44	-54,00	13,53	0,26	0,93	1469	1371	1795	2,90	23,33

567

568 The mean isotopic content in rainfall $\bar{\delta}_{in}$ shows a clear-cut linear relationship with
569 elevation (Fig. 6) that allows defining Isotopic Altitudinal Lines (IAL) for $\delta^{18}\text{O}$, $\delta^2\text{H}$
570 and dex , with slopes (i.e., vertical gradients $\nabla_z\delta^{18}\text{O}$, $\nabla_z\delta^2\text{H}$ and $\nabla_z dex$) of -1,9, -12,1
571 and 4,7 ‰/km, respectively. Vertical gradients ($\nabla_z\delta$) of mean isotopic content in
572 precipitation are common in mountain zones (see Poage and Chamberlain, 2001, and
573 references therein) and are related to the atmospheric decreasing thermal vertical profile
574 existing along the slope of the mountains. $\nabla_z\delta$ values obtained for the study zone are
575 like those obtained in other alpine areas, especially in the central Pyrenees and the Alps
576 (Table 4).

577



578

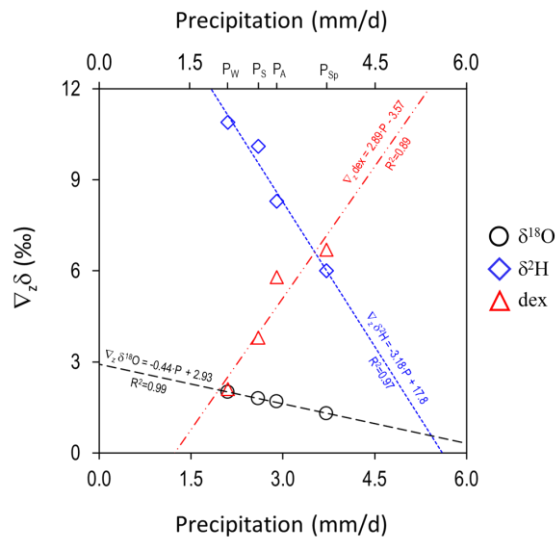
579 Fig. 6. Relationship between elevation and the mean isotopic content in precipitation and
 580 springs. (A) $\delta^{18}\text{O}$, (B) $\delta^2\text{H}$, and (C) dex . Error bars indicate the standard deviation. Dashed lines
 581 indicate the local Isotopic Altitudinal Line (IAL) of precipitation.

582

583 The vertical gradients of the mean isotopic content in precipitation depend linearly on
 584 the mean seasonal precipitation (Fig. 7). In the case of $\delta^{18}\text{O}$ and $\delta^2\text{H}$, the higher the
 585 seasonal precipitation is, the lower the seasonal gradient is. In the case of dex , the
 586 relationship is reversed, obtaining a higher $\nabla_z dex$ value as seasonal precipitation

587 increases. In a seasonal framework, recycling moisture evaporated from the land surface
588 to atmosphere may increase dex of local precipitation. Soil evaporation is maximum
589 when atmospheric vapor pressure deficit ($\Delta e = e - e_{\text{sat}}$, e being the atmospheric water
590 pressure and e_{sat} the saturating water pressure at the air parcel temperature) is
591 maximum, if the soil contains water for evaporating. Therefore, to allow soil water to
592 evaporate, it is necessary to have enough (1) soil water content, which is higher in
593 spring and autumn since these are the rainiest seasons, and (2) atmospheric vapor
594 pressure deficits (Δe). Satisfying these two conditions, $\nabla_z dex$ is maximum when the
595 difference in dex (i.e., Δe) between the highest and the lowest points of the mountain
596 slope is maximum. Given that e_{sat} is an increasing function of temperature (Gonfiantini
597 et al., 2001), Δe will decrease as temperature declines. During the cold season, despite a
598 thermal difference existing between the highest and lowest points of the mountain, the
599 difference in Δe between these points is minimum. Additionally, the commented Δe
600 difference is minimum as well when there is no thermal difference along the mountain
601 slope, a situation that is favored by the cathabaltic winds in winter (Obleitner, 1994;
602 Gladich et al., 2011) but is also favored by the vertical atmosphere air mixing during the
603 typical summer local low pressure convective rainfall events.

604



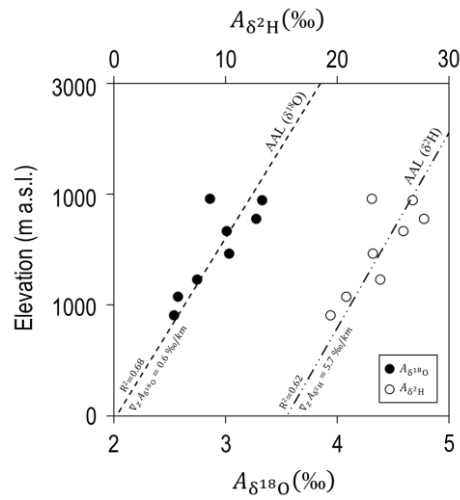
605

606 Fig. 7. Dependence of the vertical gradient of the mean isotopic content with respect to the
 607 mean seasonal precipitation. The subscripts Sp, S, A, and W stand for spring, summer, autumn
 608 and winter, respectively.

609

610 The amplitude of the seasonal variation in the isotopic content of precipitation $A_{\delta_{in}}$
 611 relates linearly to elevation (Fig. 8) to allow defining Amplitude Altitudinal Lines
 612 (AAL) for $\delta^{18}\text{O}$ and $\delta^2\text{H}$ with slopes (i.e., vertical gradients $\nabla_z A_{\delta^{18}\text{O}}$ and $\nabla_z A_{\delta^2\text{H}}$) of 0,6
 613 and 5,7 ‰/km, respectively. Similar vertical gradients have previously been reported in
 614 the central Pyrenees (Jóðar et al., 2016b) and the Bernese Alps (Jóðar et al., 2016a)
 615 (Table 4).

616



617

618 Fig. 8. Relationship between elevation and amplitude of the seasonal
 619 content ($\delta^{18}\text{O}$, $\delta^2\text{H}$) in precipitation. Dashed line and dashed-dotted line indicate the local
 620 Amplitude Altitudinal Lines (AALs) of precipitation for $\delta^{18}\text{O}$ and $\delta^2\text{H}$, respectively.

621

622 Table 4. Vertical gradients of mean isotopic water content and amplitude of the seasonal
 623 variation of the isotopic water content in precipitation.

Zone	$Z_{\min} - Z_{\max}$ (m a.s.l.)	$\nabla_z \delta^{18}\text{O}$ (‰/km)	$\nabla_z \delta^2\text{H}$ (‰/km)	$\nabla_z dex$ (‰/km)	$\nabla_z A_{\delta^{18}\text{O}}$ (‰/km)	$\nabla_z A_{\delta^2\text{H}}$ (‰/km)	Reference
Eastern Pyrenees (PCM ^a)	896-1936	-1,9	-15,2	4,7	0,6	6,1	This study
Central Pyrenees (PNOMP ^b)	772-2200	-2,2	-17,4	2,2	0,9	4,4	Jódar et al. (2016a)
Bernese Alps	874-2023	-3,0	-19,7	3,7	1,6	14,6	Jódar et al. (2016b)
Austrian Alps	580-2245	-1,9	-12,0	2,7	-	-	Froehlich et al. (2008)
Austrian Alps	469-1598	-1,3	-8,0	3,4	-	-	Froehlich et al. (2008)

Central (western flank)	Andes	2380-4250	-4,7	-42,5	2,2	-	-	Aravena et al. (1989)
Central (eastern flank)	Andes	2380-4250	-1,9	-14,3	1,1	-	-	Fiorella et al. (2015)
Central (eastern flank)	Andes	200-4080	-1,7	-11,7	2,0	-	-	Gonfiantini et al. (2001)
Western Carpathians		104-2008	-2,1	-	-	-	-	Holko et al. (2012)
Mount Cameroon		10-4050	-1,16	-11,4	1,4	-	-	Gonfiantini et al. (2001)

(a): Port del Comte Massif; (b): Ordesa and Monte Perdido National Park

624

625 The mean isotopic content of groundwater corresponding to local (perched) springs
626 shows a relationship with elevation dependence with a vertical gradient larger than that
627 of precipitation (Fig. 6), indicating the existence of aquifer recharge along the mountain
628 slope, a process also known as slope effect (Custodio and Jódar, 2016). Additionally,
629 the evolution of the isotopic content in the spring discharge shows a seasonal
630 dependence like precipitation but showing smaller amplitudes (Fig. B1 in Appendix B).
631 Even being lumped, the seasonal pattern of recharge is observed in the spring discharge,
632 indicating that MTT should not be longer than 5 or 6 years (DeWalle et al., 1997).

633

634 The isotopic altitudinal line (IAL, Fig. 6) allows estimation of the elevation of the
635 recharge zone (Z_R) corresponding to every spring by projecting their mean isotopic
636 content on IAL. Table 3 shows Z_R for all the springs, with their mean Z_R value ranging
637 between 1420 m a.s.l. (M-37) and 2136 m a.s.l. (M-17). With a known value for Z_R , it is
638 possible to calculate the amplitude of the variation in the isotopic content in
639 precipitation at the recharge zone elevation ($A_{\delta_{ZR}}$) by projecting Z_R on the amplitude

640 altitudinal line (AAL, Fig. 8). Table 2 shows $A_{\delta_{ZR}}$ for every spring. Finally, if both $A_{\delta_{ZR}}$
641 (i.e., $A_{\delta_{in}}$ at the springs recharge zone) and $A_{\delta_{out}}$ are known, it is possible to obtain a
642 first analytical estimate of MTT through [Eq. 8]. Table 5 provides the MTT values
643 obtained for all the springs. As can be shown, the obtained MTT values range between
644 0,5 and 5 yr.

645

646

Table 5. MTT values estimated for the springs sampled

Spring	$\delta^{18}\text{O}$			$\delta^2\text{H}$		
	$\tau^a(\text{yr})$	$\tau^b(\text{yr})$	$\eta(-)$	$\tau^a(\text{yr})$	$\tau^b(\text{yr})$	$\eta(-)$
S-01	4,10	2,25	1,02	3,78	3,00	1,01
S-02	2,06	1,42	1,02	2,23	1,96	1,00
S-03	4,67	2,25	1,00	3,83	2,33	1,01
S-04	4,70	2,33	1,01	5,93	2,67	1,00
S-05	3,73	2,88	1,02	4,98	2,83	1,01
S-06	3,47	2,58	1,02	4,90	2,75	1,02
M-05	1,10	-	1,00	2,22	-	1,00
M-06	0,86	-	1,00	1,49	-	1,00
M-08	1,89	-	1,00	2,32	-	1,00
M-14	0,45	-	1,00	0,53	-	1,00
M-15	0,58	-	1,00	0,69	-	1,00
M-16	0,79	-	1,00	1,09	-	1,00
M-17	1,06	-	1,00	1,54	-	1,00
M-18	0,82	-	1,00	1,04	-	1,00
M-24	1,07	-	1,00	2,61	-	1,00
M-35	0,49	-	1,00	0,5	-	1,00
M-37	1,77	-	1,00	3,99	--	1,00

(a) Analytical MTT value obtained by [Eq. 8]. (b) Numerical MTT value
obtained by FlowPC.

647

648

649 **4.2 Aquifer recharge evaluation through HBV**

650 The HBV semi-distributed conceptual rainfall–runoff model has been used to simulate
651 the observed groundwater discharge in every spring. The spring discharges were
652 measured every fortnight between July 2013 and October 2015. This period has been
653 used for calibrating the HBV parameters, which are shown in Table C4 (Appendix C).
654 The efficiency parameter R_{eff} that describes the goodness of the model fit ranges
655 between 0,55 (S-01) and 0,77 (S-05) (Table C5, Appendix C). The computed discharges
656 resemble the observed discharges by reproducing their temporal evolution in all the
657 springs (Fig. 3).

658

659 The results from the HBV model indicated that recharge is especially concentrated in
660 the open areas (VZ_1) and meadow areas (VZ_2). The yearly average effective recharge
661 ranges from 210 mm/yr (S-04) to 637 mm/yr (S-06) (Table 6). The aquifer infiltration
662 capacity ξ (i.e., the ratio between Q_{Re} – the effective recharge of the aquifer, and P_{ZR} –
663 precipitation at the spring recharge zone) ranges as the yearly average ranges from
664 28,3% (S-03) to almost 62% (S-06) (Table 6).

665

666 Table 6. Mean annual precipitation P_{ZR} , mean aquifer recharge Q_{R} , seasonal distribution of
667 recharge, infiltration capacity ξ .

Spring	P_{ZR}	Q_{R}	$\frac{Q_{\text{Re Spring}}}{Q_{\text{R}}}$	$\frac{Q_{\text{Re Summer}}}{Q_{\text{R}}}$	$\frac{Q_{\text{Re Autumn}}}{Q_{\text{R}}}$	$\frac{Q_{\text{Re Winter}}}{Q_{\text{R}}}$	ξ^a
	(mm/yr)	(mm/yr)	(%)	(%)	(%)	(%)	(%)
S-01	954	473	37,5%	15,0%	25,4%	22,1%	49,6%
S-02	1006	433	40,8%	12,3%	23,8%	23,1%	43,0%
S-03	793	227	38,1%	6,7%	27,2%	27,9%	28,6%

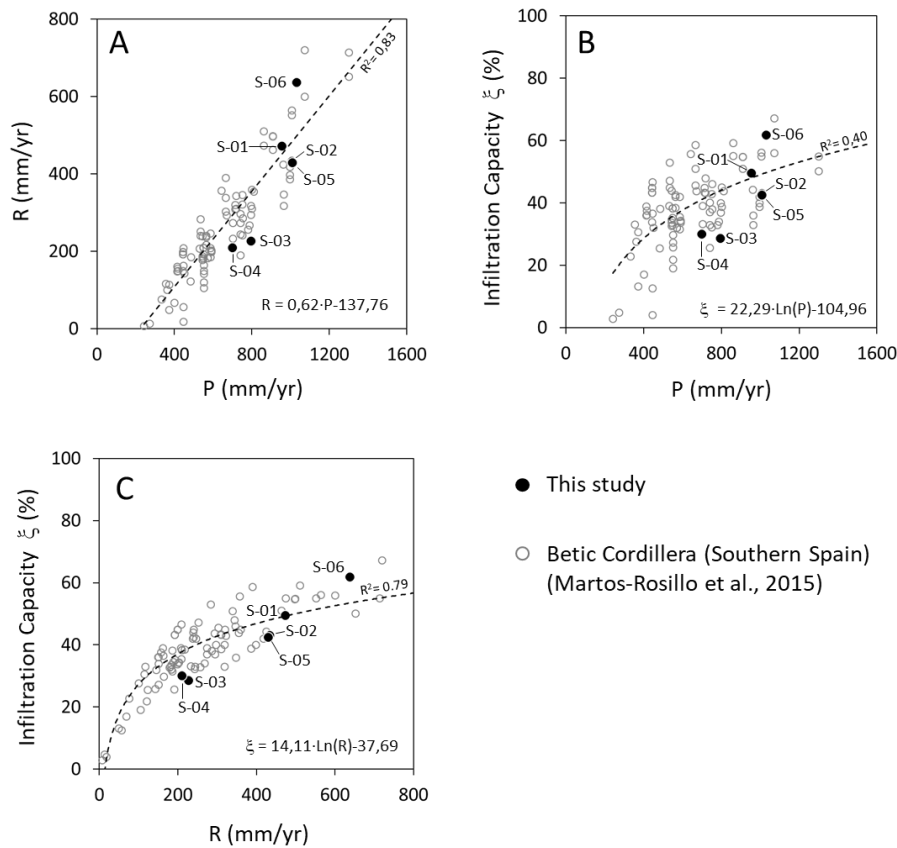
S-04	698	210	37,0%	10,2%	25,4%	27,4%	30,1%
S-05	1008	429	42,5%	14,3%	23,0%	20,2%	42,6%
S-06	1030	637	45,9%	8,9%	21,2%	24,0%	61,9%

(a) $\xi = Q_{R_e}/P_{ZR}$

668

669 Aquifer recharge follows a linear relationship similar to precipitation, as found by
670 Martos-Rosillo et al. (2015) for the mountain carbonate aquifers in the Betic Cordillera
671 (Southern Spain), where recharge is generally lower (Fig. 9A). In PCM, recharge is at a
672 maximum in spring, accounting for 40,3% of the total recharge, and this outcome is
673 explained by both rainfall and snow melt infiltration. Recharge is at a minimum (11,2%)
674 in summer, coinciding with the period of minimum seasonal precipitation.

675



676

677 Fig. 9. (A) Mean annual rainfall versus mean annual recharge, (B) Mean infiltration coefficient
678 versus mean annual rainfall, and (C) Mean infiltration coefficient versus mean annual recharge.

679

680 The relationship between ξ and P (Fig. 9B) is not as clear as the relationship between ξ
681 and R (Fig. 9C), indicating that precipitation is a necessary condition for aquifer
682 recharge, but it is not enough. In this respect, the results of the application of the linear
683 regression model between the variables Z_R , P_{ZR} , and VZ_1 , VZ_2 and VZ_3 ; shows that the
684 Z_R and is the most important predictor controlling the aquifer infiltration capacity ξ . In
685 addition, VZ_1 (karren fields and sinkholes at the highest parts of the massif) and VZ_3
686 (forest fields at the lowest of the massif) also play a role regarding ξ . These parameters

687 reflect the differences in both the karstification degree and the vegetation covering the
688 epikarst system in the PCM.

689

690 Table 7. No standardized (λ) and standardized (β) regression coefficients associated with the
691 explanatory variables used in the multiple regression method.

Explanatory Variable	λ	β
Intercept (λ_0)	-39,562	--
Z_R	0,047	0,823
P_{ZR}	-0,007	-0,054
VZ_1	6,034	0,133
VZ_2	4,018	0,072
VZ_3	258,518	0,122

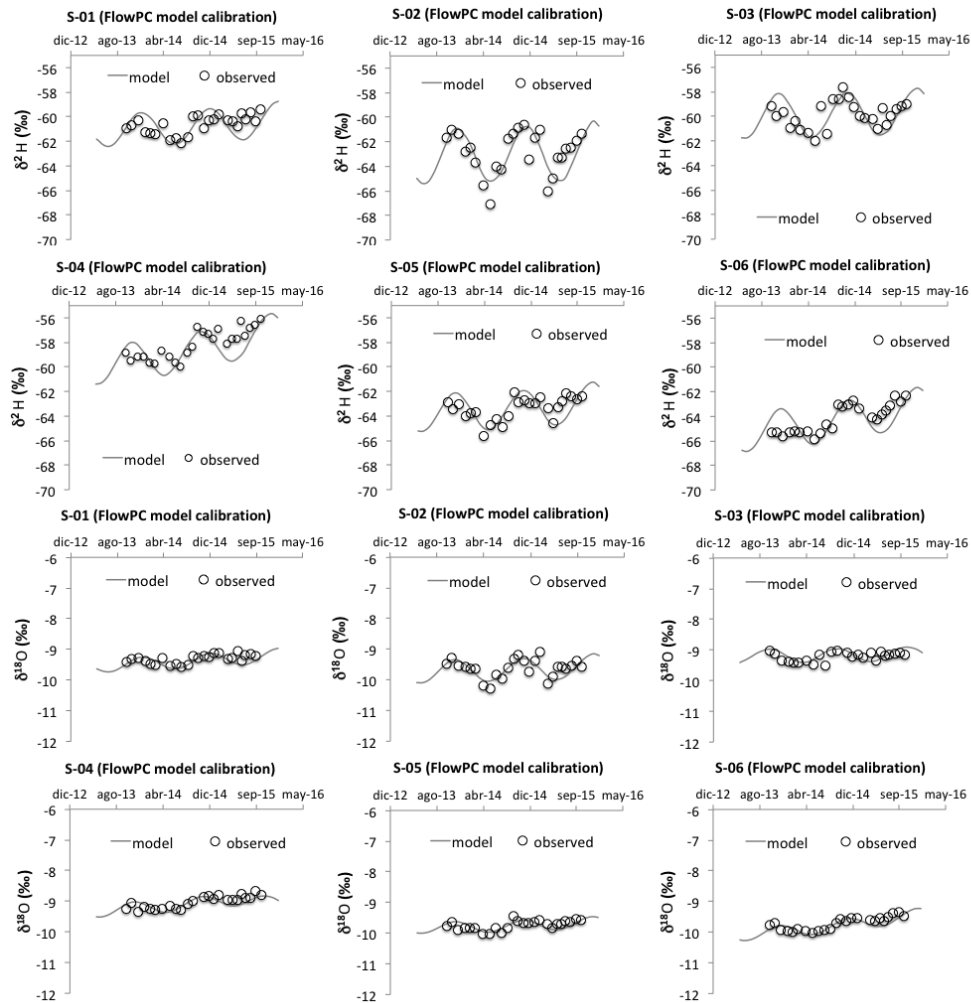
692

693

694 **4.3 Determination of spring discharge mean transit time**

695 To estimate the mean transit time of the spring discharge, the program FlowPC v3.2
696 (Małoszewski and Zuber, 1996) has been used. According to the hydrogeological
697 setting, it is assumed that the EPM flow model can describe the behavior of the aquifers
698 discharging through the springs of PCM. The lumped model parameters (η and τ) have
699 been calibrated (Table 5) by fitting the isotopic contents observed in the spring
700 discharge from December 2013 to December 2015 (Fig. 10). The goodness of fit is
701 defined in terms of RMSE, ranging between 0,02‰ (S-05) and 0,04‰ (S-02) for $\delta^{18}\text{O}$
702 (Table D1, Appendix D), and between 0,17‰ (S-03) and 0,22‰ (S-04) for $\delta^2\text{H}$ (Table
703 D2, Appendix D).

704



705

706 Fig. 10. Measured against simulated isotope content evolution with FlowPC and an EPM model.

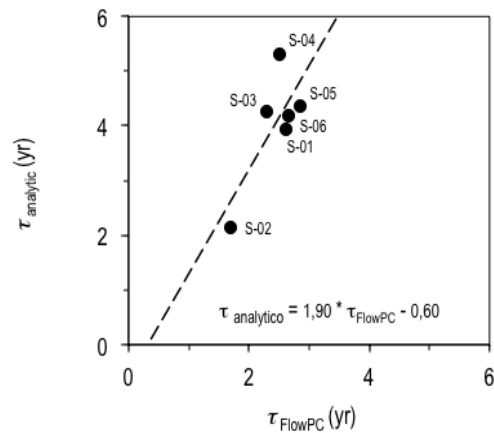
707 The gray line represents the best fit.

708

709 The estimated value of η is very close to 1 regardless of the spring, indicating that the
 710 corresponding aquifers behave as almost an exponential flow model in coherence with
 711 the behavior of a karst aquifer system discharging through a main spring. The estimated
 712 MTT with the applied methodology ranges between 1,69 yr (S-02) and 2,85 yr (S-05),

713 while in the case of the analytical approach MTT ranges between 2,14 yr (S-02) and
714 5,31 yr (S-04).

715



716

717 Fig. 11. Graph showing the MTT values estimated based on the lumped parameter model
718 FlowPC (Maloszewski, 1996) versus the MTT values estimated based on the analytical model
719 [Eq. 8] (Maloszewski et al., 1983)

720

721 The MTT values obtained by this numerical approach are 1,9 times shorter than the
722 MTT values analytically obtained through [Eq. 8] that compares the amplitude of the
723 seasonal isotopic content of recharge with the seasonal isotopic content in the spring
724 discharge [Fig 11]. In the numerical case, the monthly isotopic content in recharge is
725 weighted by the monthly volumetric recharge rate, whereas in the analytical case, the
726 isotopic content weighting coefficients for the monthly recharge are all equal to 1
727 because recharge is assumed constant (i.e., steady state) for the whole period covered by
728 the isotopic content time series. This assumption is worth keeping in mind when using
729 [Eq. 8] for estimating groundwater mean transit times. In other words, if aquifer
730 recharge shows a seasonal pattern, then the numerical approach should be used instead
731 of the analytical approach to estimate MTT. The transit time discrepancies between both

732 approaches may be critical when MTT is used as a vulnerability indicator for karst-
733 fissure aquifers (Malík et al, 2016). The results obtained suggest that the numerical
734 approach based explicitly on considering the recharge series in the LPM model provides
735 a more accurate evaluation of hydraulic dynamics throughout the system. This allows
736 better MTT estimations, similar of what concluded Vitvar et al. (1999) in pre-alpine
737 non-karst aquifers. The MTT values obtained in this work are consistent with the
738 conceptual model of the karst system. The aquifer presents specific zones with rapid
739 recharge through surficial karstic elements (e.g. swallow holes) and slow recharge
740 through meadows and forest.

741

742 In terms of MTT, the results obtained in this study are similar to those obtained in other
743 hydrological karst systems located in mountain zones: (1) In the case of the Ordesa and
744 Monte Perdido karst aquifer system (Central Pyrenees, Spain), which is the highest
745 calcareous massif in Western Europe, Lambán et al. (2015) and Jódar et al. (2016b)
746 estimated MMT for several springs. For each spring the authors fitted a sinusoidal
747 function [Eq. 1] to the measured tracer ($\delta^{18}\text{O}$ and $\delta^2\text{H}$) content time series
748 corresponding to rainfall entering the system as recharge and the spring discharge,
749 obtaining the amplitude of the seasonal variation of both the input and output system
750 tracer function ($A_{\delta_{\text{in}}}$ and $A_{\delta_{\text{out}}}$, respectively; Fig. 4). Besides, the authors assumed a
751 constant recharge rate along the year. This hypothesis allowed obtaining an analytical
752 solution to the convolution integral [Eq. 5] (Jódar et al., 2014) but also applying [Eq. 8]
753 to directly estimate MTT, that ranged between 1,12 and 4,48 yr.

754

755 (2) In the Wimbach high-alpine karst system (Berchtesgaden Alps) Einsiedl et al.
756 (2009) estimated MTT with FlowPC. To this end, they used as tracer input function the

757 time series of ^3H content in rainfall measured in a meteorological station close to the
758 study zone, and as system output the time series of ^3H content in groundwater discharge
759 for different springs and also at the outlet of the hydrological catchment. They obtained
760 MTT ranging between 4 and 5 yr for the considered springs, and 5 yr for the whole
761 hydrologic catchment. For the same catchment, Maloszewski et al. (1992) evaluated the
762 MTT by using monthly recharge time series instead of rainfall time series. The aquifer
763 recharge time series was obtained by applying a seasonal infiltration coefficient to the
764 observed monthly precipitation time series. With this approach they estimated a MTT of
765 4,15 yr. This value is close to that obtained by Einsiedl et al. (2009). Additionally,
766 Garvelmann et al. (2017) expanded the previous studies in the Berchtesgaden Alps for a
767 total of eight springs. For each spring they estimated MTT using two different methods;
768 (A) by numerically solving the convolution integral [Eq. 5], and (B) though [Eq. 8] by
769 previously conducting a sin-wave analysis [Eq. 1] to the input (i.e. rainfall) and output
770 tracer functions. The MTT obtained by both methods did not show large discrepancies
771 for the same spring. In terms of the obtained MTT the sampled springs were be
772 classified in two groups: a first group with relatively short MTTs (0,7 to 1,9 yr) and a
773 second group with longer MTTs (7,3 to 12,5 yr).

774

775 (3) In the Schneealpe massif Rank et al. (1992) used the environmental tracers to study
776 the karstic-fissured-porous aquifer system of Schneealpe, The aquifer system that is
777 drained by two principal springs is the main drinking water resource for Vienna
778 (Austria). It is composed of a fissured-porous aquifer with a high storage capacity that
779 partially feeds a karst aquifer conformed by a high- conductivity drainage channel
780 network. For each aquifer they estimated MTT by calibrating a LPM with a 8 years long
781 time series of environmental tracer data, using ^3H and $\delta^{18}\text{O}$ for the fissured-porous and

782 the karst aquifer, respectively. In the former case MTTs ranged between 2,5 and 4,5 yr,
783 whereas in the karst aquifer the estimated MTT was only 2 months. Maloszewski et al.
784 (2002) recalibrated both LPMs by refining and extending up to 20 years the length of
785 the observed time series of ^3H and $\delta^{18}\text{O}$ measurements. In the case of the fissured-
786 porous aquifer the obtained MTTs ranged between 14 and 26 yr, being significantly
787 larger than those obtained by Rank et al (1992). Nevertheless, in the case of the karst
788 aquifer the obtained MTTs were similar ranging between 1,2 and 1,5 months. The large
789 discrepancy between the MTT associated to the Fissured-Porous and karst aquifer
790 indicates that water enters the aquifer system at the surface and flows through it towards
791 the conductive drainage channels until reaching the springs. Nevertheless, the short
792 MTTs associated to the karst aquifer reveal a direct hydraulic connection between the
793 sinkholes at the surface and the drainage channel network.

794

795 (4) In the Wetterstein Mountains karst aquifer system Lauber and Goldscheider (2014)
796 used both artificial (uranine) and environmental tracers (^{18}O and ^2H) to investigate the
797 hydrological behavior of the system. Despite the low recovery of artificial tracer during
798 the tracer test, the fast tracer arrival observed in all the sampled springs, with peak times
799 between 1,8 and 3,2 days, indicates as in the previous case, the existence of well-
800 developed flow paths through thick (>1000 m) USZ. This result underlines the role that
801 may play the USZ conditioning the hydrologic response of the karst system. The
802 authors estimated the aquifer MTT with FlowPC by using as input tracer content that of
803 precipitation, and assuming a constant (without any seasonality) aquifer recharge rate.
804 The obtained MTT values ranged between 3 and 5 months, being significantly shorter
805 than those MTT presented above for the other karst systems.

806

**Comment [JJ16]: Answer to Reviewer #1– General Comment 3
Answer to Reviewer #3– Q2
Answer to Reviewer #4– Q1**

807 The hydrological system MTT reflects the diversity of aquifer flow paths and
808 groundwater mixing from the recharge zone to the discharge point. Considering that the
809 different aquifers constituting the PCM show an exponential flow model (EM)
810 behavior, and provided that MTT (τ ; Table 5) and the aquifer mean recharge flow rate
811 (Q_R ; Table 6) are known, it is possible to estimate the aquifer storage (i.e., mixing)
812 volume by using [Eq. 7]. In Table 8, the stored dynamic volume ('mobile water volume
813 $-V_m$ '; Małoszewski and Zuber (2002); where: $V_m = Q_R \cdot \tau$) is associated with the
814 catchment areas (Fig. A1 of the Appendix A) discharging through the springs S-01 to S-
815 06. S-05 and S-02 play a major role in terms of both groundwater discharge and aquifer
816 storage. The springs S-05 and S-02 present a similar area and a similar discharge.
817 Nevertheless, from a geometrical point of view, they are different: S-05 is rounded in
818 shape whereas S-02 is elongated. Considering that aquifer recharge is produced mainly
819 in the highest parts of PCM, it is clear that the distance between the recharge and
820 discharge points is larger in the case of S-02. This difference is interesting if one
821 considers that the mean transit time of S-02 is shorter than the mean transit time of S-
822 05. The shorter transit time would indicate a higher development of the karst water
823 conducting features in the catchment area of S-02. The springs S-04 and S-06 denote
824 their perched character with the associated low discharge flow rates and groundwater
825 reserve volumes.

826

827 Table 8. Estimation of dynamic volume V_m stored in the aquifer for the springs analyzed

Spring	V_m (hm ³)
S-01	2,44 + 0,49
S-02	11,54 + 2,61
S-03	1,72 + 0,04

S-04	0,03 + 0,01
S-05	19,39 + 0,20
S-06	0,09 + 0,01

828

829 The few available groundwater level depth data from old water wells in the PCM
830 suggest the karst aquifer presents low regional hydraulic gradients in the phreatic zone
831 ranging between 1 - 2%. Nevertheless, while considering the expected mean phreatic
832 level above the horizontal plane from the spring levels (i.e., the groundwater that
833 contributes to each spring discharge), the 3D geological model evaluates the total
834 aquifer formation volume (V_{aq}) associated with the regional springs S-01, S-02, S-03
835 and S-05. Assuming V_{aq} as known, the mean aquifer interconnected porosity (ϕ) can
836 therefore be estimated as the ratio V_{GW}/V_{aq} . In the PCM, the average ϕ obtained is
837 3,1%. This result agrees with the value obtained for other carbonate aquifers of the
838 Betic Cordillera (Southern Iberian Peninsula) with an average value of 3% (Pulido-
839 Bosch et al., 2004; Martos- Rosillo et al., 2014).

840

841 This work is aimed to characterize the hydrological behavior of a high mountain karst
842 system with a overlaying thick UZS that plays a relevant role along with in the system
843 response. The applied approach allows accounting the effects of the extreme alpine
844 climate conditions on both the aquifer recharge rates and the isotopic composition of
845 recharge. The used approach provides a more reliable assessment of the hydrological
846 behavior of these alpine karst systems than the obtained applying the traditional
847 approaches found in the scarce bibliography. The methodology used in this work for
848 characterizing the hydrological behavior of PCM can be applied in many analogue high
849 mountain karst systems whose hydrologic behavior still remains unknown. In this sense,
850 Table 9 shows a brief summary of the available bibliography at the pan-European zone

851 focused on high-mountain karst aquifers with a thick USZ in which this methodology
 852 could be tested (Fig. 12).

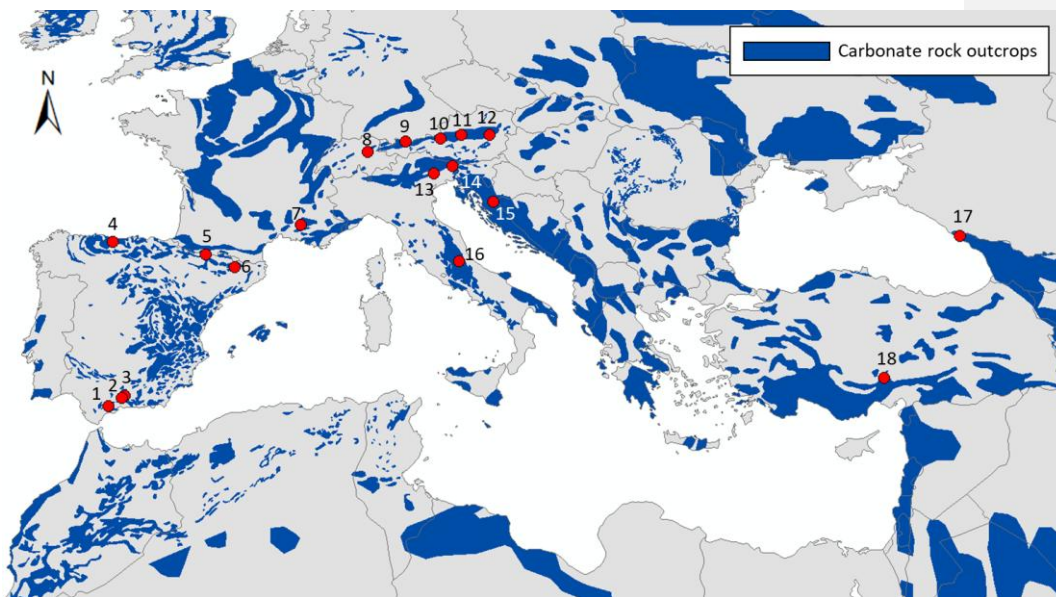
853

854 Table 9. Brief summary of published research studies of groundwater flow karst systems in
 855 mountain areas with thick USZ the pan-European zone.

Code	High mountain karst system	NSZ Thickness	Reference
1	Yunqueira-Sierra de las Nieves	1000	Andreo et al. (2004); Pardo-Iguzquiza et al. (2015)
2	Alta Cadena	700	Mudarra and Andreo (2011)
3	Sierra Gorda	500	Mudarra and Andreo (2015)
4	Picos de Europa	1500	Ballesteros et al. (2015a); Ruiz and Poblete (2012)
5	Ordesa y Monte Perdido	1500	Lambán et al. (2015); Jódar et al. (2016b)
6	Port del Comte	1000	(This research)
7	Fontaine Vaucluse	800	Fleury et al. (2007)
8	Schlichenden Brünnen - Muotathal	1000	Jeannin (2001)
9	Wetterstein Mountains (Zugspitze)	1000	Lauber and Goldscheider (2014)
10	Wimbachtal catchment	1500	Maloszewski et al. (1992)
11	Totes Gebirge	1000	Laimer (2010)
12	Schneecalpe Massif	900	Rank et al 1992; Maloszewski et al. (2002)
13	Cansiglio-Cavallo karst aquifer	800	Filippini et al. (2018)
14	Mount Kanin	2000	Zini et al. (2015); Turk et al. (2015)
15	Gacka	1000	Ozyurt et al. (2014)
16	Gran Sasso aquifer	1500	Falcone et al. (2008); Amuroso et al. (2013)
17	Arabika Massif	2500	Klimchouk (2009)
18	Aladaglar Mountains	2000	Ozyurt and Bayari (2008)

856

857



858

859 Fig. 12. Spatial distribution of carbonate rock outcrops at the pan-Mediterranean zone. Red
860 points indicate the position of those high mountain karst aquifers zones with a thick (<500 m)
861 NSZ referenced in the existing bibliography (map modified from the *World Map of Carbonate*
862 *Rock Outcrops v.3.0*. Source: http://www.fos.auckland.ac.nz/our_research/karst). Numbers in
863 bullets correspond to the codes shown in Table 9.

864

865 4.4 Evaluation of results for groundwater management purposes

866 MTT is a corner stone for groundwater management strategies, and many authors have
867 used this variable as a proxy of vulnerability assessment in hydrogeological systems
868 (Einsiedl et al., (2009) and Malik et al., (2016), among others). This work provides the
869 first estimation of the MTT associated with most important springs discharging the
870 PCM karst system. From the perspective of aquifer vulnerability, the intensive cattle
871 grazing conducted in the PCM is the most threatening activity to the groundwater
872 resources stored in the underlying aquifer so far. The relatively large MTTs (2,25 yr)
873 along with the exponential flow model describing the hydrologic behavior of PCM,

Comment [JJ17]: Answer to Reviewer #3- Q2
Answer to Reviewer #4- Q1

874 points to groundwater mixing as a natural attenuation/dilution process inside the aquifer
875 system. However, it must be taken in mind that the presence of unnoticed but likely
876 well-developed flow paths through the USZ and also the existence of karst conductive
877 features in the saturated zone of the PCM may favor fast contaminant migration from
878 the recharge areas to the groundwater discharge points of this aquifer system, but this is
879 investigation is out of the scope of this work.

880

881 From the perspective of water resources management the storage and dynamic volumes
882 associated with the PCM aquifer system are also valuable information obtained in this
883 study. In this line, it is worth to comment that the PCM aquifer system has an integrated
884 groundwater storage capacity (V_{GW}) of 35,2 hm³, and generates an overall mean annual
885 groundwater discharge of 15,35 hm³/yr, that represents 15% of the mean annual water
886 consumption in the city of Barcelona (Barcelona City Council, 2018). Moreover, the
887 average discharge of S-05, which is one of the main groundwater springs of the PCM
888 represents 7% of the mean annual water consumption of Barcelona city. This discharge
889 tributes to the Llobregat River Basin, which in turns provides critical water resources to
890 the Barcelona metropolitan area. It is important keeping these numbers in mind to
891 estimate the water resources availability given the increased frequency and severity of
892 the Mediterranean droughts reported by the experts (Hoerling et al., 2012; Vicente-
893 Serrano et al., 2014).

894

895 In the Pyrenean range, climate models forecast a precipitation decrease up to 14% with
896 respect to the observed mean precipitation and a temperature increase between 2 and 4
897 °C that will reduce the amount of solid precipitation and the corresponding snowmelt
898 runoff (López-Moreno et al., 2008, 2009). In addition, the duration of the snowpack will

899 be shorter, shifting the timing of the snowmelt (Adam et al., 2009). The PCM is in the
900 pre-Pyrenean zone to the South of the Pyrenean axial zone. Here, the elevation of the
901 mountains is lower, and the climate conditions are not so severe, accelerating the impact
902 of the forecast temperature increase on snow precipitation, snowmelt runoff generation
903 and the dynamics of the hydrological systems located in this area. Therefore, the
904 geographical and hydrogeological settings of the PCM, along with the groundwater
905 transit times calculated, make the PCM aquifer system an exceptional observatory for
906 anticipating and studying the climate change impact on southern Europe. In this line, it
907 would be extremely important to maintain the observation research program to fully
908 understand the hydrogeological behavior of this aquifer system.

Comment [JJ18]: Answer to Reviewer #23– Q17

910 **4.5 Future works in PCM**

911 This study is the first stage in the full hydrogeological characterization of this aquifer
912 system. The next step is to conduct the hydrogeochemical characterization of recharge
913 and groundwater springs discharge to complement the results obtained in this work by
914 focusing in relevant unsolved questions like (1) the role play by the epikarst zone in the
915 total transit time of groundwater and how this role is reflected in the hydrogeochemical
916 evolution of the springs discharge after important rainfall events and during low-flows
917 and (2) the use of artificial tracers and environmental isotopes (e.g. ^{34}S , ^{15}N) to
918 characterize not only the mean transit time (i.e. the first moment of the transit-time
919 distribution) but also to profile the groundwater transit-time distribution in terms of fast,
920 intermediate and slow groundwater flows. This investigation is crucial to evaluate the
921 aquifer vulnerability.

Comment [JJ19]: Answer to Reviewer #1– General Comment 2

922 **5. Conclusions**

923 A distributed rainfall-runoff model and a lumped-parameter model have been combined
924 to estimate MTT in high-mountain karst systems with an overlying thick unsaturated
925 zone by using the stable isotopes of precipitation as environmental tracers. The
926 presented approach accounts for the effects of the alpine climate conditions on both the
927 aquifer recharge rates and the isotopic composition of recharge. The used approach
928 provides a more reliable assessment of mean transit time compared to traditional
929 methods for such alpine karst systems.

930

931 The approach presented in this work has been used to characterize the hydrological
932 behavior of the Port del Comte Massif, a high mountain karst aquifer with a 1000 m
933 thick unsaturated zone located in the southeastern part of the Pyrenees. The percentage
934 of precipitation that enters into the hydrogeological system as aquifer recharge reaches
935 61,9% (the highest studied spring in the area). This elevated infiltration capacity is
936 controlled by the presence of karren fields and sinkholes at the highest parts of Port del
937 Comte Massif, at elevations between 2050 and 2300 m a.s.l. The evolution of the
938 isotopic content in the sampled springs shows a sinusoidal pattern that reflects the
939 seasonal variation of the isotopic composition of recharge. This is consistent with the
940 relatively short groundwater transit times (2,25 yr) obtained for the hydrological system,
941 which is in agreement with its karstic nature of the aquifer system, and emphasizes the
942 high vulnerability of the aquifer system to variations in recharge.

943

944 The mean annual groundwater discharge and the mean water storage of the Port del
945 Comte Massif hydrogeological system represent 16 and 34% of the mean annual water
946 consumption in the city of Barcelona, underlying the important role as a strategic water

947 resource that the Port del Comte Massif may play for stakeholders and water resources
948 managers when facing the drought episodes that the Mediterranean region iteratively
949 suffers. Moreover, given the geographical position of the study zone, located to the
950 south of the Pyrenean axial zone, and the hydrogeological settings of the associated
951 karst aquifer system, the Port del Comte Massif is an exceptional watchtower for
952 anticipating the impact of climate change in Southern Europe.

Comment [JJ20]: Answer to Reviewer
#12- Q5

953

954

955 **6. Acknowledgments**

956 This research was supported by Agencia Estatal de Investigación (AEI) from the
957 Spanish Government and the European Regional Development Fund (FEDER) from
958 EU, REMEDIATION (CGL2014-57215-C4-1-R), and PACE-ISOTEC (CGL2017-
959 87216-C4-1-R) projects, the PIRAGUA project (EFA210/16/ PIRAGUA) which is
960 funded by the European Union through the Interreg-POCTEFA territorial cooperation
961 program, the Catalan Government projects to support consolidated research groups
962 MAG (Mineralogia Aplicada, Geoquímica i Geomicrobiologia, 2017SGR-1733) from
963 Universitat de Barcelona (UB) and GREM (Grup de Recerca de Minería Sostenible)
964 from the Universitat Politècnica de Catalunya (UPC), and the Junta de Andalucía
965 research group RNM-308 (Hydrogeology Group). We also thank the Institut Cartogràfic
966 i Geològic de Catalunya (Hydrogeology and Geothermics Team) and CCiT from the
967 Universitat de Barcelona (UB) for their technical assistance, and especially Raul Carrey
968 from the MAiMA group for the help in the laboratory analyses. The Meteorological
969 Service of Catalonia (SMC) has kindly provided the meteorological data. The
970 constructive comments and interesting suggestions from four anonymous reviewers are
971 greatly appreciated since they have led to a substantial improvement of the final article

972

973 **7. References**

974 Adam, J.C., Hamlet, A.F., & Lettenmaier, D.P., 2009. Implications of global climate
975 change for snowmelt hydrology in the twenty-first century. *Hydrological*
976 *Processes: An International Journal*, 23(7), 962-972.
977 <https://doi.org/10.1002/hyp.7201>

978 Agencia Estatal de Meteorología de España (AEMET) and Instituto de Meteorologia –
979 Portugal (IMA). 2011. Iberian climate atlas. Air temperature and precipitation
980 (1971-2000).

981 [https://www.aemet.es/documentos/es/conocermas/publicaciones/Atlas-](https://www.aemet.es/documentos/es/conocermas/publicaciones/Atlas-climatologico/Atlas.pdf)
982 [climatologico/Atlas.pdf](https://www.aemet.es/documentos/es/conocermas/publicaciones/Atlas-climatologico/Atlas.pdf)

983 Allocca, V., De Vita, P., Manna, F., Nimmo, J.R. 2015. Groundwater recharge
984 assessment at local and episodic scale in a soil mantled perched karst aquifer in
985 southern Italy. *Journal of Hydrology*, 529 (2015) 843–853.
986 <https://doi.org/10.1016/j.jhydrol.2015.08.032>

987 Amin I.E., Campana, M.E. 1996. A general lumped parameter model for the
988 interpretation of tracer data and transit time calculation in hydrologic systems. *J*
989 *Hydrol*; 179 (1–4):1–21 [https://doi.org/10.1016/0022-1694\(95\)02880-3](https://doi.org/10.1016/0022-1694(95)02880-3)

990 Andreo, B., Linan, C., Carrasco, F., De Cisneros, C. J., Caballero, F., Mudry, J. 2004.
991 Influence of rainfall quantity on the isotopic composition (^{18}O and 2H) of water
992 in mountainous areas. Application for groundwater research in the Yunquera-
993 Nieves karst aquifers (S Spain). *Applied Geochemistry*, 19(4), 561-574.
994 <https://doi.org/10.1016/j.apgeochem.2003.08.002>

995 Araguás-Araguás, L.J., Díaz-Teijeiro, M.F. 2005. Isotope composition of precipitation
996 and water vapour in the Iberian Peninsula. In “Isotopic Composition of

997 Precipitation in the Mediterranean Basin in Relation to Air Circulation Patterns
998 and Climate” (pp. 173-190). IAEA-TECDOC-1453.

999 Aravena, R., Peña, H., Grilli, A., Suzuki, O., Mordeckai, M., 1989. Evolución isotópica
1000 de las lluvias y origen de las masas de aire en el altiplano chileno. *Isotope*
1001 hydrology investigations in Latin America. IAEA-TECDOC-502. IAEA, Vienna,
1002 pp. 129–142.

1003 Bakalowicz, M. (2005). Karst groundwater: a challenge for new resources.
1004 *Hydrogeology Journal*, 13(1), 148-160. [https://doi.org/10.1007/s10040-004-0402-](https://doi.org/10.1007/s10040-004-0402-9)
1005 9

1006 Ballesteros, D., Jiménez-Sánchez, M., Giralt, S., García-Sansegundo, J., Meléndez-
1007 Asensio, M. 2015a. A multi-method approach for speleogenetic research on alpine
1008 karst caves. Torca La Texa shaft, Picos de Europa (Spain). *Geomorphology*, 247,
1009 35-54.

1010 Ballesteros, D., Arnauld Malard., A., Pierre-Yves Jeannin, P-Y., Jimenez-Sanchez M.,
1011 García-Sansegundo, J., Meléndez-Asensio, M., Sendra, G. 2015b. KARSYS
1012 hydrogeological 3D modeling of alpine karst aquifers developed in geologically
1013 complex areas: Picos de Europa National Park (Spain). *Environ Earth Sci.*
1014 Volume 74, Issue 12, pp 7699–7714. <https://doi.org/10.1007/s12665-015-4712-0>

1015 Barberá, J.A., Jódar, J., Custodio, E., González-Ramón, A., Jiménez-Gavilán, Vadillo,
1016 I., Pedrera, A., Martos-Rosillo, S., 2018a. Groundwater dynamics in a
1017 hydrologically-modified alpine watershed from an ancient managed recharge
1018 system (Sierra Nevada National Park, Southern Spain): insights from
1019 hydrogeochemical and isotopic information. *Science of the Total Environment*
1020 640–641, 874–893, <https://doi.org/10.1016/j.scitotenv.2018.05.305>

1021 Barberá, J. A., Mudarra, M., Andreo, B., De la Torre, B., 2018b. Regional-scale
1022 analysis of karst underground flow deduced from tracing experiments: examples
1023 from carbonate aquifers in Màlaga province, southern Spain. *Hydrogeology*
1024 *Journal*, 26(1), 23-40. <https://dx.doi.org/10.1007/s10040-017-1638-5>

1025 Barcelona City Council, 2018. Evolution of water consumption in the city of Barcelona.
1026 <http://www.bcn.cat/estadistica/angles/dades/economia/consum/evoconsum/coev04>
1027 [.htm](#) (last access 08/07/2018).

1028 Barnett, T.P., Adam, J.C., Lettenmaier, D.P., 2005. Potential impacts of a warming
1029 climate on water availability in snow-dominated regions. *Nature*, 438(7066),
1030 <https://dx.doi.org/10.1038/nature04141>

1031 Bergström, S., 1976. Development and Application of a Conceptual Runoff Model For
1032 Scandinavian Catchments, SMHI, Report No. RHO 7 (134 pp Norrköping).

1033 Braun, L.N., Renner, C.B., 1992. Application of a conceptual runoff model in different
1034 physiographic regions of Switzerland. *Hydrological Sciences Journal*, 37(3), 217-
1035 231. <https://doi.org/10.1080/02626669209492583>.

1036 Butscher C, Huguenberger P., 2007. Implications for karst hydrology from 3D
1037 geological modeling using the aquifer base gradient approach. *J Hydrol*; 342 (1–
1038 2):184–98. <https://doi.org/10.1016/j.jhydrol.2007.05.025>

1039 Celle-Jeanton,H., Travi, Y., Blavoux, B., 2001. Isotopic typology of the precipitation in
1040 the Western Mediterranean region at three different time scales. *Geophysical*
1041 *Research Letters*, Vol. 28, no. 7, pages 1215-1218

1042 Cervi, F., Marcaccio, M., Petronici, F., Borgatti, L., 2014. Hydrogeological
1043 characterization of peculiar Apenninic springs. *Proceedings of the International*
1044 *Association of Hydrological Sciences*, 364, 333-338.

1045 Chen, Z., 2017. Modeling a geologically complex karst aquifer system, Hochifen-
1046 Gottesacker, Alps. PhD. Thesis. Karlsruher Instituts für Technologie, Germany.
1047 <https://d-nb.info/1136660852/34>

1048 Chueca, J., Julián, A., López-Moreno, J.I., 2007. Recent evolution (1981–2005) of the
1049 Maladeta glaciers, Pyrenees, Spain: extent and volume losses and their relation
1050 with climatic and topographic factors. *Journal of glaciology*, 53(183), 547-557.
1051 <https://doi.org/10.3189/002214307784409342>

1052 Clark, I.D., Fritz, P. 1997. *Environmental isotopes in hydrogeology*. Lewis Publishers,
1053 New York.

1054 Coplen 2011. Guidelines and recommended terms for expression of stable-isotope-ratio
1055 and gas-ratio measurement results. *Rapid Commun. Mass Spectrom.* 2011, 25,
1056 2538–2560.

1057 CREAM, 2009. Land Cover Map of Catalonia (MCSC) 1:250,000. 4a edition (2009).
1058 <http://www.creaf.uab.es/mcsc/usa/index.htm>

1059 Custodio, E., Llamas, M.R. (Eds.), 1976. *Hidrología subterránea [Groundwater
1060 hydrology]*. 2 Vols: 1–2350. Ediciones Omega, Barcelona.

1061 Custodio, E., Jódar, J., 2016. Simple solutions for steady–state diffuse recharge
1062 evaluation in sloping homogeneous unconfined aquifers by means of atmospheric
1063 tracers. *J. Hydrol.* <http://dx.doi.org/10.1016/j.jhydrol.2016.06.035>

1064 De Jong, C., Lawler, D., Essery, R., 2009. Mountain hydroclimatology and snow
1065 seasonality and hydrological change in mountain environments. *Hydrological
1066 Processes* 23, 955–961. <https://doi.org/10.1002/hyp.7193>

1067 De Walle, D.R., Edwards, P.J., Swistock, B.R., Aravena, R., Drimmie, R.J., 1997.
1068 Seasonal isotope hydrology of three Appalachian forest catchments. *Hydrological*

1069 Processes, 11(15), 1895-1906. [https://doi.org/10.1002/\(SICI\)1099-](https://doi.org/10.1002/(SICI)1099-)
1070 1085(199712)11:15<1895::AID-HYP538>3.0.CO;2-#

1071 Einsiedl, F., 2005. Flow system dynamics and water storage of a fissured-porous karst
1072 aquifer characterized by artificial and environmental tracers. *J Hydrol* 312:312–
1073 321. <https://doi.org/10.1016/j.jhydrol.2005.03.031>

1074 Einsiedl, F., Maloszewski, P., Stichler, W., 2009. Multiple isotope approach to the
1075 determination of the natural attenuation potential of a high-alpine karst system.
1076 *Journal of Hydrology* 365 (2009) 113–121.
1077 <https://doi.org/10.1016/j.jhydrol.2008.11.042>

1078 Epting, J., M. Page, R., Auckenthaler, A., Huggenberger, P. 2018. Process-based
1079 monitoring and modeling of Karst springs – Linking intrinsic to specific
1080 vulnerability. *Sci. Total Environ.* 625, 403-415-
1081 <https://doi.org/10.1016/j.scitotenv.2017.12.272>

1082 Falcone, R.A., Falgiani, A., Parris, B., Petitta, M., Spizzico, M., Tallini, M. 2008.
1083 Chemical and isotopic ($\delta^{18}\text{O}\%$, $\delta^2\text{H}\%$, $\delta^{13}\text{C}\%$, ^{222}Rn) multi-tracing for
1084 groundwater conceptual model of carbonate aquifer (Gran Sasso INFN
1085 underground laboratory–central Italy). *Journal of hydrology*, 357(3-4), 368-388.

1086 Farlin, J., Maloszewski, P., 2013. On the use of spring baseflow recession for a more
1087 accurate parameterization of aquifer transit time distribution functions. *Hydrology*
1088 *and Earth System Sciences*, 17(5), 1825-1831. <https://doi.org/10.5194/hess-17->
1089 1825-2013

1090 Fiorella, R.P., Poulsen, C.J., Pillco Zolá, R.S., Barnes, J.B., Tabor, C.R., Ehlers, T.A.,
1091 2015. Spatiotemporal variability of modern precipitation $\delta^{18}\text{O}$ in the central Andes
1092 and implications for paleoclimate and paleoaltimetry estimates. *Journal of*

1093 Geophysical Research: Atmospheres, 120(10), 4630-4656.
1094 <https://dx.doi.org/10.1002/2014JD022893>

1095 Fleury, P., Plagnes, V., Bakalowicz, M. 2007. Modelling of the functioning of karst
1096 aquifers with a reservoir model: Application to Fontaine de Vaucluse (South of
1097 France). Journal of Hydrology 345, 38– 49.
1098 <https://doi.org/10.1016/j.jhydrol.2007.07.014>

1099 Filippini, M., Squarzone, G., De Waele, J., Fiorucci, A., Vigna, B., Grillo, B., Riva, A.,
1100 Rossetti, S., Zini, L., Casagrande, G., Stumpp, C., Gargini, A. 2018.
1101 Differentiated spring behavior under changing hydrological conditions in an
1102 alpine karst aquifer. Journal of Hydrology, 556, 572-584.
1103 <https://doi.org/10.1016/j.jhydrol.2017.11.040>

1104 Freixes, A., 2014. Els aqüífers càrstics dels Pirineus de Catalunya. Interès estratègic i
1105 sostenibilitat [The karstic aquifers of the Catalanian Pyrenees. Strategic interest
1106 and sustainability]. PhD. Thesis. Universitat de Barcelona.
1107 <http://hdl.handle.net/2445/65187>

1108 Froehlich, K., Gibson, J.J., Aggarwal, P., 2001. Deuterium excess in precipitation and
1109 its climatological significance. In Study of environmental change using isotope
1110 techniques (Vol. 13, pp. 54-66). IAEA.

1111 Froehlich, K., Kralik, M., Papesch, W., Rank, D., Scheifinger, H., Stichler, W., 2008.
1112 Deuterium excess in precipitation of Alpine regions—moisture recycling. Isotopes
1113 in Environmental and Health Studies, 44(1), 61-70.
1114 <https://doi.org/10.1080/10256010801887208>

1115 García-Ruiz, J.M., López-Moreno, J.I., Vicente-Serrano, S.M., Lasanta-Martínez, T.,
1116 Beguería, S., 2011. Mediterranean water resources in a global change scenario.

1117 Earth-Science Reviews, 105(3-4), 121-139.
1118 <https://doi.org/10.1016/j.earscirev.2011.01.006>

1119 Garvelmann, J., Warscher, M., Leonhardt, G., Franz, H., Lotz, A., Kunstman, H. 2017.
1120 Quantification and characterization of the dynamics of spring and stream water
1121 systems in the Berchtesgaden Alps with a long-term stable isotope dataset.
1122 *Environ Earth Sci* 76:766 <https://doi.org/10.1007/s12665-017-7107-6>

1123 Giorgi, F., Lionello, P., 2008. Climate change projections for the Mediterranean region.
1124 *Global and planetary change*, 63(2-3), 90-104.
1125 <https://doi.org/10.1016/j.gloplacha.2007.09.005>

1126 Gladich, I., Gallai, I., Giaiotti, D. B., & Stel, F. 2011. On the diurnal cycle of deep
1127 moist convection in the southern side of the Alps analysed through cloud-to-
1128 ground lightning activity. *Atmospheric Research*, 100(4), 371-376.
1129 <https://doi.org/10.1016/j.atmosres.2010.08.026>

1130 Goldscheider, N., 2005. Fold structure and underground drainage pattern in the alpine
1131 karst system Hochifien-Gottesacker. *Eclogae Geologicae Helvetiae*, 98(1), 1-17.
1132 <https://doi.org/10.1007/s00015-005-1143-z>

1133 Goldscheider N, Drew D (eds) (2007) *Methods in Karst Hydrogeology*. International
1134 Contributions to Hydrogeology 26, International Association of Hydrogeologists,
1135 Taylor & Francis, London, 264 pp. ISBN 978-0-415-42873-6

1136 Goldscheider, N., Meiman, J., Pronk, M., Smart, C., 2008. Tracer tests in karst
1137 hydrogeology and speleology. *International Journal of Speleology*, 37(1), 3.
1138 <http://dx.doi.org/10.5038/1827-806X.37.1.3>

1139 Goldscheider, N., 2011. Alpine Hydrogeologie [Alpine hydrogeology]. *Grundwasser*
1140 16:1–1. <https://doi.org/10.1007/s00767-010-0157-2>

1141 Gonfiantini, R., Roche, M.A., Olivry, J.C., Fontes, J.C., Zuppi, G.M., 2001. The altitude
1142 effect on the isotopic composition of tropical rains. *Chemical Geology*, 181(1-4),
1143 147-167. [https://doi.org/10.1016/S0009-2541\(01\)00279-0](https://doi.org/10.1016/S0009-2541(01)00279-0)

1144 Gremaud, V., Goldscheider, N., Savoy, L., Favre, G., Masson, H., 2009. Geological
1145 structure, recharge processes and underground drainage of a glacierised karst
1146 aquifer system, Tsanfleuron-Sanetsch, Swiss Alps. *Hydrogeol. J.* 17, 1833–1848.
1147 <https://doi.org/10.1007/s10040-009-0485-4>

1148 Grunewald, K., Scheithauer, J., 2010. Europe's southernmost glaciers: response and
1149 adaptation to climate change. *Journal of glaciology*, 56(195), 129-142.
1150 <https://doi.org/10.3189/002214310791190947>

1151 Hernández-Mora, N., del Moral Ituarte, L., La-Roca, F., La Calle, A., Schmidt, G.,
1152 2014. Interbasin water transfers in Spain: Interregional conflicts and governance
1153 responses. In *Globalized Water* (pp. 175-194). Springer, Dordrecht. ISBN 978-94-
1154 007-7322-6. https://doi.org/10.1007/978-94-007-7323-3_13

1155 Hargreaves, G.H. and Samani, Z.A. 1982. Estimating potential evapotranspiration.
1156 *Journal of Irrigation and Drainage Engineering*, 108, 223-230

1157 Hoerling, M., Eischeid, J., Perlwitz, J., Quan, X., Zhang, T., Pegion, P., 2012. On the
1158 increased frequency of Mediterranean drought. *Journal of Climate*, 25(6), 2146-
1159 2161. <https://doi.org/10.1175/JCLI-D-11-00296.1>

1160 Holko, L., Dóša, M., Michalko, J., Šanda, M. 2012. Isotopes of oxygen-18 and
1161 deuterium in precipitation in Slovakia. *Journal of Hydrology and*
1162 *Hydromechanics*, 60(4), 265-276. <https://doi.org/10.2478/v10098-012-0023-2>

1163 Hood, J.L., Hayashi, M., 2010. Assessing the application of a laser rangefinder for
1164 determining snow depth in inaccessible alpine terrain. *Hydrology and Earth*
1165 *System Sciences*, 14(6), 901. <http://dx.doi.org/10.5194/hess-14-901-2010>

1166 Hottelet, Ch., Braun, L.N., Leibundgut, Ch., Rieg, A., 1993. Simulation of Snowpack
1167 and Discharge in an Alpine Karst Basin. IAHS Publication No. 218, pp. 249–260

1168 ICGC, 2007. Mapa geològic comarcal de Catalunya 1:50 000. Full Alt Urgell
1169 (BDGC50M). [http://www.icgc.cat/ca/Administracio-i-
1170 empresa/Descarregues/Cartografia-geologica-i-geotematica/Cartografia-
1171 geologica/Mapa-geologic-comarcal-de-Catalunya-1-50.000/Mapa-geologic-
1172 comarcal-de-Catalunya-1-50.000](http://www.icgc.cat/ca/Administracio-i-empresa/Descarregues/Cartografia-geologica-i-geotematica/Cartografia-geologica/Mapa-geologic-comarcal-de-Catalunya-1-50.000/Mapa-geologic-comarcal-de-Catalunya-1-50.000)

1173 Jeelani, G., Shah, R.A., Deshpande, R.D., Fryar, A.E., Perrin, J., Mukherjee, A., 2017.
1174 Distinguishing and estimating recharge to karst springs in snow and glacier
1175 dominated mountainous basins of the western Himalaya, India. Journal of
1176 hydrology, 550, 239-252. <https://doi.org/10.1016/j.jhydrol.2017.05.001>

1177 Jeannin, P-Y. 2001. Modeling flow in phreatic and epiphreatic karst conduits in the
1178 Hölloch cave (Muotatal, Switzerland). Water Resources Research. Vol. 37, No. 2,
1179 pp 191-200. <https://doi.org/10.1029/2000WR900257>

1180 Jiménez-Martínez, J. y Custodio, E., 2008. El exceso de deuterio en la lluvia y en la
1181 recarga a los acuíferos en el área circum-mediterránea y en la costa mediterránea
1182 española. Boletín Geológico y Minero, 119 (1): 21-32.

1183 Jódar, J., Lambán, L.J., Medina, A., Custodio, E., 2014. Exact analytical solution of the
1184 convolution integral for classical hydrogeological lumped-parameter models and
1185 typical input tracer functions in natural gradient systems. J. Hydrol. 519, 3275–
1186 3289. <http://dx.doi.org/10.1016/j.jhydrol.2014.10.027>.

1187 Jódar, J., Custodio, E., Liotta, M., Lambán, L.J., Herrera, C., Martos-Rosillo, S.,
1188 Sapriza, G., Rigo, T., 2016a. Correlation of the seasonal isotopic amplitude of
1189 precipitation with annual evaporation and altitude in alpine regions. Sci. Total
1190 Environ., 550: 27-37. <https://dx.doi.org/10.1016/j.scitotenv.2015.12.034>

1191 Jódar, J., Custodio, E., Lambán, L.J., Martos-Rosillo, S., Herrera-Lameli, C., Sapriza-
1192 Azuri, G., 2016b. Vertical variation in the amplitude of the seasonal isotopic
1193 content of rainfall as a tool to jointly estimate the groundwater recharge zone and
1194 transit times in the Ordesa and Monte Perdido National Park aquifer system,
1195 north-eastern Spain. *Sci. Total Environ.* 573, 505–517.
1196 <https://dx.doi.org/10.1016/j.scitotenv.2016.08.117>

1197 Jódar, J., Cabrera, J.A., Martos-Rosillo, S., Ruiz-Constan, A., Gonzalez-Ramón, A.,
1198 Lambán, L.J., Herrera, C., Custodio, E., 2017. Groundwater discharge in high-
1199 mountain watersheds: a valuable resource for downstream semi-arid zones. The
1200 case of the Bérchules River in Sierra Nevada (Southern Spain). *Science of The*
1201 *Total Environment*, <https://doi.org/10.1016/j.scitotenv.2017.03.190>

1202 Jódar, J., Carpintero, E., Martos-Rosillo, S., Ruiz-Constán, A., Marín-Lechado, C.,
1203 Cabrera-Arrabal, J.A., Navarrete-Mazariego, E., González-Ramón, A., Lambán,
1204 L.J., Herrera, C., González-Dugo, M.P. 2018. Combination of lumped
1205 hydrological and remote-sensing models to evaluate water resources in a semi-
1206 arid high altitude ungauged watershed of Sierra Nevada (Southern Spain). *Sci.*
1207 *Total Environ.*, 625: 285-300. [https://doi-](https://doi-org.recursos.biblioteca.upc.edu/10.1016/j.scitotenv.2017.12.300)
1208 [org.recursos.biblioteca.upc.edu/10.1016/j.scitotenv.2017.12.300](https://doi-org.recursos.biblioteca.upc.edu/10.1016/j.scitotenv.2017.12.300)

1209 Katsuyama, M., Tani, M., Nishimoto, S., 2010. Connection between streamwater mean
1210 residence time and bedrock groundwater recharge/discharge dynamics in
1211 weathered granite catchments. *Hydrological Processes*, 24(16), 2287-2299.
1212 <https://doi.org/10.1002/hyp.7741>

1213 Kazakis, N., Chalikakis, K., Mazzilli, M., Ollivier, C., Manakos, A., Voudouris, K.,
1214 2018. Management and research strategies of karst aquifers in Greece: Literature
1215 overview and exemplification based on hydrodynamic modelling and

1216 vulnerability assessment of a strategic karst aquifer. *Sci. Total Environ.*, 643:
1217 592–609. <https://doi.org/10.1016/j.scitotenv.2018.06.184>

1218 Klimchouk, A. Samokhin, G.V., Kasian, Y.M. 2009. The deepest cave in the world in
1219 the arabika massif (western caucasus) and its hydrogeological and
1220 paleogeographic significance. 2009 ICS Proceedings. 15th International Congress
1221 of Speleology

1222 Konz, M., Seibert, J., 2010. On the value of glacier mass balances for hydrological
1223 model calibration. *Journal of hydrology*, 385(1-4), 238-246.
1224 <https://doi.org/10.1016/j.jhydrol.2010.02.025>

1225 Kurylyk, B.L., Hayashi, M., 2017. Inferring hydraulic properties of alpine aquifers from
1226 the propagation of diurnal snowmelt signals. *Water Resources Research*.
1227 <https://doi.org/10.1002/2016WR019651>

1228 Laimer, H.J. 2010. Neue Ergebnisse zur Karsthydrogeologie des westlichen Toten
1229 Gebirges (Österreich). (New karst hydrogeological research in the western Totes
1230 Gebirge, Austria). *Grundwasser*. Volume 15, Issue 2, pp 113–122

1231 Lambán, L.J., Jódar, J., Custodio, E., Soler, A., Sapriza, G. and Soto, R., 2015. Isotopic
1232 and hydrogeochemical characterization of high-altitude karst aquifers in complex
1233 geological settings. The Ordesa and Monte Perdido National Park (Northern
1234 Spain) case study. *Sci. Total Environ.*, 506–507: pp 466–479,
1235 <https://doi.org/10.1016/j.scitotenv.2014.11.030>

1236 Lauber, U., Kotyla, P., Morche, D., Goldscheider, N., 2014. Hydrogeology of an Alpine
1237 rockfall aquifer system and its role in flood attenuation and maintaining baseflow.
1238 *Hydrology and Earth System Sciences*, 18(11), 4437.
1239 <http://dx.doi.org/10.5194/hess-18-4437-2014>

1240 Lauber, U., Goldscheider, N., 2014. Use of artificial and natural tracers to assess
1241 groundwater transit-time distribution and flow systems in a high-alpine karst
1242 system (Wetterstein Mountains, Germany). *Hydrogeology Journal*, 22(8), 1807-
1243 1824. <http://dx.doi.org/10.1007/s10040-014-1173-6>

1244 Liu, Z., Tian, L., Yao, T., & Yu, W. 2008. Seasonal deuterium excess in Nagqu
1245 precipitation: influence of moisture transport and recycling in the middle of
1246 Tibetan Plateau. *Environmental Geology*, 55(7), 1501-1506.
1247 <http://dx.doi.org/10.1007/s00254-007-1100-4>

1248 López-Moreno, J.I., García-Ruiz, J.M., 2004. Influence of snow accumulation and
1249 snowmelt on streamflow in the central Spanish Pyrenees/Influence de
1250 l'accumulation et de la fonte de la neige sur les écoulements dans les Pyrénées
1251 centrales espagnoles. *Hydrological Sciences Journal*, 49(5).
1252 <https://doi.org/10.1623/hysj.49.5.787.55135>

1253 López-Moreno, J. I., Goyette, S., Beniston, M., 2008. Climate change prediction over
1254 complex areas: spatial variability of uncertainties and predictions over the
1255 Pyrenees from a set of regional climate models. *International Journal of*
1256 *Climatology*, 28(11), 1535-1550. <https://doi.org/10.1002/joc.1645>

1257 López-Moreno, J.I., Revuelto, J., Rico, I., Chueca-Cía, J., Julián, A., Serreta, A.,
1258 Serrano, E., Vicente-Serrano, S.M., Azorin-Molina, C., Alonso-González, E.,
1259 García-Ruiz, J.M., 2016. Thinning of the Monte Perdido Glacier in the Spanish
1260 Pyrenees since 1981. *The Cryosphere*, 10(2), 681-694. [https://doi.org/10.5194/tc-](https://doi.org/10.5194/tc-10-681-2016)
1261 [10-681-2016](https://doi.org/10.5194/tc-10-681-2016)

1262 Mądrala, M., Wąsik, M., Małoszewski, P., 2017. Interpretation of environmental tracer
1263 data for conceptual understanding of groundwater flow: an application for
1264 fractured aquifer systems in the Kłodzko Basin, Sudetes, Poland. *Isotopes in*

1265 environmental and health studies, 53(5), 466-483.
1266 <https://dx.doi.org/10.1080/10256016.2017.1330268>

1267 Malard, A., Jeannin, P.Y., Vouillamoz, J. et al 2015. An integrated approach for
1268 catchment delineation and conduit-network modeling in karst aquifers: application
1269 to a site in the Swiss tabular Jura. *Hydrogeol J* 23: 1 1341–1357.
1270 <https://doi.org/10.1007/s10040-015-1287-5>

1271 Malard, A., Sinreich, M., Jeannin, P.Y., 2016. A novel approach for estimating karst
1272 groundwater recharge in mountainous regions and its application in Switzerland.
1273 *Hydrological Processes*, 30(13), 2153-2166. <https://doi.org/10.1002/hyp.10765>

1274 Malík, P., Svasta, J., Michalko, J., Gregor, M., 2016. Indicative mean transit time
1275 estimation from $\delta^{18}\text{O}$ values as groundwater vulnerability indicator in karst-
1276 fissure aquifers. *Environmental Earth Sciences*. 75. [10.1007/s12665-016-5791-2](https://doi.org/10.1007/s12665-016-5791-2).

1277 Małoszewski, P., Rauert, W., Stichler, W., Herrmann, A., 1983. Application of flow
1278 models in an alpine catchment area using tritium and deuterium data. *Journal of*
1279 *Hydrology*, 66: 319–330. [http://dx.doi.org/10.1016/0022-1694\(83\)90193-2](http://dx.doi.org/10.1016/0022-1694(83)90193-2)

1280 Małoszewski, P., Rauert, W., trimborn, P., Herrmann, A., Rau, R. 1992. Isotope
1281 hydrological study of mean transit times in an alpine basin (Wimbachtal,
1282 Germany). *Journal of Hydrology*, 140: 343-360. [https://doi.org/10.1016/0022-](https://doi.org/10.1016/0022-1694(92)90247-S)
1283 [1694\(92\)90247-S](https://doi.org/10.1016/0022-1694(92)90247-S)

1284 Małoszewski, P., Zuber, A., 1996. Lumped parameter models for the interpretation of
1285 environmental tracer data. *Manual on mathematical models in isotope hydrology*.
1286 IAEA-TECDOC 910. Vienna (Austria): IAEA; 1996

1287 Małoszewski, P., Zuber, A., 2002. *Manual on lumped parameter models used for the*
1288 *interpretation of environmental tracer data in groundwaters (IAEA-UIAGS/CD--*
1289 *02-00131). International Atomic Energy Agency (IAEA)*

1290 (https://inis.iaea.org/search/search.aspx?orig_q=RN:33037906, last access
1291 12/04/2018)

1292 Marti, R., Gascoin, S., Houet, T., Ribière, O., Laffly, D., Condom, T., Monnier, S.,
1293 Schmutz, M., Camerlynck, C., Tihay, J.P., Soubeyroux, J.M., 2015. Evolution of
1294 Ossoue Glacier (French Pyrenees) since the end of the Little Ice Age. The
1295 Cryosphere, 9(5), 1773-1795. <http://dx.doi.org/10.5194/tc-9-1773-2015>.

1296 Martos-Rosillo, S., Marín-Lechado, C., Pedrera, A., Vadillo, I., Motyka, J., Molina,
1297 J.L., Ortiz, P., Martín-Ramírez, J.M., 2014. Methodology to evaluate the renewal
1298 period of carbonate aquifers: a key tool for their management in arid and semiarid
1299 regions, with the example of Becerrero aquifer, Spain. Hydrogeology Journal,
1300 22(3), 679-689. <http://dx.doi.org/10.1007/s10040-013-1086-9>

1301 Martos-Rosillo, S., González-Ramón, A., Jiménez-Gavilán, P., Andreo, B., Durán, J.J.,
1302 Mancera, E., 2015. Review on groundwater recharge in carbonate aquifers from
1303 SW Mediterranean (Betic Cordillera, S Spain). Environ Earth Sci. 74: 7571.
1304 <https://doi.org/10.1007/s12665-015-4673-3>

1305 Merz, R., Blöschl, G., 2004. Regionalisation of catchment model parameters. Journal of
1306 hydrology, 287(1-4), 95-123. <http://dx.doi.org/10.1016/j.jhydrol.2003.09.028>

1307 Milano, M., Ruelland, D., Fernandez, S., Dezetter, A., Fabre, J., Servat, E., Fritsch,
1308 J.M., Ardoin-Bardin, S., Thivet, G., 2013. Current state of Mediterranean water
1309 resources and future trends under climatic and anthropogenic changes.
1310 Hydrological Sciences Journal, 58(3), 498-518.
1311 <http://dx.doi.org/10.1080/02626667.2013.774458>

1312 Molina, A., Melgarejo, J., 2016. Water policy in Spain: seeking a balance between
1313 transfers, desalination and wastewater reuse. International Journal of Water

1314 Resources Development, 32(5), 781-798.
1315 <http://dx.doi.org/10.1080/07900627.2015.1077103>

1316 Mook, W.G., De Vries, J.J., 2000. Volume I, Introduction: theory methods review.
1317 Environmental Isotopes in the Hydrological Cycle—Principles and Applications,
1318 International Hydrological Programme (IHP-V). Technical Documents in
1319 Hydrology (IAEA/UNESCO) No, 39 vol. 1 ([http://www-](http://www-naweb.iaea.org/napc/ih/IHS_publication.html)
1320 [naweb.iaea.org/napc/ih/IHS_publication.html](http://www-naweb.iaea.org/napc/ih/IHS_publication.html), last access 12/04/2018).

1321 Mudarra, M., Andreo, B. 2011. Relative importance of the saturated and the unsaturated
1322 zones in the hydrogeological functioning of karst aquifers: The case of Alta
1323 Cadena (Southern Spain). Journal of Hydrology 397, 263–280.
1324 <https://doi.org/10.1016/j.jhydrol.2010.12.005>

1325 Mudarra, M., Andreo, B., Marín, A.I., Vadillo, I., Barberá, J.A., 2014. Combined use of
1326 natural and artificial tracers to determine the hydrogeological functioning of a
1327 karst aquifer: the Villanueva del Rosario system (Andalusia, southern Spain).
1328 Hydrogeology journal, 22(5), 1027-1039. [http://dx.doi.org/10.1007/s10040-014-](http://dx.doi.org/10.1007/s10040-014-1117-1)
1329 [1117-1](http://dx.doi.org/10.1007/s10040-014-1117-1)

1330 Mudarra, M., Andreo, B., 2015. Role of the Soil-Epikarst-Unsaturated Zone in the
1331 Hydrogeological Functioning of Karst Aquifers. The Case of the Sierra Gorda de
1332 Villanueva del Trabuco Aquifer (Southern Spain). Hydrogeological and
1333 Environmental Investigations in Karst Systems. (ed. Andreo, B., Carrasco, F.,
1334 Durán, J.J., Jiménez, P., LaMoreaux.) Series: Environmental Earth Sciences.
1335 Springer. 638 pp.

1336 Nimon, K.F., Oswald, F.L., 2013. Understanding the results of multiple linear
1337 regression: Beyond standardized regression coefficients. Organizational Research
1338 Methods, 16(4), 650-674.

1339 Nogués-Bravo, D., Araújo, M.B., Lasanta, T., López-Moreno, J.I., 2008. Climate
1340 change in Mediterranean mountains during the 21st century. *AMBIO: A Journal*
1341 *of the Human Environment*, 37(4), 280-285. [https://doi.org/10.1579/0044-](https://doi.org/10.1579/0044-7447(2008)37[280:CCIMMD]2.0.CO;2)
1342 [7447\(2008\)37\[280:CCIMMD\]2.0.CO;2](https://doi.org/10.1579/0044-7447(2008)37[280:CCIMMD]2.0.CO;2)

1343 Obleitner, F., 1994. Climatological features of glacier and valley winds at the
1344 Hintereisferner (Ötztal Alps, Austria). *Theoretical and Applied Climatology*,
1345 49(4), 225-239. <https://doi.org/10.1007/BF00867462>

1346 Ozyurt, N.N., Bayari, C.S. 2008. Temporal variation of chemical and isotopic signals in
1347 major discharges of an alpine karst aquifer in Turkey: implications with respect to
1348 response of karst aquifers to recharge. *Hydrogeology Journal* 16: 297–309.
1349 <http://dx.doi.org/10.1007/s10040-007-0217-6>

1350 Ozyurt, N.N., Lutz, H.O., Hunjak, T., Mance, D., Roller-Lutz, Z. 2014. Characterization
1351 of the Gacka River basin karst aquifer (Croatia): Hydrochemistry, stable isotopes
1352 and tritium-based mean residence times. *Sci. Total Environ.* 87 245–254.
1353 <http://dx.doi.org/10.1016/j.scitotenv.2014.04.018>

1354 Pardo-Igúzquiza, E., Durán, J.J., Luque-Espinar, J.A., Robledo-Ardila, P.A., Martos-
1355 Rosillo, S., Guardiola-Albert, C., Pedrera, A. 2015. Karst massif susceptibility
1356 from rock matrix, fracture and conduit porosities: a case study of the Sierra de las
1357 Nieves (Málaga, Spain). *Environ Earth Sci.* 74:7583–7592.
1358 <http://dx.doi.org/10.1007/s12665-015-4545-x>

1359 Peel, M.C., Finlayson, B.L., McMahon, T.A., 2007. Updated world map of the Köppen–
1360 Geiger climate classification. *Hydrol. Earth Syst. Sci.* 11, 1633–1644.
1361 <http://dx.doi.org/10.5194/hess-11-1633-2007>

1362 Poage, M.A., Chamberlain, C.P., 2001. Empirical relationships between elevation and
1363 the stable isotope composition of precipitation and surface waters: considerations

1364 for studies of paleoelevation change. *Am. J. Science* 301 (1), 1–15.
1365 <http://dx.doi.org/10.2475/ajs.301.1.1>

1366 René, P., 2013. *Glaciers des Pyrénées: le réchauffement climatique en images*. Éd.
1367 Cairn.

1368 Ribalaygua, J., Pino, M.R., Pórtoles, J., Roldán, E., Gaitán, E., Chinarro, D., Torres, L.,
1369 2013. Climate change scenarios for temperature and precipitation in Aragón
1370 (Spain). *Science of the Total Environment*, 463, 1015-1030.
1371 <https://doi.org/10.1016/j.scitotenv.2013.06.089>

1372 Rodgers, P., Soulsby, C., Waldron, S., 2005. Stable isotope tracers as diagnostic tools in
1373 upscaling flow path understanding and residence time estimates in a mountainous
1374 mesoscale catchment. *Hydrol Process* 19(11):2291–2307.
1375 <http://dx.doi.org/10.1002/hyp.5677>

1376 Ruiz-Constán, A., Marín-Lechado, C., Martos-Rosillo, S., Fernández-Leyva, C., García-
1377 Lobón, J. L., Pedrera, A., López-Geta, J.A., Hernández-Bravo, J.A., Rodríguez-
1378 Hernández, L., 2015. Methodological Procedure for Evaluating Storage Reserves
1379 in Carbonate Aquifers Subjected to Groundwater Mining: The Solana Aquifer
1380 (Alicante, SE Spain). In *Hydrogeological and Environmental Investigations in*
1381 *Karst Systems* (pp. 255-262). Springer, Berlin, Heidelberg.
1382 http://dx.doi.org/10.1007/978-3-642-17435-3_28

1383 Sánchez-Murillo, R., Brooks, E.S., Elliot, W.J., Boll, J., 2015. Isotope hydrology and
1384 baseflow geochemistry in natural and human-altered watersheds in the Inland
1385 Pacific Northwest, USA. *Isotopes in environmental and health studies*, 51(2), 231-
1386 254. <http://dx.doi.org/10.1080/10256016.2015.1008468>

1387 Schotterer, U., Froehlich, K., Stichler, W., Trimborn, P., 1993. Temporal variation of
1388 ^{18}O and deuterium excess in precipitation, river and spring waters in Alpine

1389 regions of Switzerland. In *Isotope Techniques in the study of Past and Current*
1390 *Environmental Changes in the Hydrosphere and the Atmosphere*. Edited by
1391 IAEA. Proceedings series, ISSN 0074-1884, STI/PUB/908, ISBN 92-0-103293-5
1392 (https://inis.iaea.org/search/search.aspx?orig_q=RN:25027909, last access
1393 12/04/2018).

1394 Seibert, J., 2005. *HBV Light Version 2. User's Manual*. Uppsala University, Dept. of
1395 Earth Science, Hydrology, Uppsala, Sweden.

1396 Seibert, J., Vis, M.J.P., 2012. Teaching hydrological modelling with a user-friendly
1397 catchment-runoff-model software package, *Hydrol. Earth Syst. Sci.*, 16(9), 3315–
1398 3325. <http://dx.doi.org/10.5194/hess-16-3315-2012>, 102012

1399 Seibert, J., Jenicek, M., Huss, M., Ewen, T., 2015. Snow and ice in the hydrosphere. In
1400 *Snow and Ice-Related Hazards, Risks and Disasters* (pp. 99-137). ISBN: 978-0-
1401 12-394849-6. <https://doi.org/10.1016/B978-0-12-394849-6.00004-4>

1402 Solder, J.E., Stolp, B.J., Heilweil, V.M., Susong, D.D., 2016. Characterization of mean
1403 transit time at large springs in the Upper Colorado River Basin, USA: a tool for
1404 assessing groundwater discharge vulnerability. *Hydrogeology Journal*, Volume
1405 24, Issue 8, pp 2017–2033, <https://doi.org/10.1007/s10040-016-1440-9>

1406 Staudinger, M., Stoelzle, M., Seeger, S., Seibert, J., Weiler, M., Stahl, K., 2017.
1407 Catchment water storage variation with elevation. *Hydrological Processes*, 31(11),
1408 2000-2015. <https://doi.org/10.1002/hyp.11158>

1409 Turnadge, C., Smerdon, B.D. 2014. A review of methods for modelling environmental
1410 tracers in groundwater: advantages of tracer concentration simulation. *Journal of*
1411 *Hydrology*, 519, 3674-3689. <https://doi.org/10.1016/j.jhydrol.2014.10.056>

1412 Turk, J., Malard, A., Jeannin, P.-Y., Petric M., Gabrovšek, F., Ravbar, N., Vouillamoz,
1413 J., Slabe, T., Sordet, V., 2015. Hydrogeological characterization of groundwater

1414 storage and drainage in an alpine karst aquifer (the Kanin massif, Julian Alps).
1415 Hydrological Processes 29(8), 1986-1998. <https://doi.org/10.1002/hyp.10313>

1416 Uhlenbrook, S., Seibert, J.A.N., Leibundgut, C., Rodhe, A., 1999. Prediction
1417 uncertainty of conceptual rainfall-runoff models caused by problems in
1418 identifying model parameters and structure. Hydrological Sciences Journal, 44(5),
1419 779-797. <https://doi.org/10.1080/02626669909492273>

1420 Vergés, J. 1999. Estudi geològic del vessant sud del Pirineu oriental i central. Evolució
1421 cinemàtica en 3D. PhD Thesis. University of Barcelona (UB), Faculty of
1422 Geology, 180 pp.

1423 Vicente-Serrano, S.M., Lopez-Moreno, J.I., Beguería, S., Lorenzo-Lacruz, J., Sanchez-
1424 Lorenzo, A., García-Ruiz, J.M., Azorin-Molina, C., Morán-Tejeda, E., Revuelto,
1425 J., Trigo, R., Coelho, F., Espejo, F., 2014. Evidence of increasing drought severity
1426 caused by temperature rise in southern Europe. Environmental Research Letters,
1427 9(4), 044001. <https://doi.org/10.1088/1748-9326/9/4/044001>

1428 Vitvar, T., Gurtz, O., Lang, H. 1999. Application of GIS-based distributed hydrological
1429 modelling for estimation of water residence times in the small Swiss pre-alpine
1430 catchment Rietholzbach. Integrated Methods in Catchment Hydrology—Tracer.
1431 Remote Sensing and New Hydrometric Techniques (Proceedings of IUGG 99
1432 Symposium HS4, Birmingham, July 1999). IAHS Publ. no. 258, 1999

1433 Viville, D., Ladouche, B. and Bariac, T., 2006. Isotope hydrological study of mean
1434 transit time in the granitic Strengbach catchment (Vosges Massif, France).
1435 Application of the FlowPC model with modified input function. Hydrol. Process.
1436 20, 1737–1751. <https://doi.org/10.1002/hyp.5950>

1437 Viviroli, D., Weingartner, R., 2004. The hydrological significance of mountains: from
1438 regional to global scale. *Hydrology and Earth System Sciences* 8, 1016–1029.
1439 <https://doi.org/10.5194/hess-8-1017-2004>

1440 Viviroli, D., Dürr, H.H., Messerli, B., Meybeck, M., Weingartner, R., 2007. Mountains
1441 of the world— water towers for humanity: typology, mapping and global
1442 significance. *Water Resources Research* 43 (7), W07447.
1443 <https://doi.org/10.1029/2006WR005653>

1444 Wassenaar, L. I., Ahmad, M., Aggarwal, P., van Duren, M., Pölsenstein, L., Araguas,
1445 L., & Kurttas, T. 2012. Worldwide proficiency test for routine analysis of $\delta^2\text{H}$
1446 and $\delta^{18}\text{O}$ in water by isotope-ratio mass spectrometry and laser absorption
1447 spectroscopy. *Rapid Communications in Mass Spectrometry*, 26(15), 1641-1648.
1448 <https://doi.org/10.1002/rcm.6270>

1449 Wetzel, K., 2004. On the hydrogeology of the Partnach area in the Wetterstein
1450 Mountains (Bavarian Alps). *Erdkunde* 58:172–186.
1451 <http://www.jstor.org/stable/25647659>

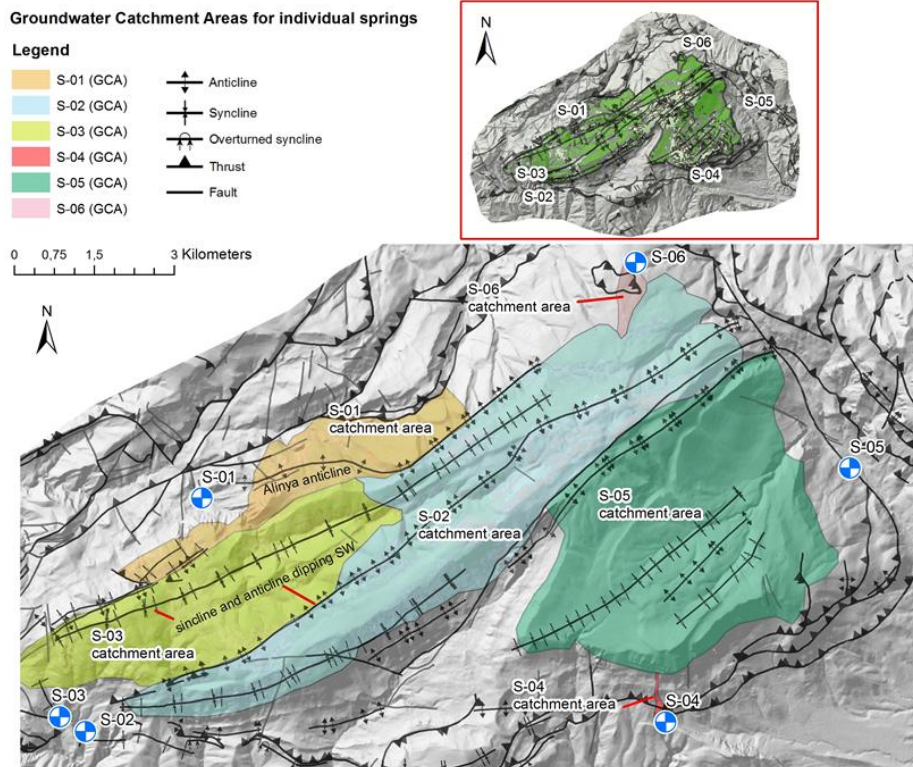
1452 Zini, L., Casagrande, G., Calligaris, C., Cucchi, F., Manca, P., Treu, F., Zavagno, E.,
1453 Biolchi, S. 2015. The Karst Hydrostructure of the Mount Canin (Julian Alps, Italy
1454 and Slovenia). *Hydrogeological and Environmental Investigations in Karst*
1455 *Systems*. (ed. Andreo, B., Carrasco, F., Durán, J.J., Jiménez, P., LaMoreaux.)
1456 Series: *Environmental Earth Sciences*. Springer. 638 pp.
1457 <https://doi.org/10.1007/978-3-642-17435-3>

1458

1459 **Appendix A: Groundwater catchment areas for the springs S-01 to S-06.**

1460

Comment [JJ21]: Answer to Reviewer #2- Q9



1461

1462 **Fig. A1. Groundwater catchment areas for the springs S-01 to S-06.**

1463

1464 **Table A1. Distribution of geographical and elevation zones considered into the HBV semi-**
 1465 **distributed rainfall-runoff model into the groundwater catchment zones. The areas of the**
 1466 **different vegetation zones (VZs) are provided, considering the three different elevation zones**
 1467 **into which every GWC is divided.**

Index	GWC Associated Spring	Elevation Zones			Vegetation Zone Areas			Percentage Areas		
		Z _{min} (m a.s.l.)	Z _{max} (m a.s.l.)	EZ _{ij} ^a (ha)	VZ ₁ ^b (ha)	VZ ₂ ^c (ha)	VZ ₃ ^d (ha)	VZ ₁ /EZ _{ij} (%)	VZ ₂ /EZ _{ij} (%)	VZ ₃ /EZ _{ij} (%)
1	S-01	1334	1600	204,0	41,8	56,8	105,5	20,5	27,8	51,7
		1601	1851	219,1	19,0	67,7	132,4	8,7	30,9	60,4
		1851	2141	122,8	4,8	6,8	111,1	3,9	5,5	90,5
2	S-02	1122	1543	106,9	8,2	26,0	72,7	7,7	24,3	68,0
		1544	1965	756,5	32,2	210,3	514,0	4,3	27,8	67,9

		1966	2385	1389,5	183,8	443,5	762,2	13,2	31,9	54,9
3	S-03	1201	1443	102,3	1,7	36,9	63,7	1,7	36,1	62,3
		1444	1686	561,2	19,5	178,9	362,8	3,5	31,9	64,6
		1687	1927	522,6	12,6	119,4	390,6	2,4	22,8	74,7
4	S-04	1468	1710	9,1	0,1	2,8	6,2	1,1	30,8	68,1
		1711	1847	0,9	0,1	0,5	0,3	11,1	55,6	33,3
		1848	1875	0,1	0,0	0,1	0,0	0,0	100,0	0,0
5	S-05	1421	1663	234,3	8,1	24,4	201,8	3,5	10,4	86,1
		1664	1973	635,5	45,4	126,0	464,1	7,1	19,8	73,0
		1974	2348	1278,4	215,5	495,0	568,0	16,9	38,7	44,4
6	S-06	1838	1926	11,9	0,7	0,7	10,5	5,9	5,9	88,2
		1927	2014	20,7	0,1	1,8	18,8	0,5	8,7	90,8
		2015	2101	13,4	0,0	2,3	11,2	0,0	17,2	83,6

(a) For a given elevation zone EZ_{ij} the subscripts "i" (from 1 to 6) and "j" refer to the corresponding groundwater catchment zone and elevation zone number, respectively; (b) VZ_1 corresponds to open areas; (c) VZ_2 corresponds to mountain meadows; (d) VZ_3 corresponds to forest zones

1468

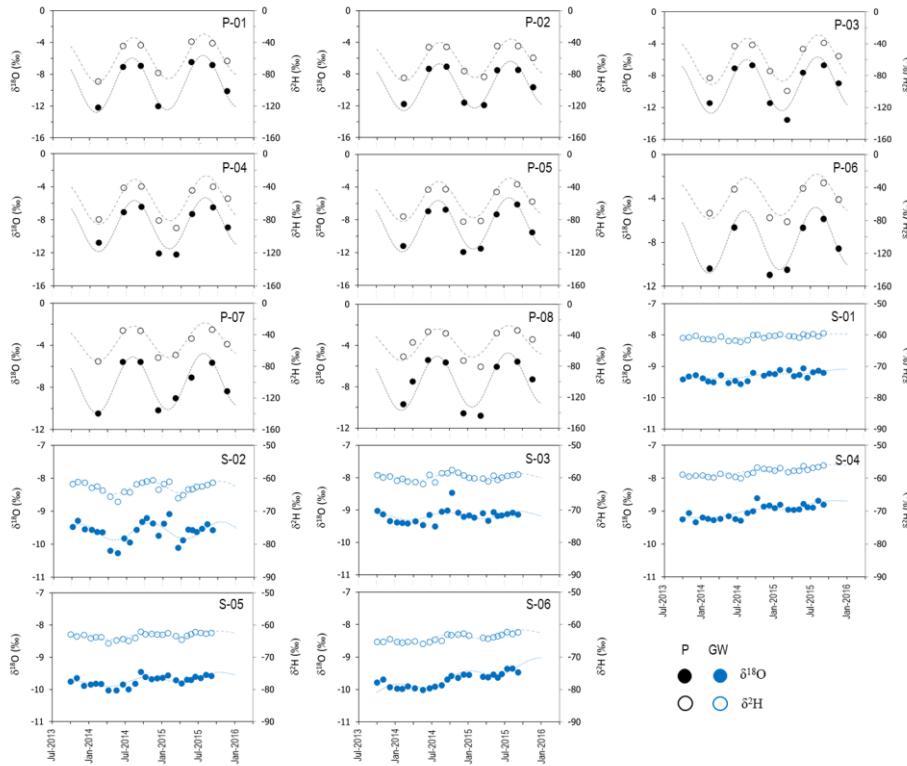
1469

1470

1471 **Appendix B: Sinusoidal functions fitting the measuring the isotopic content**

1472 **($\delta^{18}\text{O}$ and $\delta^2\text{H}$) variation in precipitation and spring discharges.**

1473



1474

1475 Fig. B1. Isotopic content of precipitation (P; black symbols) and spring discharge (GW; blue
1476 symbols). $\delta^{18}\text{O}$ and $\delta^2\text{H}$ are indicated by solid and empty symbols, respectively The dashed lines
1477 indicate the fitted sinusoidal function [Eq.1]. The identification codes correspond to those in
1478 Table 1.

1479

1480 **Appendix C: HBV hydrological modeling**

1481 Table C1. List of abbreviations for the vegetation zone parameters of HBV (Seibert, 2005)

Parameter	Units	Valid range	Description
TT	°C	(-inf,inf)	Threshold temperature to produce accumulation of precipitation as snow. Melt of snow starts if temperatures are above TT calculated with a simple degree-day (degree-Δt in case of a non-daily time step) method
CFMAX	mm/Δt/°C	[0,inf)	Degree-Δt factor - CFMAX varies normally between 1.5 and 4 mm oC-1 day-1 (in Sweden), with lower values for forested areas. As approximation the values 2 and 3.5 can be used for CFMAX in forested and open landscape respectively.
SFCF	-	[0,inf)	Snowfall correction factor
CFR	-	[0,inf)	Refreezing coefficient
CWH	-	[0,inf)	Water holding capacity, according to: refreezing meltwater = CFR·CFMAX(TT-T)'
FC	mm	(0,inf)	Maximum soil moisture storage
LP	-	[0,1)	Soil moisture value above which AET reaches PET
BETA	-		Parameter that determines the relative contribution to runoff from rain or snowmelt

1482 Table C2. List of abbreviations for the catchment parameters of HBV (Seibert, 2005)

Parameter	Units	Valid range	Description
PERC	mm/Δt	[0,inf)	Threshold parameter
UZL	mm	[0,inf)	Threshold parameter
K0	1/Δt	[0,1)	Storage (or recession) coefficient 0
K1	1/Δt	[0,1)	Storage (or recession) coefficient 1
K2	1/Δt	[0,1)	Storage (or recession) coefficient 2
MAXBAS	Δt	[1,100]	Length of triangular weighting function

1484

1485 Table C3. Objective functions for the calibration of the HBV hydrologic model, where Q_{obs_i}
 1486 and Q_{sim_i} are the measured and computed of spring discharge values, respectively, $\overline{Q_{obs}}$ is the
 1487 arithmetic mean of the observed spring discharge values, and $\overline{Q_{sim}}$ is the arithmetic mean of the
 1488 computed spring discharge values.

Objective function	Observations
$R_{eff} = 1 - \frac{\sum_{i=1}^N (Q_{sim_i} - Q_{obs_i})^2}{\sum_{i=1}^N (Q_{obs_i} - \overline{Q_{obs}})^2}$	$R_{eff} = 1$ means perfect fit $R_{eff} = 0$, indicates that the model fits the observed data no better than a horizontal line through $\overline{Q_{obs}}$ $R_{eff} < 0$ means very poor fit
$R^2 = \frac{(\sum_{i=1}^N (Q_{obs_i} - \overline{Q_{obs}}) * (Q_{sim_i} - \overline{Q_{sim}}))^2}{\sum_{i=1}^N (Q_{obs_i} - \overline{Q_{obs}})^2 * \sum_{i=1}^N (Q_{sim_i} - \overline{Q_{sim}})^2}$	R^2 is the determination coefficient. The higher the R^2 value the better the model performance

1489

1490

1491 Table C4. Calibrated values of the parameters in the HBV-light model

Catchment Parameters	Units	S-01	S-02	S-03	S-04	S-05	S-06
Snow Routine (VZ ₁)							
TT	°C	-0,2	-4,52	-1,6	-1,1	-1	-1,1
CFMAX	mm/d/°C	1,9	2,4	2	1,7	2,8	1,2
SFCF	-	1	2,38	0,5	1	1,2	1,5
CFR	-	1	2,5	0,7	0,5	0,6	0,6
CWH	-	0,5	2	2	1	0,8	0,8
Snow Routine (VZ ₂)							
TT	°C	-0,2	-4,39	-1,6	-0,5	-3	-0,46
CFMAX	mm/d/°C	1,9	1	2	1,6	1	2,1
SFCF	-	1	2,6	0,7	1	1,2	1,16
CFR	-	1	2,5	0,7	0,3	1	1
CWH	-	1	2	1	1	0,2	0,2
Snow Routine (VZ ₃)							

TT	°C	4	6	6	0	5,5	6,5
CFMAX	mm/d/°C	1,5	1	1,5	1,5	1	4
SFCF	-	0,001	0,001	0,001	0,01	0,001	0,001
CFR	-	0,7	1	0,7	0,2	0,4	0,4
CWH	-	2	2	3	1	1	1
Soil Moisture Routine							
(VZ ₁)							
FC	mm	95	75	80	75	50	80
LP	-	0,07	0,01	0,02	0,02	0,01	0,01
BETA	-	0,60	0,40	1,54	1,70	0,30	2,5
Soil Moisture Routine							
(VZ ₂)							
FC	mm	180	120	150	125	139	150
LP	-	0,07	0,01	0,06	0,01	0,01	0,01
BETA	-	0,60	2,20	3,90	3,45	1,80	2,7
Soil Moisture Routine							
(VZ ₃)							
FC	mm	750	550	490	750	660	700
LP	-	0,00	0,01	0,01	0,01	0,01	0,01
BETA	-	6,00	3,00	5,70	6,00	3,50	4,00
Response Routine							
PERC	mm/d	5	20,0	2,2	1,1	25,0	1,7
UZL	mm	100	80	100	110	100	100
K0	1/d	0,20	0,50	0,20	0,20	0,20	0,40
K1	1/d	0,07	0,11	0,13	0,17	0,20	0,20
K2	1/d	0,01	0,02	0,04	0,04	0,05	0,05
Routing Routine							
MAXBAS	d	1,7	6,2	2	2,45	4,3	4,22

1492

1493

1494

1495

Table C5. Goodness of the result of the HBV calibrations for each spring model

HBV model	$R_{\text{eff}}(-)$	$R^2(-)$
S-01	0,55	0,55
S-02	0,66	0,67
S-03	0,73	0,78
S-04	0,57	0,73
S-05	0,77	0,80
S-06	0,62	0,66

1496

1497

1498 **Appendix D: FlowPC modeling**

1499 Table D1. Fitted parameters of the exponential-piston flow model (EPM) for the estimated
 1500 mean transit times (τ) with FlowPC model and $\delta^{18}\text{O}$ data

Parameters	S-01	S-02	S-03	S-04	S-05	S-06
β (%) ^a	0	0	0	0	0	0
δ_{β} (‰) ^b	0	0	0	0	0	0
η (-) ^c	1,02	1,02	1,00	1,01	1,02	1,02
τ (yr)	2,25	1,42	2,25	2,33	2,88	2,58
RMSE (‰)	0,03	0,04	0,03	0,03	0,02	0,03

(a) A constant discharge component as a fraction (usually older) of the total spring volumetric discharge flow rate. (b) Constant isotopic content of β . (c) η is the ratio of the total volume to the volume with exponential distribution transit time (TTD). $\eta = 1$ means the Exponential model (EM) and $\eta > 1$ for Exponential-piston flow model (EPM)

1501

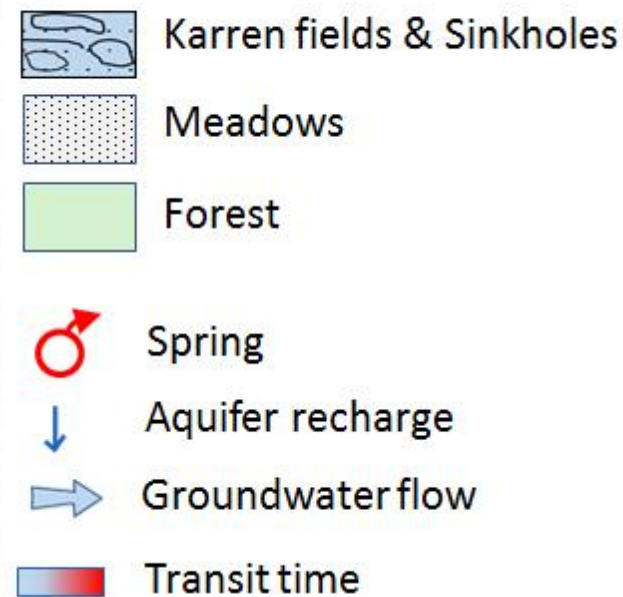
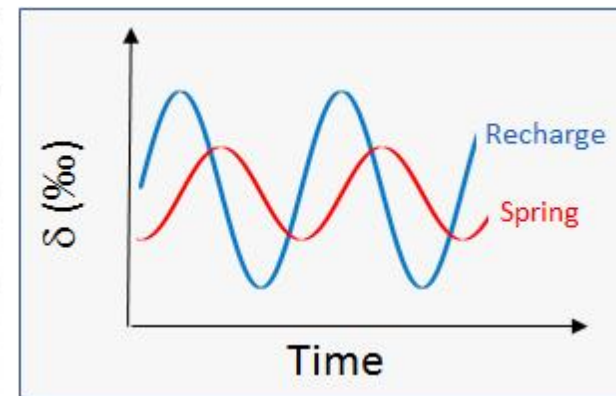
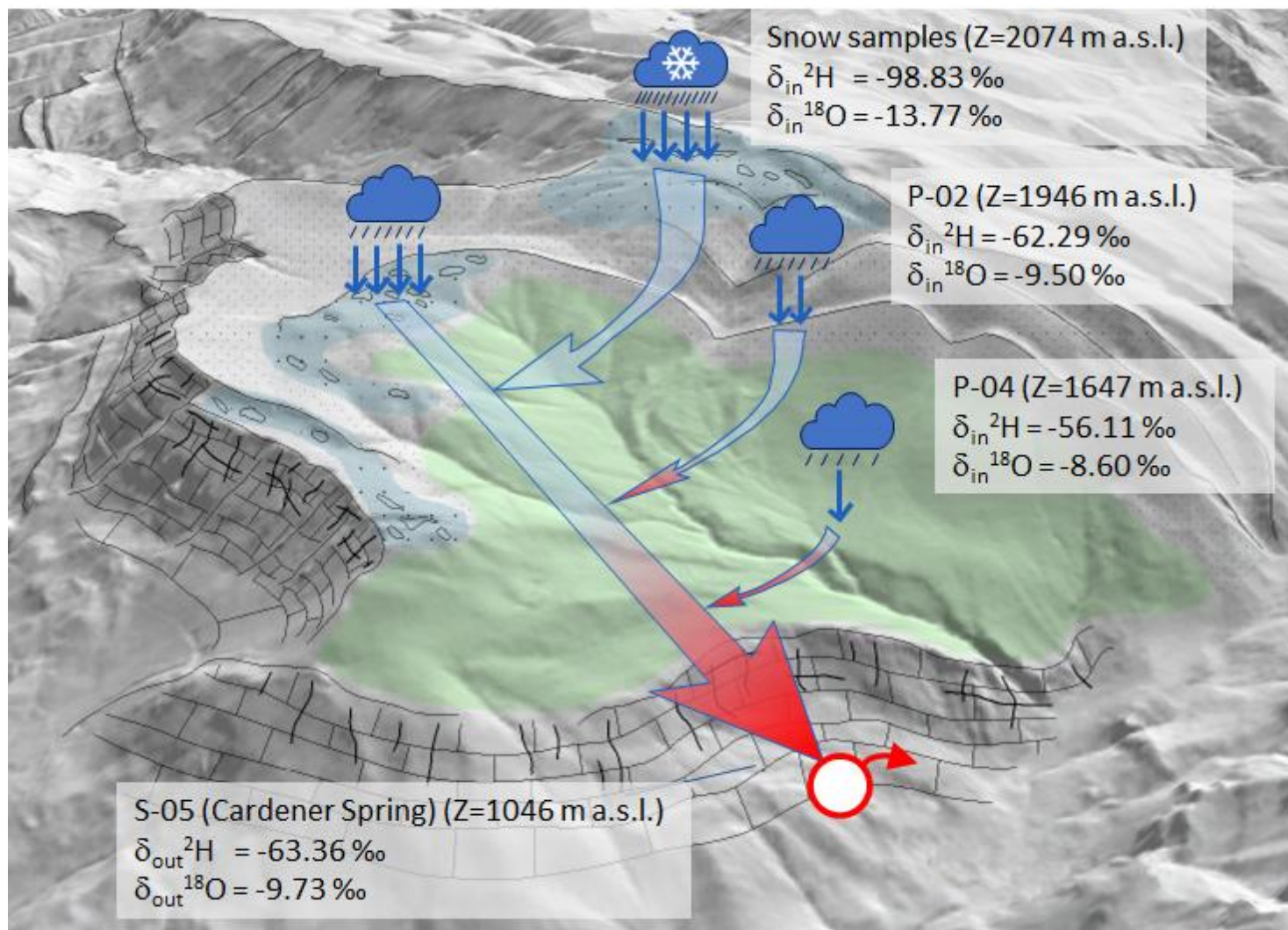
1502

1503 Table D2. Fitted parameters of the exponential-piston flow model (EPM) for the estimated
 1504 mean transit times (τ) with FlowPC model and $\delta^2\text{H}$ data

Parameters	S-01	S-02	S-03	S-04	S-05	S-06
β (%) ^a	0	0	0	0	0	0
δ_{β} (‰) ^b	0	0	0	0	0	0
η (-) ^c	1,01	1,00	1,01	1,00	1,01	1,02
τ (yr)	3,00	1,92	2,33	2,67	2,83	2,75
RMSE (‰)	0,19	0,21	0,17	0,22	0,18	0,20

(a) A constant discharge component as a fraction (usually older) of the total spring volumetric discharge flow rate. (b) Constant isotopic content of β . (c) η is the ratio of the total volume to the volume with exponential distribution transit time (TTD). $\eta = 1$ means the Exponential model (EM) and $\eta > 1$ for Exponential-piston flow model (EPM)

1505



Amplitude of seasonal isotopic composition of rainfall depends on elevation

Moisture generating rainfall in the study zone comes from the Mediterranean

The aquifer main recharge zones located at elevations between 2700 and 2100 m a.s.l

Considering transient recharge improves the estimations of mean transit times

Transit times in agreement with the karstic nature of the aquifer system

1 Contribution of isotopic research techniques to characterize
2 high-mountain-Mediterranean karst aquifers: The Port del
3 Comte (Eastern Pyrenees) aquifer.

4

5 Herms, I.^a, Jódar, J.^{b,*}, Soler, A.^c, Vadillo, I.^d, Lambán, L.J.^e, Martos-
6 Rosillo, S.^e, Núñez, J.A.^a, Arnó, G.^a, Jorge, J.^f

7

8 (a) Àrea de Recursos Geològics. Institut Cartogràfic i Geològic de Catalunya (ICGC), Barcelona, Spain

9 (b) Groundwater Hydrology Group. Dept. Civil Engineering and Environment, Technical University of
10 Catalonia (UPC), Barcelona, Spain & Aquageo Proyectos S.L., Spain

11 (c) Grup de Mineralogia Aplicada i Geoquímica i Geomicrobiologia, Departament de Mineralogia,
12 Petrologia i Geologia Aplicada, Facultat de Ciències de la Terra, Universitat de Barcelona (UB),
13 Barcelona, Spain

14 (d) Centro de Hidrogeología, Universidad de Málaga (UMA), Málaga, Spain

15 (e) Instituto Geológico Minero de España (IGME), Spain

16 (f) Departament d'Enginyeria Minera, Industrial i TIC. Universitat Politècnica de Catalunya (UPC),
17 Manresa, Spain

18 * Corresponding author: Jorge Jódar (jorge.jodar@hydromodelhost.com). Telf:(+34)
19 619712122

20

21

22 **Abstract**

23 Water resources in high mountain karst aquifers are usually characterized by high
24 rainfall, recharge and discharge that lead to the sustainability of the downstream
25 ecosystems. Nevertheless, these hydrological systems are vulnerable to the global
26 change impact. The mean transit time (MTT) is a key parameter to describe the behavior

27 of these hydrologic systems and also to assess their vulnerability. This work is focused
28 on estimating MTT by using environmental tracers in the framework of high-mountain
29 karst systems with a very thick unsaturated zone (USZ). To this end, it is adapted to
30 alpine zones a methodology that combines a semi-distributed rainfall-runoff model to
31 estimate recharge time series, and a lumped-parameter model to obtain MTT. The
32 methodology has been applied to the Port del Comte Massif (PCM) hydrological system
33 (Southeastern Pyrenees, NE Spain), a karst aquifer system with an overlying 1000 m
34 thick USZ. Six catchment areas corresponding to most important springs of the system
35 are considered. The obtained results show that hydrologically the behavior of the system
36 can be described by an exponential flow model (EM), with MTT ranging between 1.9
37 and 2.9 years. These MTT values are shorter than those obtained by considering a
38 constant recharge rate along time, which is the easiest and most applied aquifer recharge
39 hypothesis when estimating MTT through lumped-parameter models.

40

41 **Keywords:** Stable isotopes; Seasonal isotopic amplitude; Altitudinal line; Recharge;
42 Mean transit time; Karst.

43

44 **1. Introduction**

45 High mountain zones are known as "water towers" because they generate the main
46 water resources feeding the most important rivers in the world (Viviroli et al., 2007).
47 This phenomenon is especially important in the drought-prone Mediterranean area
48 (Vicente-Serrano et al 2014), where water availability is scarce and greatly dependent
49 on runoff from headwater basins (De Jong et al., 2009). Moreover, water discharge from
50 mountain areas is critical to ensure water supply in the lowland and coastal fringe

51 (Viviroli and Weingartner, 2004; García-Ruiz et al 2011), where human activity
52 (agriculture, industry, tourism) concentrates.

53

54 Future scenarios for climate change in the whole Mediterranean region forecast an
55 increase in temperature and a decrease in precipitation at the end of the 21st century
56 (Giorgi and Lionello, 2008). These effects may well impact the Mediterranean high
57 mountain zones (Nogués-Bravo et al., 2008; Lopez-Moreno et al., 2009; Ribalaygua et
58 al., 2013), modifying the hydrological behavior of their headwater basins (Barnett et al.,
59 2005; García-Ruiz et al. 2011, and references therein). Nevertheless, the first evidence
60 of such changes has already been reported in the Pyrenees, the southernmost European
61 range where glaciers can be found (Grunewald and Scheithauer, 2010). Pyrenean
62 glaciers have undergone an intense retreat since the middle of the last century, causing
63 most of them to face a certain close extinction (Chueca et al., 2007; René 2013; Marti et
64 al., 2015; López-Moreno et al., 2016). In addition, during this period, both mean annual
65 precipitation and number of rainy days have shown a clear decreasing trend in this zone
66 (Lopez-Moreno et al., 2010), along with a lesser snowfall and snow accumulation
67 (López-Moreno, 2005). These effects directly impact the water storage capacity of the
68 associated headwater systems (Seibert et al., 2015), as well as their associated
69 hydrological response in terms of both river discharge flowrates and timing of
70 maximum discharges (López-Moreno and García-Ruiz, 2004; Gremaud et al., 2009).
71 These changes will directly impact the downstream zones by complicating the current
72 water stress situation in the Mediterranean zone (Milano et al., 2013; Hernández-Mora
73 et al., 2014, Molina and Melgarejo, 2016). Because of the hydrological outlook that is
74 not so promising, it is essential to understand the functioning of the mountain
75 hydrological systems of the Mediterranean area, especially those scenarios in which

76 groundwater (GW) plays a major role in the headwater discharge, because mountain
77 aquifers maintain base flows to rivers during the recurrent Mediterranean dry periods
78 (Hoerling et al 2012; Vicente-Serrano et al., 2014).

79

80 Despite playing a strategic role, most high mountain hydrogeological systems are still
81 insufficiently understood (Goldscheider, 2011). Conventional hydrogeological
82 investigation techniques (Bakalowicz, 2005; Goldscheider and Drew, 2007) are often
83 difficult to apply in alpine regions because of the difficult access and the harsh working
84 conditions, along with the types of instruments needed for conducting research in high
85 mountain zones (Lauber et al., 2014; Hood and Hayashi, 2010). However, a growing
86 number of publications are focusing on the importance of groundwater in the
87 functioning of high-mountain watershed rivers in different geological settings, including
88 alluvial/rockfall/talus aquifers (Lauber and Goldscheider, 2014; Kurylyk and Hayashi,
89 2017), fractured aquifers (Jódar et al., 2017; Barberá et al., 2018a) and karst systems
90 (Wetzel, 2004; Goldscheider, 2005; Gremaud et al., 2009; Mudarra et al., 2014; Allocca
91 et al., 2015; Lambán et al., 2015; Chen, 2017; Barberá et al., 2018b; Kazakis et al.,
92 2018). Determining the magnitude of groundwater recharge and aquifer Mean Transit
93 Time (MTT) are key issues for understanding and managing alpine groundwater
94 systems. Spring hydrograph analysis and environmental tracer methods allow for
95 characterizing aquifer recharge and discharge processes, estimating recharge zone
96 elevation and transit times, determining drainage structures, and assessing spring
97 vulnerability, as well as calculating water resources in headwater aquifers (Wetzel,
98 2004; Rodgers et al., 2005; Einsiedl, 2005; Farlin and Maloszewski, 2013; Jódar et al.,
99 2016b; Malard et al., 2016; Epting et al., 2018).

100

101 In high-altitude alpine karst aquifers, groundwater recharge processes highly depend on
102 temporal and spatial distribution of precipitation and snowmelt (Lauber and
103 Goldscheider, 2014). The estimation of MTT in karst systems is conditioned by the
104 existence of variable flow conditions. These systems normally show triple-porosity and
105 different connected parts: the karstic conduits that allows rapid flow, and the fissured-
106 porous matrix that shows intermediate to slow flow. Artificial tracer test normally
107 injected in preferential flow paths (i.e. the channels) doesn't consider the fissured-
108 porous matrix of the aquifer, which can be important as far as the total karst water
109 volumes (Maloszewski et al., 2002). In this respect, the use of artificial tracers to
110 characterize such hydrological systems is not enough since it doesn't allow
111 characterizing all the components of the flow. Others important factors that govern the
112 suitability of injection test for MTT estimations is the existence of a thick unsaturated
113 zones (USZ): conducting tracer tests by injecting it at the surface of the thick USZ is
114 likely a failing tracer test given the large uncertainties regarding the likelihood of
115 hydraulic connection between the tracer injection point and the sampled system
116 discharge point (Lauber and Goldscheider, 2014). Additionally, the adverse working
117 conditions and the type of material of the instruments necessary to correctly perform the
118 tracer test (Goldscheider et al., 2008) in high-mountain areas make it difficult to execute
119 them.

120

121 As a result, the hydrogeological behavior of most of the mountain karst systems with an
122 associated thick USZ remain uncharacterized, despite of being the exploration of these
123 systems on the focus of speleogenetic research since the last decades (Ballesteros et al.,
124 2015a, and references therein).

125

126 Lumped parameter models (LPMs) are useful to simulate the behavior of such complex
127 mountain karst systems, even when they are poorly characterized. These models do not
128 require a detailed hydrological knowledge of the physical system. Moreover, LPMs
129 naturally integrate the USZ of the aquifer as a part of the whole hydrological system to
130 be modeled (Turnadge and Smerdon, 2014). Additionally, the stable isotopes of water
131 ($\delta^{18}\text{O}$ and $\delta^2\text{H}$) in rainfall have proved to be good environmental tracers for
132 investigating the dynamics of such hydrological systems karst systems (Andreo et al.,
133 2004). These tracers enter the system as recharge, migrate downgradient exploring the
134 whole hydrological system, and leave the karst aquifer with spring discharge or by
135 lateral mass transfer to other hydrogeologically connected aquifer units. In this line, this
136 work is devoted to estimate MTT of a high-mountain karst aquifer with a thick
137 unsaturated zone by using ^{18}O and ^2H as environmental tracers along with LPMs. To this
138 end, it is considered the approach presented by Vitvar et al. (1999) to estimate MTT in a
139 small Swiss pre-alpine aquifer. The original approach is adapted to high mountain zones
140 by considering the existing vertical gradients of precipitation and air temperature along
141 the slope of high mountains, but also the role played by the snow accumulation and
142 ablation processes in the runoff generation. The resulting method combines in series
143 two LPMs: (1) a semi-distributed rainfall-runoff HBV model (Bergström, 1976; Seibert,
144 2005) that simulates the observed hydrodynamical system response while taking into
145 account the elevation dependences of the different hydrometeorological variables (i.e.
146 Precipitation and temperature) and associated processes (e.g. snow accumulation and
147 ablation), and (2) a FlowPC model (Małoszewski and Zuber, 1996) that estimates the
148 mean transit time of the hydrological system while simulating the environmental tracer
149 content evolution in the system discharge. This is done by numerically integrating a
150 convolution integral (Maloszewski et al., 1983; Jódar et al., 2014). In our case, the

151 FlowPC model uses as input data: a) the recharge time series of the aquifer obtained
152 with the HBV model, and b) the time series isotope content ($\delta^{18}\text{O}$ and $\delta^2\text{H}$) in recharge,
153 which is obtained through a spatiotemporal characterization of the isotope contained of
154 precipitation.

155

156 The methodology is applied to the hydrological system of Port del Comte Massif (PCM;
157 NE Spain), a karst aquifer with a 1000 m thick USZ. The hydrological system mainly
158 discharges through the Cardener springs into the homonym river, which is the main
159 tributary of the Llobregat River, the first water resources provider to the city of
160 Barcelona (NE Spain). Despite the strategic role of Cardener springs the hydrologic
161 behavior of the karst system remains unknown. This study contributes to a better
162 hydrological characterization of PCM hydrological system. Moreover, the proposed
163 methodology can be applied to characterize other high mountain karst aquifers with an
164 overlying thick USZ that are common in many alpine zones elsewhere the globe.

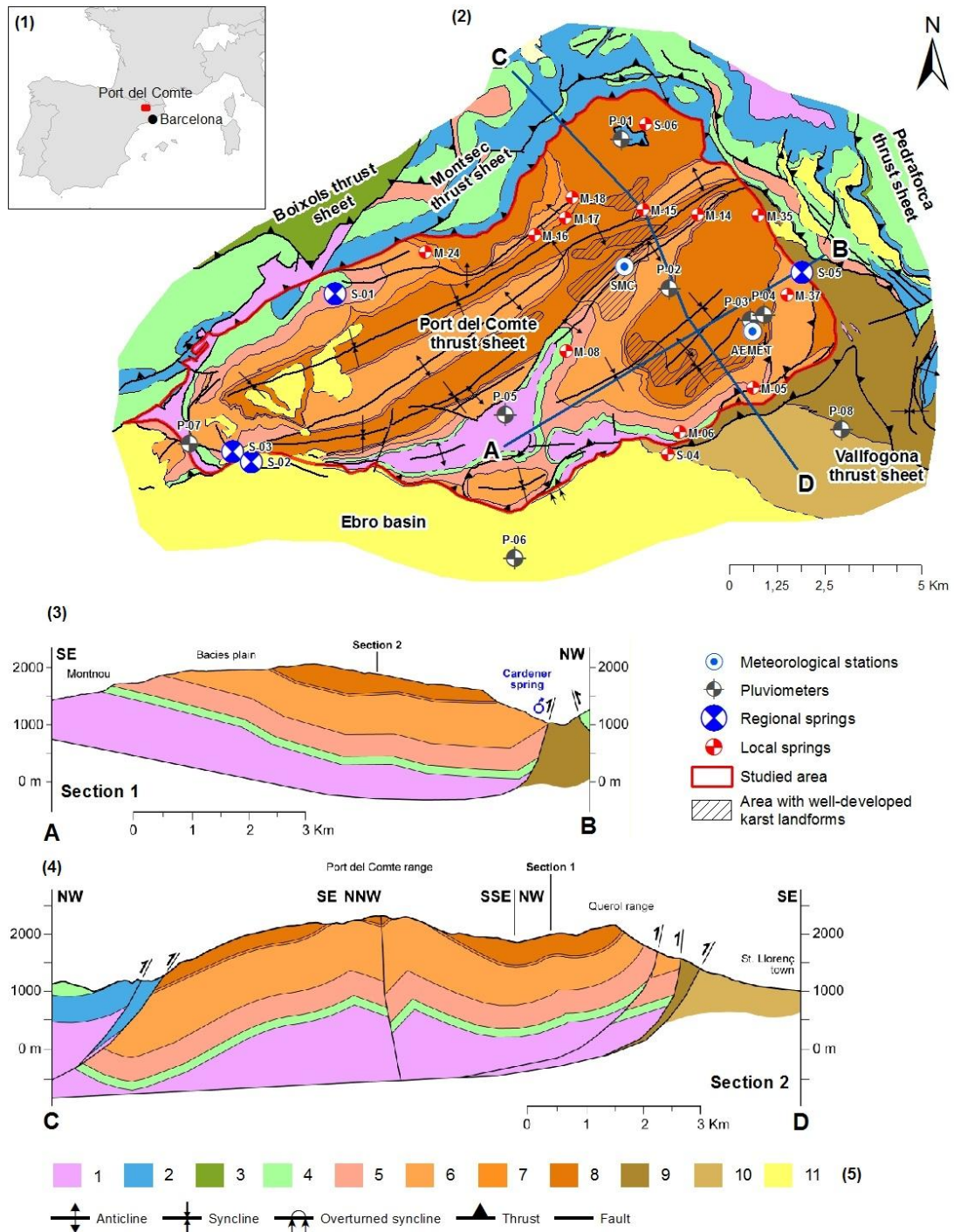
165

166

167 **2. Study area**

168 The study area is located at the Port del Comte Massif (PCM), which is situated in the
169 eastern part of the Pyrenees, NE Spain (Fig. 1). The elevation of the watershed ranges
170 from approximately 900 m a.s.l., up to 2387 m a.s.l., at the ‘Pedró dels Quatre Batlles’
171 peak. With approximately 110 km², it contains one of the main mountain karst aquifers
172 of the Catalan Pyrenees. The watershed of the massif divides the river basin of the
173 Cardener River at the E and S and the river basin of the Segre River at the NW and SW.
174 The massif constitutes an independent structural and hydrogeological unit.

175



176

177 Fig. 1. (1) Location map of the study zone. (2) Geological map (geological map modified from
 178 ICGC, 2007). (3) Geological cross-section A-B. (4) Geological cross-section C-D. (5)
 179 Geological legend: [1] Triassic – shales, limestones, dolomites and evaporates; [2] Jurassic –
 180 marls, bioclastic limestones and dolomites; [3] Lower Cretaceous – mudstones, ammonite
 181 limestones and marl; [4] Upper Cretaceous – limestones, marls, calcarenites and terrigenous

182 deposit; [5] Garumnian – red shales and limestones; [6] Lower Eocene – fissured and karstified
183 alveoline limestones and dolomites; [7] Lower Eocene – marls, sandstones and limestone; [8]
184 Lower Eocene – fissured and karstified micritic and bioclastic limestones; [9] Middle Eocene –
185 sandstones, marls, conglomerates, limestones and evaporates; [10] Upper Eocene – continental
186 alluvial systems: conglomerates and sandstones; [11] Oligocene – continental alluvial systems:
187 conglomerates, breccias and sandstones.

188

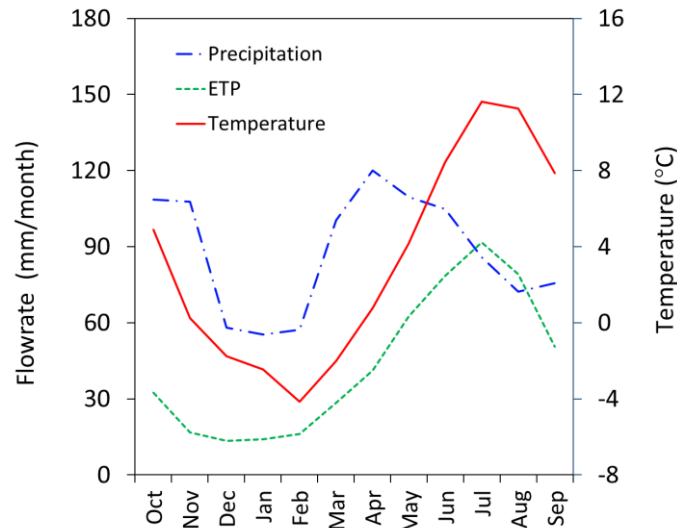
189 **2.1 Meteorological setting**

190 From a climatic point of view, and according to the Köppen-Geiger classification (Peel
191 et al., 2007), the study zone has a cold climate without dry season and temperate
192 summer (defined as ‘Dfb’ type; accordingly to AEMET and IMA, 2011). At the
193 meteorological station MS-01 (Fig. 1), which is located at 2315 m a.s.l., the average
194 values of precipitation (P), temperature (T) and potential evapotranspiration (ETP)
195 calculated with the Hargreaves and Samani (1982) equation are 1055 mm/yr, 3,24 °C
196 and 525 mm/yr, respectively. These three variables show a seasonal variation (Fig. 2)
197 and an elevation dependence. The measured vertical gradients (lapse rate) of
198 precipitation ($\nabla_z P$), atmospheric temperature ($\nabla_z T$) and potential evapotranspiration
199 ($\nabla_z ETP$) are 8,9 mm/yr/100 m, $-0,74$ °C/100 m and $-32,3$ mm/yr/100 m, respectively.
200 The snow cap is present in the upper zones of the basin in winter and spring, maintained
201 annually for 3 to 4 months since 1800 m a.s.l., meaning that precipitation is partly
202 produced as snow.

203

204 Despite the high average rainfall above 1000 mm/year, in most of the study area the
205 surface runoff is almost nonexistent, and it is not observed until reaching lower
206 altitudes.

207



208

209 Fig. 2. Seasonal variation of precipitation, potential evapotranspiration and temperature
 210 measured at the meteorological station MS-01 (see Table 1) located at 2315 m a.s.l. for the
 211 period Sep 2005- Apr 2016.

212

213 2.2 General settings of the study zone

214 From a geological perspective, the massif belongs to the PCM thrust sheet that presents
 215 complex structural relationships in its contours (Fig. 1). On the E, the PCM mantle
 216 borders on the mantle of Cadí, coinciding with the point of origin for the Cardener
 217 River (spring S-05; Fig. 1). To the NE and NW, the PCM is limited by the tectonic
 218 plates of the mantles of Sierras Marginales, Montsec and Boixols. To the S, the PCM
 219 mantle overlaps with the conglomeratic materials of the Ebro Basin, the southern
 220 foreland basin of the Pyrenees. The internal structure of the PCM mantle is formed by a
 221 set of folds and thrusts detached above the Triassic. These folds have a constant
 222 direction NE-SW parallel to the NW limit of the mantle (Vergés, 1999). The
 223 stratigraphic series contains materials from the Triassic, Jurassic, Cretaceous and
 224 Paleogene with a total of approximately 1000 m thickness. The main karst aquifer
 225 inside PCM massif is in the Paleocene - Eocene carbonate rocks. The geologic structure
 226 and stratigraphy of the PCM thrust strongly influence the location of the existing karst

227 springs, their groundwater geochemistry and their hydrologic behavior. The lower
228 Upper Cretaceous/Paleocene (Garumnian facies) substrate materials underlying the
229 Palaeocene aquifer are composed of sandstone, siltstone and shale. These materials
230 constitute an impervious layer for the overlaying aquifer system.

231

232 From the geomorphological point of view, the PCM has a characteristic triangular
233 geometry. The PCM has a smooth rounded landscape with a plain in the highest part
234 without vegetation cover and with almost no soil, which corresponds to approximately
235 10% of the total area. The rest of the massif is covered by mountain meadows (29%)
236 and forest (61%) with scarce soil depth up to medium developed soil cover. Different
237 karstic forms progressively appear from 1950 m a.s.l. upwards, being well developed at
238 2050 m a.s.l., with sinkholes, dry caves, dolines and karren fields, generating a
239 heterogeneous karstified hydrogeological system.

240

241 The hydrogeological conceptual model of the PCM aquifer system considers that
242 recharge is produced by infiltration of precipitation as rainfall and snowmelt. The
243 magnitude and distribution of infiltration is conditioned by the development of the karst
244 landforms. The infiltration is produced (1) in a concentrated way through the local
245 karstic elements such as dolines and (2) in a diffuse way by rain and snowmelt along the
246 whole PCM area. The epikarst unsaturated zone (NSZ) presents a thickness close to
247 1000 m in the highest zones of the PCM. The infiltrated water flows vertically through
248 the NSZ towards the saturated zone.

249

250 The hydrogeological system naturally discharges through the large number of existing
251 springs. Approximately 100 springs have been found in the PCM showing large

252 discrepancies in their mean discharge flow rate, ranging from values $\ll 1$ L/s up to
 253 values > 100 L/s. Most of these springs discharge a local subhorizontal interflow
 254 characteristic of a small entity (i.e., Local springs, Table 1). However, in terms of
 255 groundwater discharge, there are six important springs in the PCM (i.e., Regional
 256 springs, Table 1). These springs have been monitored regularly for this research,
 257 showing that all of them have a highly variable discharge flow rate (Fig. 3). Four of
 258 these regional springs (S-01, S-02, S-03 and S-05) are the principals discharging points
 259 of the whole hydrogeological system. The four springs are located at elevations between
 260 944 and 1098 m a.s.l. (see Table 1). Through these main springs, the hydrogeological
 261 system discharges at two principal watersheds: the Cardener River watershed to the east
 262 and the Segre River watershed to the northwest. Groundwater flow direction is
 263 conditioned by the geological structure of PCM. Nevertheless, the exact position of the
 264 regional groundwater table is poorly known.

265

266 Table 1. Meteorological stations, pluviometers and springs in the study zone sampled during the
 267 period July 2013 – October 2015.

Code	Type	Name	Elevation (m a.s.l.)	Num. water samples (-)	Discharge rate (L/s)
MS-01	Met. Station	SMC-Z8	2315	-	-
MS-02	Met. Station	AEMET-0127O	1800	-	-
P-01	Pluviometer	Refugi de l'Arp	1936	7	-
P-02	Pluviometer	Bassa Clot de la Vall	1946	8	-
P-03	Pluviometer	Refugi Bages	1768	8	-
P-04	Pluviometer	Casa X&A	1657	8	-
P-05	Pluviometer	Casa Ramonet	1450	8	-
P-06	Pluviometer	Casa Cavallera	1216	7	-
P-07	Pluviometer	Camp. La Comella	1062	8	-

P-08	Pluviometer	Camp. Morunys	896	9	-
S-01	Regional Spring	Font Aiguaneix	1098	25	8 - 73
S-02	Regional Spring	Font Sant Quintí	944	25	70 – 575
S-03	Regional Spring	Font Can Sala	1062	25	0,25 – 148
S-04	Local Spring	Font Coll de Jou	1464	25	0,07 - 0,59
S-05	Regional Spring	Fonts del Cardener	1032	25	57 – 904
S-06	Local Spring	Font carretera Refugi Arp	1858	25	0,04 – 7
M-05	Local Spring	Font del Ginebró	1730	4	<0,001
M-06	Local Spring	Font de la Garganta	1657	4	0,02-0,49
M-08	Local Spring	Font Orris 02	1871	4	0,1 – 0,7
M-14	Local Spring	Font Estivella	2053	4	0,07 – 5
M-15	Local Spring	Font Arderic	2158	3	0,03 – 2,8
M-16	Local Spring	Font del Casalí	2077	1	<0,001
M-17	Local Spring	Font del Diumenge	1989	2	0,004 – 0,026
M-18	Local Spring	Font barraca Sangonella	1940	1	0,001 - 0,01
M-24	Local Spring	Font dels Acens	1550	4	0,06 – 0,23
M-35	Local Spring	Font Ca l'Arreplagant	1330	4	<0,001 – 0,02
M-37	Local Spring	Font La Part (esllav.)	1315	4	0,5 – 1

268

269

270 **3. Materials and methods**

271 **3.1 Field work**

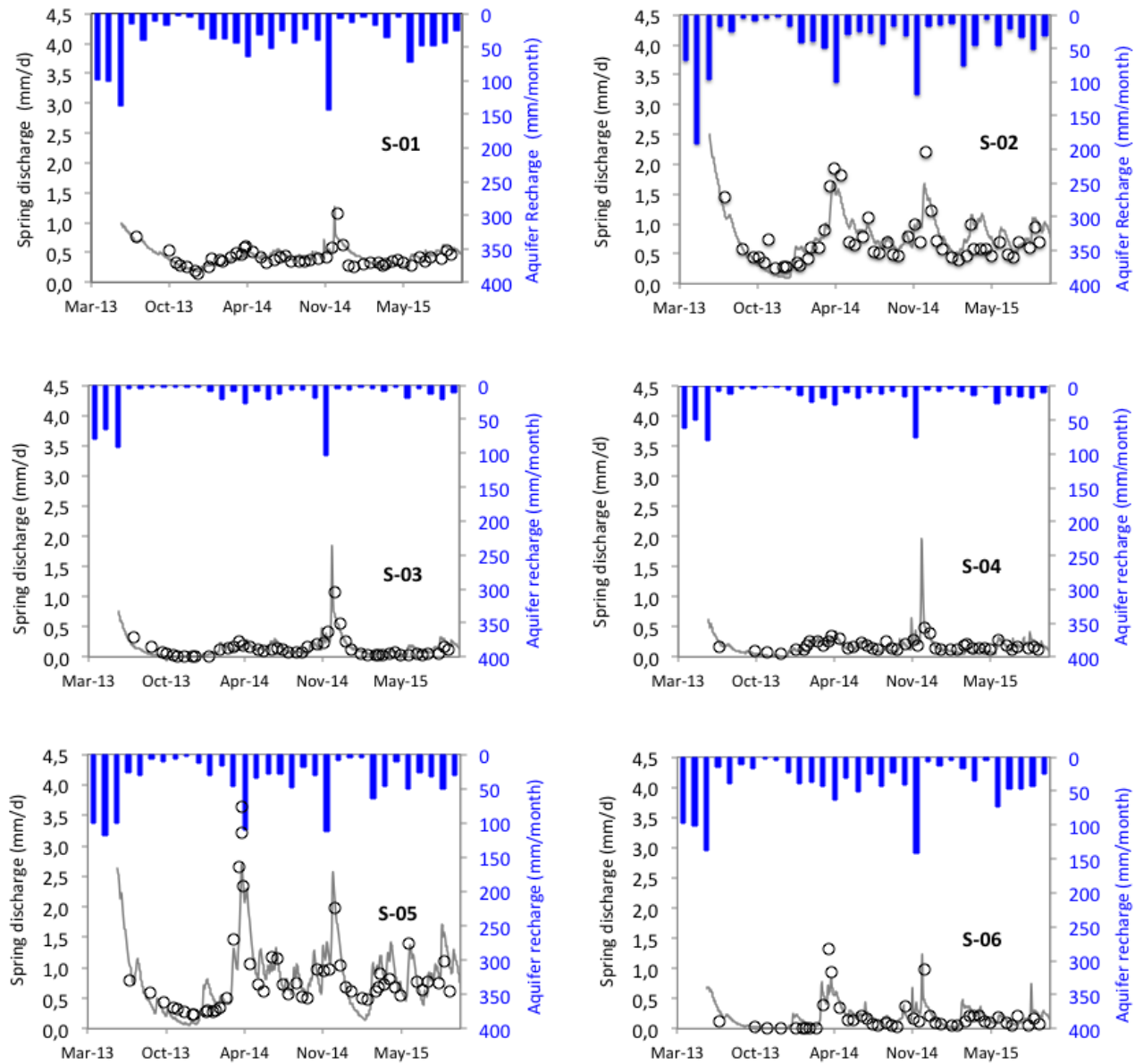
272 To collect precipitation samples, a network of 8 cumulative precipitation gauges
 273 (pluviometers) of the type CoCoRaHS RG202 Official-4 was installed at elevations
 274 between 896 and 1935 m a.s.l. (P-01 a P-08; Fig. 1). The pluviometers consist of a
 275 polycarbonate cylindrical deposit with a diameter of 10,8 cm. The pluviometers include
 276 a top funnel that captures and guides precipitation into the storing deposit, where

277 according to the technical procedure for the stations of the Global Network of Isotopes
278 in Precipitation (GNIP) of the International Atomic Energy Agency (IAEA), a 0,5 cm
279 paraffin oil floating layer is added to avoid evaporation. The pluviometers were sampled
280 seasonally (except the first winter with two campaigns), a total of 9 campaigns from
281 Dec. 2013 to Dec. 2015. Additionally, one snow sampling survey was conducted in
282 December 2003. The snow samples were obtained by drilling through the entire snow
283 depth (Lambán et al., 2015) and were taken at different locations with elevations
284 ranging from 1935 to 2150 m a.s.l.

285

286 Groundwater samples were collected under different hydrodynamic conditions between
287 Oct. 2013 and Dec. 2015. In this period, the springs S-01 to S-06 were sampled
288 approximately monthly, for a total of 25 sampling campaigns. Groundwater samples
289 were taken before the snow arrival in autumn (Oct. 2013 and Oct. 2014), and after the
290 snow-melting season (Apr. 2014 and Apr. 2015). In these springs, groundwater
291 discharge was measured once every two weeks from Jul. 2013 to Oct. 2015 (Fig. 3). In
292 springs S-01, S-02, S-03 and S-05 the discharge flow rate was measured by conducting
293 slug-injection salt dilution tests (Cervi et al., 2014), whereas the volumetric method was
294 used for the precision discharge measurement in springs S-04 and S-06. The M-##
295 springs (Table 1) showed a tiny and intermittent discharge. Therefore, groundwater
296 samples were only taken with uneven frequency when it was possible.

297



298

299 Fig. 3. Measured spring discharge (circles) in the six monitored springs (S-01 to S-06, Table 1)
 300 of the PCM hydrogeological system. Gray lines indicate the spring discharge numerically
 301 simulated with the HBV model (Seibert and Vis, 2012). For each spring, blue columns
 302 indicate the recharge values time series used as input data to the corresponding HBV model.

303

304 The isotopic composition ($\delta^2\text{H}$ and $\delta^{18}\text{O}$) of all low salinity water samples was
 305 determined in the Center of Hydrogeology of the University of Málaga (CEHIUMA),
 306 where a Picarro® “L2130-I” isotopic water analyzer was used. The analytical

307 uncertainties for $\delta^{18}\text{O}$ and $\delta^2\text{H}$ are $\pm 0.2\text{ ‰}$ and $\pm 1.0\text{ ‰}$, respectively. According to
308 Coplen et al., (2011) several international and laboratory standards have been
309 interspersed for normalization of analyses. The standards used (WICO-13, WICO-14,
310 WICO-15) were calibrated in an interlaboratory comparison (Wassenaar et al., 2012).
311 All results are given relative to the V-SMOW standard.

312

313 **3.2 Approach for spring catchment delineation**

314 A critical aspect to understand the behavior of karst hydrogeological flow systems is the
315 delineation of the spring capture zones (i.e., recharge areas) and their boundaries
316 (Goldscheider and Drew, 2007). Ideally, the delineation should be based on the proven
317 information of connection between recharge areas and the discharge points. In high
318 mountain zones, this connection may be confirmed by conducting tracer tests
319 (Goldscheider et al., 2008; Mudarra et al., 2014; Barberá et al., 2018b). When this
320 information is not available, the spring capture zone can be indirectly inferred by
321 considering inputs from other classical information sources such as geophysics,
322 structural geology and geomorphology data interpretation. However, 3D conceptual
323 modeling techniques are currently being used to delineate the spring capture zones:
324 Malard et al. (2015) analyze spring discharge hydrographs based on geological three-
325 dimensional (3D) conceptual modeling (Butscher and Huggenberger, 2007, 2008;
326 Martos-Rosillo et al., 2014; Ruiz-Costán et al., 2015; Malard et al., 2015; Ballesteros et
327 al., 2015b; Epting et al., 2018).

328

329 In this work, a combined 3D conceptual methodology has been used to delineate the
330 catchment areas associated with each spring. The delineating criteria are based on the

331 information provided by three complementary methods: (1) the interpretation of the
332 geological structure and the subsurface catchments relative to each spring location. To
333 this end, a 3D geological model has been developed in the 3DMove software platform
334 (Midland Valley Exploration Ltd.); (2) the analysis of the disposition and location of the
335 karst landforms over the area, and (3) the analysis through GIS spatial analysis tools of
336 the ground surface structure, including type of soils (CREAF, 2009) and vegetation
337 (Appendix A) at the spring recharge elevation zones. In the case of the regional springs
338 S-01, S-02, S-03 and S-05, the three listed methods have been applied to delineate their
339 catchment zone, whereas in the case of the perched springs S-04 and S-06, only the
340 previous methods (2) and (3) could be applied. Fig. A1 (Appendix A) shows the
341 catchment zones (i.e., aquifer units) obtained for the selected springs.

342

343 The delineated catchment zones associated with the regional springs divide PCM into
344 two main blocks: (1) a southwestern block that includes only the catchment zone
345 associated with S-05. This catchment zone is characterized by a syncline dipping NW
346 structure (Fig. 1). From a functional point of view, this zone is hydrodynamically
347 independent of the rest of PCM given the existence of an anticline and a main NE-SW
348 fault that prevents lateral flows. (2) The northeastern block formed by the catchment
349 zone associated with springs S-01, S-02 and S-03. The geological structure of this block
350 regulates the regional groundwater flows, so as the Alinyà anticline controls the
351 discharge of spring S-01, and the main syncline-anticline system dips SW along with
352 the minor faults and synclines dipping south conditions the discharge of springs S-02
353 and S-03. Table A1 (Appendix A) provides the geographical details of the delineated
354 groundwater catchment zones.

355

365 3.3 Characterizing the seasonal variation of environmental tracers

367 The evolution of some environmental variables is linked to the atmospheric temperature
368 variation. As a result, these variables often show a similar seasonal pattern that can be
369 characterized with a general sinusoidal function $\delta(t)$ (Jódar et al., 2014). This function
370 consists of two additive terms, a sine-wave function [Eq. 1] plus a temporal linear trend
361 for the mean [Eq. 2].

362

$$\delta(t) = A \sin(\omega(t - t_0) + \varphi) + \bar{\delta} \quad (1)$$

$$\bar{\delta} = \alpha(t - t_0) + \bar{\delta}_0 \quad (2)$$

363

364 where A is the amplitude of the sinusoidal function, ω is the angular frequency, φ is the
365 angular initial at time t_0 , α is the slope of the linear trend, and $\bar{\delta}_0$ is the linear trend
366 value at time t_0 . The parameters A , α and $\bar{\delta}_0$ can be estimated by using the solution of
367 any of the commonly available spreadsheet software's or manually. In this work, the
368 root-mean-squared error (RMSE) is used as the selection criterion for the best fit to the
369 measured isotope content time series.

370

371 In the case time series with a short amount of data (e.g., associated with the M-##
372 springs in Table 1), it is not possible to obtain reliable estimates for, α , A , and $\bar{\delta}_0$ by
373 using the method proposed above. In this case, no linear trend in the mean value is
374 assumed ($\alpha = 0$), and $\bar{\delta}_0$ and A are estimated as:

$$\bar{\delta}_0 = \frac{1}{N} \sum_{i=1}^N \delta_i \quad (3)$$

$$A = \max(\text{Abs}(\bar{\delta}_0 - \delta_i)); \forall i = 1 \div N \quad (4)$$

375

376 where N is the number of the isotopic content value of the time series.

377

378 Hydrogeological systems transfer the isotopic input signal of recharge. The tracer input
379 seasonal signal is buffered and delayed as it propagates through the aquifer towards the
380 discharging point (Fig. 4). This tracer transport process through the hydrological system
381 can be described by the convolution integral that relates the tracer input content in
382 recharge δ_{in} to the tracer input content in the spring discharge δ_{out} as shown below.

383

$$\delta_{out}(t) = \int_{-\infty}^t \delta_{in}(t')g(t - t')dt' \quad (5)$$

384

385 where t is the time of tracer entry as recharge, t' is the integration variable and $g(t')$ is a
386 weighting function describing the Transit Time Distribution (TTD) exit of tracer content
387 that entered the aquifer at different times in the past. The differences between the input
388 and the output tracer signals are related to the aquifer system MTT (τ) which is the first
389 moment of the system TTD and is given by

$$\tau = \int_0^{\infty} tg(t)dt \quad (6)$$

390

391 where V is the volume of mobile water in the system (Małozzewski et al., 1983), and Q
392 is the volumetric flow rate through the system. In the case of natural gradient
393 hydrogeological systems, MTT corresponds to the mean amount of time for
394 groundwater to travel from the recharge zone to the discharging spring. In this situation,
395 MTT is related to the spring discharge flow rate Q , and the aquifer storage V as follows
396 (Custodio and Llamas, 1976):

$$\tau = \frac{V}{Q} \quad (7)$$

397

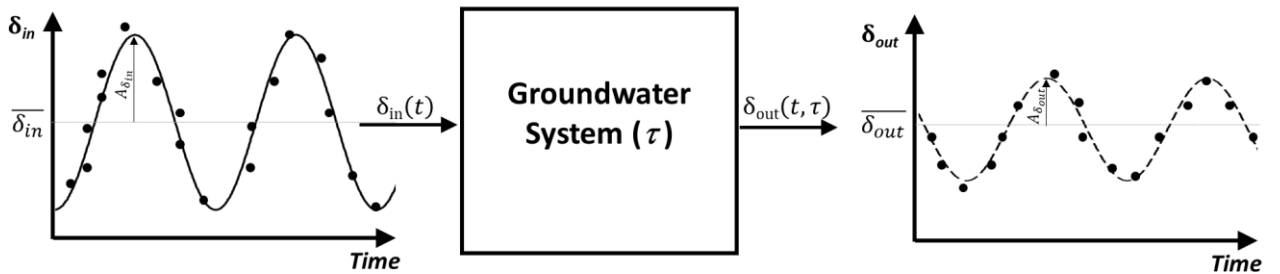
398 Additionally, in natural gradient hydrogeological systems with a seasonal varying input
 399 tracer function, MTT can be estimated as (Małozzewski et al., 1983):

$$\tau = \frac{1}{\omega} \sqrt{\left(\frac{A_{\delta_{in}}}{A_{\delta_{out}}}\right)^2 - 1} \quad (8)$$

400

401 where $A_{\delta_{in}}$ and $A_{\delta_{out}}$ are the amplitudes of the seasonal variation of the isotopic content
 402 in the aquifer recharge and the spring discharge, respectively. As can be shown, the
 403 above equation compares $A_{\delta_{in}}$ with respect to $A_{\delta_{out}}$, so the larger the amplitude
 404 dampening is, the longer the transit time.

405



406

407 Fig. 4. Schematic representation of the groundwater system response $\delta_{out}(t, \tau)$ to a
 408 hypothetical input tracer function $\delta_{in}(t)$ (modified from Jódar et al., 2016b), where τ
 409 means MTT.

410

411 **3.4 Numerical approach for simulating the aquifer behavior**

412 To reproduce the observed spring discharge flow rates and the associated isotopic
 413 content, a two-step methodology has been used:

414

415 (1) Simulation of the hydrodynamic behavior of the hydrogeological system. To this
416 end, the freely available version of the semi-distributed conceptual
417 precipitation–runoff model HBV-Light (Seibert and Vis, 2012) is used. HBV is
418 a conceptual rainfall-runoff model for catchment hydrology modeling that solves
419 a general water balance equation. HBV has been used in different alpine
420 mountain hydrologic research studies (Braun and Renner, 1992; Hottelot, et al.,
421 1993; Uhlenbrook et al., 1999; Merz and Blöschl, 2004; Konz and Seibert, 2010;
422 Staudinger et al., 2017; Epting, et al., 2018; Jódar et al., 2018). This model has
423 become a standard tool for simulating high mountain snow-dominated
424 hydrological systems. This code requires as input data some hydroclimatic
425 catchment information such as the relative weight with respect to the total area
426 of the different altitude and associated vegetation zones in the catchment, the
427 vertical lapse rates $\nabla_z P$ and $\nabla_z T$, as well as the time series of daily P, T, and
428 ETP. The hydrological catchment can be separated into numerous elevation
429 zones, depending on the elevation gap between the lowest and the highest points
430 of the catchment. In this work, every zone has been divided into three elevation
431 zones (Table A1 in Appendix A). Additionally, every elevation zone can be
432 divided into different vegetation zones. Based on the Land Cover Map of
433 Catalonia (CREAF, 2009), three vegetation zones are considered: (1) open areas
434 corresponding to zones of both poor or no soils where karst landforms are very
435 well-developed (karren fields, sinkholes, dolines, etc.), (2) areas with mountain
436 meadows and soil moderately developed, and (3) alpine forest zones with
437 moderate to well-developed soils. A two stacked linear reservoir is used to
438 simulate the hydrological system dynamics. The upper reservoir is used to
439 generate surface and subsurface runoff whereas the lower reservoir generates

440 groundwater runoff. The model considers vegetation zones parameters and
441 catchment zone parameterer (Tables C1 and C2 of Appendix C, respectively).
442 They are can be automatically calibrated by minimizing an efficiency objective
443 function (R_{eff} ; Table C3, Appendix C), which is already implemented in HBV.
444 The model output includes the daily time series of aquifer recharge Q_R , which is
445 used in the following step.

446

447 (2) Simulation of the transient isotopic content variation in the groundwater
448 discharge. The temporal variation of the isotopic content in the spring discharge
449 is simulated with FlowPC (Małoszewski and Zuber, 1996, 2002), a lumped
450 parameter model typically used to estimate groundwater MTTs with the aid of
451 observed environmental tracer data (Viville et al., 2006; Einsiedl et al., 2009;
452 Katsuyama et al., 2010; Lauber and Goldscheider, 2014; Sánchez-Murillo et al.,
453 2015; Mađrala et al., 2017). The program solves the convolution integral [Eq. 5]
454 and transforms the isotopic input tracer signal $\delta_{\text{in}}(t)$ entering the hydrogeological
455 system as recharge into the isotopic output tracer signal $\delta_{\text{out}}(t)$ leaving the
456 system through the spring discharge. To this end, FlowPC includes among
457 others two parametric TTDs which are especially well suited for simulating karst
458 aquifer systems: (A) The exponential model (EM), also known as a “good
459 mixing model”, is typically applied in systems where the groundwater flow lines
460 tend to converge towards the water sampling points (Zuber, 1986; Amin and
461 Campana, 1996). (B) The Exponential-Piston model (EPM) or “real system
462 model”, which combines two parts in line, an unconfined upstream part where
463 recharge enters the system and an exponential distribution of transit times is
464 assumed, and a confined downstream part where the flow scheme is

465 approximated like the piston flow model (Zuber, 1986). The weighting function
 466 for EPM is described by the following equation.

467

$$g(t) = \begin{cases} 0 & t < \tau \left(1 - \frac{1}{\eta}\right) \equiv t_\tau \\ \frac{1}{\tau} \eta e^{-\frac{\eta}{\tau} + \eta - 1} & t \geq t_\tau \end{cases} \quad (9)$$

468

469 where η is the ratio of total volume of the hydrogeological system to the volume
 470 of the system in which the exponential TDD exists, and τ is MTT. [Eq. 9] also
 471 describes the EM weighting functions when $\eta = 1$, which is the lowest bound of
 472 this parameter. The model parameters (η and τ) are calibrated by minimizing the
 473 RMSE function.

474

475 FlowPC requires the time series of (1) monthly aquifer recharge \widehat{Q}_R (hereinafter,
 476 a circumflex accent over a flow or an isotopic content variable indicates that the
 477 variable is cumulated monthly or averaged, respectively), which is obtained
 478 from the HBV model outputs for each simulation, and (2) the corresponding
 479 monthly averaged isotopic content of the recharge $\widehat{\delta}_R$. Given the karstic nature of
 480 the hydrogeological system, we assume that the isotopic content of local
 481 recharge and its seasonal characteristics (i.e., $\bar{\delta}_{in}, A_{\delta_{in}}$) are the same as the
 482 isotopic content and seasonal characteristics of local precipitation ($\bar{\delta}_p, A_{\delta_p}$).
 483 Since $\bar{\delta}_p$ and A_{δ_p} are known, then $\delta_p(t)$ is analytically obtained through [Eq.1].
 484 As $\delta_p(t)$ is a daily time function, it is necessary to transform it into $\widehat{\delta}_p$. For the

485 j^{th} month, $\widehat{\delta}_{P_j}$ is obtained by weighting the daily values of recharge isotopic
 486 content $\delta_{P_{ij}}$ by the corresponding daily recharge rate $Q_{R_{ij}}$ as

$$\widehat{\delta}_{R_j} \sim \widehat{\delta}_{P_j} = \frac{\sum_{i=1}^N \delta_{P_{ij}} Q_{R_{ij}}}{\sum_{i=1}^N Q_{R_{ij}}} \quad (10)$$

487 where N is the number of days of the j^{th} month. The Appendix D includes all the
 488 technical details corresponding to the different FlowPC models used in this work

489

490 **3.5 Statistical analysis of the relationship between the infiltration coefficient** 491 **and recharge**

492 To analyze the factors that controls the mean calculated infiltration coefficient (ξ) in the
 493 PCM, a linear regression model has been built, expressing the dependent variable ξ as a
 494 linear function of N explanatory variables Ψ_i as

$$\xi = \lambda_0 + \sum_{i=1}^N \lambda_i \Psi_i \quad (11)$$

495 where λ_0 is the intercept (constant) term, and λ_i ($i \geq 1 \div N$) are the regression coefficients
 496 associated with the predictors Ψ_i . In this study, the predictor variables of the linear
 497 regression model of the [Eq.11] are the elevation of the spring recharge zone Z_R (Table
 498 3), the mean precipitation at the spring recharge zone P_{ZR} (Table 6), and the percentages
 499 of open areas, mountain meadows and forest in the spring catchment zones (VZ_1 , VZ_2
 500 and VZ_3 , respectively; Table A1 in Appendix A). The coefficient of determination of
 501 the regression is one, so the model reproduces the whole variance of ξ . Table 7 shows
 502 the intercept value λ_0 , the regression coefficients λ_i , and their corresponding
 503 standardized value β_i ($i \geq 1 \div N$). The standardized value β_i measures the expected
 504 change in ξ , in standard deviation units, for a one standard deviation change in Ψ_i ,

505 provided that other explanatory variables in the model ($\Psi_j, \forall i \neq j$) are fixed (Nimon and
506 Oswald, 2013). The larger the absolute value of β_i , the more important the
507 corresponding predictor Ψ_j is.

508

509

510 **4. Results and discussion**

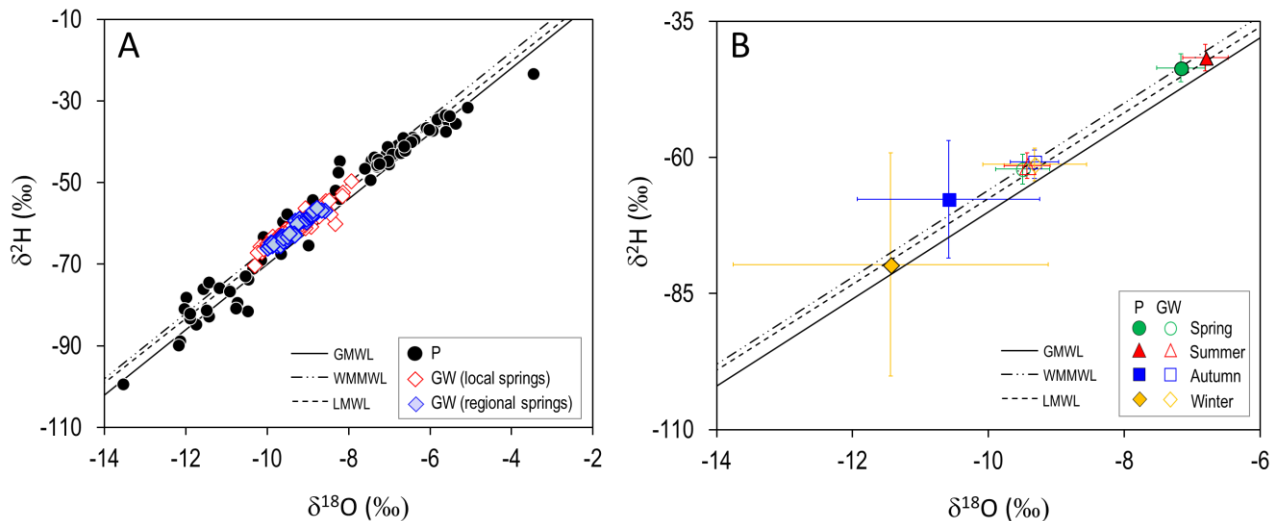
511 **4.1 Results from observed data**

512 The isotopic content of the precipitation corresponding to the water samples taken is
513 shown in Fig. 5A. The mean isotopic content of precipitation is lighter in winter and
514 autumn than that in spring and summer, as one would expect given the dependence
515 between the isotopic content in rainfall and temperature (Mook and De Vries, 2000).
516 The obtained values are aligned between the Global Meteoric Water Line (GMWL) and
517 the West Mediterranean Meteoric Water Line (WMMWL) (Fig. 5A). The local water
518 meteoric water line (LMWL) that is obtained by linear regression ($N= 76; R^2= 0,97$) is
519 defined as $\delta^2\text{H} = 8,05 \cdot \delta^{18}\text{O} + 12,74$. From a seasonal point of view, the isotopic content
520 of precipitation in autumn and winter presents a larger variability than the isotopic
521 content of precipitation in spring and summer, as shown in Fig. 5B by the error bars
522 indicating the standard deviation associated with every seasonal value. The isotopic
523 content in groundwater changes seasonally much less, than the isotopic content in
524 precipitation (Fig. 5B), pointing out the existence of a good mixing flow process in the
525 discharging points of the aquifer.

526

527 The geographical location of the study zone postulates the Mediterranean as the most
528 important source of precipitation. This assumption is supported by the overall mean
529 deuterium excess ($dex= \delta^2\text{H} - 8 \cdot \delta^{18}\text{O}$) value of $12,03 \pm 3,37 \text{ ‰}$ obtained for all the

530 precipitation samples analyzed (Celle-Jeanton et al., 2001; Jiménez-Martínez and
 531 Custodio, 2008). Nevertheless, the Atlantic fingerprint in rainfall can be observed in the
 532 above *dex* value through its variation interval, which provides a minimum *dex* value of
 533 8,66 ‰ (Froehlich et al., 2001; Araguás-Araguás and Díaz-Teijeiro, 2005).
 534



535
 536
 537 Fig. 5. (A) Values of $\delta^{18}\text{O}$ and $\delta^2\text{H}$ in precipitation (P; solid circles) and groundwater (GW)
 538 from local springs (empty red diamonds) and from regional springs (solid blue diamonds) for
 539 the period Oct. 2013 – Dec. 2015. (B) Seasonal overall averages of $\delta^{18}\text{O}$ and $\delta^2\text{H}$ for
 540 precipitation (P; solid symbols) and groundwater (GW; empty symbols). The spring, summer
 541 autumn and winter values are indicated by green circles, red triangles, blue squares and orange
 542 diamonds, respectively. GMWL (Clarke and Fritz, 1997) is the Global Meteoric Water Line
 543 (slope 8 and *dex*=10‰), WMMWL is the Western Mediterranean Meteoric Water Line (slope 8
 544 and *dex*=14‰) and LMWL is the Local Meteoric water Line (slope 8,05 and *dex*=12,74‰).
 545
 546 The isotopic composition of precipitation and spring discharge show a seasonal
 547 variation, which is not reflected in the deuterium excess. A seasonal variation in *dex*
 548 would indicate the existence of different moisture sources generating rainfall in the

549 study zone by following a certain seasonal pattern (Schotterer et al 1993; Liu et al 2008;
 550 Froehlich et al 2008). The lack of such seasonal pattern supports the Mediterranean as
 551 the main rainfall source.

552

553 A sine-wave function [Eq.1] is used to characterize every one of the measured seasonal
 554 time series of isotopic content in water from the sampling points (Fig. B1 in Appendix
 555 B). Tables 2 and 3 show the calibrated mean isotopic content ($\bar{\delta}$) and amplitude (A)
 556 corresponding to the time series of isotopic content of precipitation and spring
 557 discharge, respectively.

558

559 Table 2. Mean value $\bar{\delta}_{in}$ and amplitude $A_{\delta_{in}}$ of the seasonal variation in the isotopic content of
 560 precipitation for the sampled pluviometers.

Pluviometer	$\bar{\delta}_{in}$ (‰)			$A_{\delta_{in}}$ (‰)	
	$\delta^{18}\text{O}$	$\delta^2\text{H}$	<i>dex</i>	$\delta^{18}\text{O}$	$\delta^2\text{H}$
P-01	-9.20	-59.91	14.56	3.34	26.89
P-02	-9.50	-62.29	13.88	2.87	23.23
P-03	-9.20	-60.25	12.94	3.29	27.92
P-04	-8.60	-56.11	12.87	3.02	26.05
P-05	-8.60	-55.65	12.37	3.05	23.31
P-06	-7.80	-51.10	9.53	2.76	23.96
P-07	-7.50	-49.06	10.24	2.59	20.92
P-08	-7.50	-50.22	9.40	2.55	19.53

561

562

563 Table 3. Mean value $\bar{\delta}_{out}$ and amplitude $A_{\delta_{out}}$ of the seasonal variation in the isotopic content of
 564 groundwater for the springs sampled. For every spring, the elevation of the corresponding
 565 recharge zone Z_R is included. For this elevation, the associated amplitude $A_{\delta_{ZR}}$ of the seasonal
 566 variation in isotopic content of precipitation is shown.

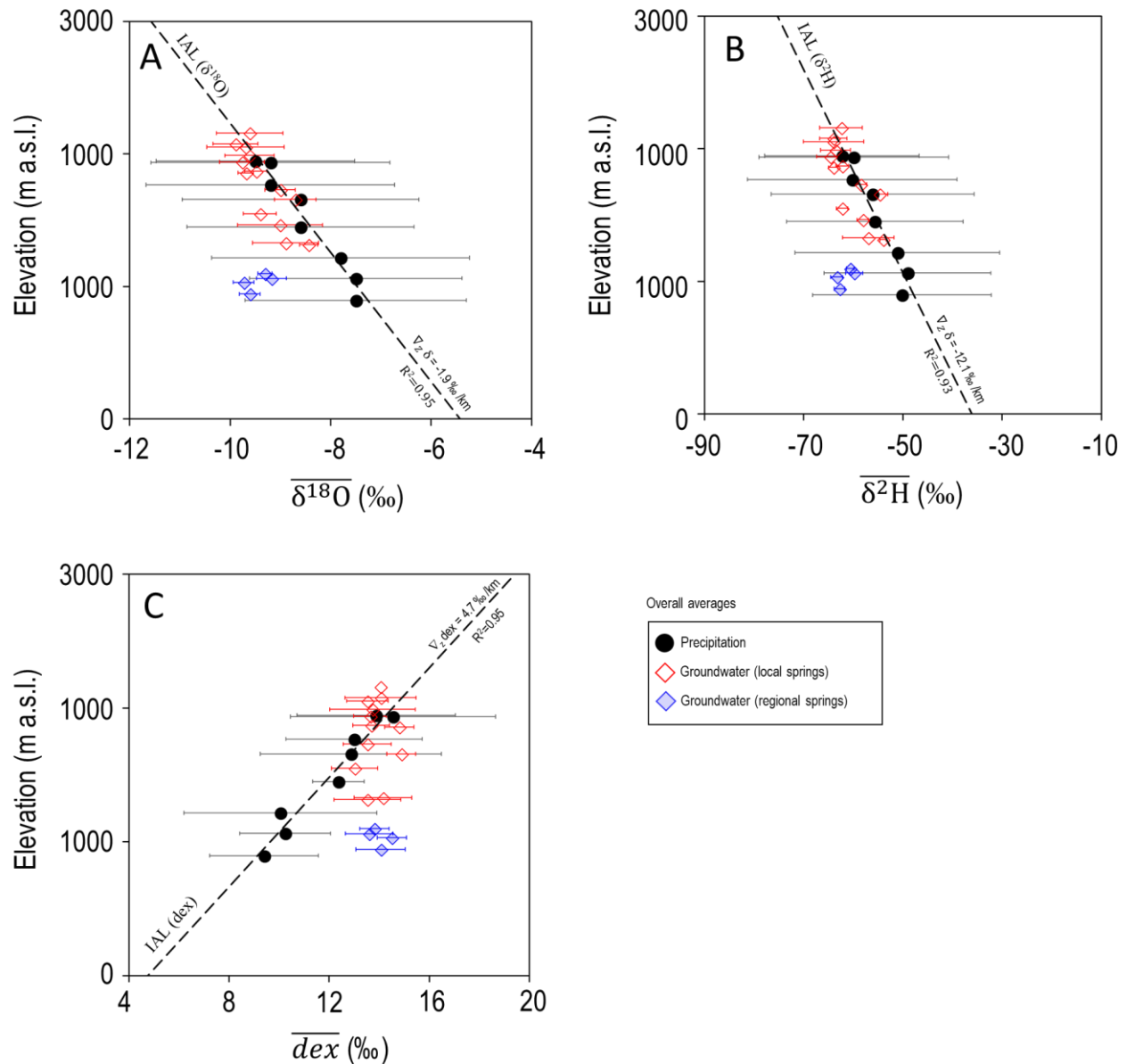
$\bar{\delta}_{out}$ (‰)	$A_{\delta_{out}}$ (‰)	Z_R (m a.s.l)	$A_{\delta_{ZR}}$ (‰)
--------------------------	------------------------	-----------------	-----------------------

Spring	$\delta^{18}\text{O}$	$\delta^2\text{H}$	dex	$\delta^{18}\text{O}$	$\delta^2\text{H}$	$\delta^{18}\text{O}$	$\delta^2\text{H}$	dex	$\delta^{18}\text{O}$	$\delta^2\text{H}$
S-01	-9,31	-60,65	13,81	0,12	1,10	1892	1881	1852	3,16	26,23
S-02	-9,61	-62,82	14,06	0,25	1,93	2038	2046	1902	3,24	27,18
S-03	-9,18	-59,85	13,60	0,11	1,07	1830	1819	1702	3,12	25,88
S-04	-9,01	-58,11	13,95	0,10	0,67	1745	1686	1881	3,07	25,12
S-05	-9,73	-63,36	14,50	0,14	0,88	2099	2088	1994	3,28	27,41
S-06	-9,69	-64,03	14,80	0,15	0,90	2078	2140	1798	3,27	27,71
M-05	-9,01	-58,53	13,52	0,44	1,81	1744	1718	1793	3,07	25,31
M-06	-8,70	-54,75	14,88	0,54	2,51	1597	1428	2071	2,98	23,65
M-08	-9,49	-62,22	13,68	0,27	1,84	1979	2001	1826	3,21	26,92
M-14	-9,69	-64,01	13,53	1,08	8,01	2079	2138	1795	3,27	27,70
M-15	-9,73	-63,81	14,05	0,87	6,24	2099	2123	1901	3,28	27,61
M-16	-9,77	-64,13	14,05	0,65	4,00	2118	2147	1902	3,29	27,75
M-17	-9,76	-64,32	13,73	0,49	2,86	2110	2161	1836	3,29	27,83
M-18	-9,59	-63,12	13,64	0,62	4,12	2031	2070	1817	3,24	27,31
M-24	-9,41	-62,26	13,02	0,47	1,64	1941	2004	1690	3,19	26,93
M-35	-8,90	-57,02	14,14	0,94	7,54	1690	1602	1920	3,04	24,65
M-37	-8,44	-54,00	13,53	0,26	0,93	1469	1371	1795	2,90	23,33

567

568 The mean isotopic content in rainfall $\bar{\delta}_{in}$ shows a clear-cut linear relationship with
569 elevation (Fig. 6) that allows defining Isotopic Altitudinal Lines (IAL) for $\delta^{18}\text{O}$, $\delta^2\text{H}$
570 and dex , with slopes (i.e., vertical gradients $\nabla_z\delta^{18}\text{O}$, $\nabla_z\delta^2\text{H}$ and $\nabla_z dex$) of -1,9, -12,1
571 and 4,7 ‰/km, respectively. Vertical gradients ($\nabla_z\delta$) of mean isotopic content in
572 precipitation are common in mountain zones (see Poage and Chamberlain, 2001, and
573 references therein) and are related to the atmospheric decreasing thermal vertical profile
574 existing along the slope of the mountains. $\nabla_z\delta$ values obtained for the study zone are
575 like those obtained in other alpine areas, especially in the central Pyrenees and the Alps
576 (Table 4).

577



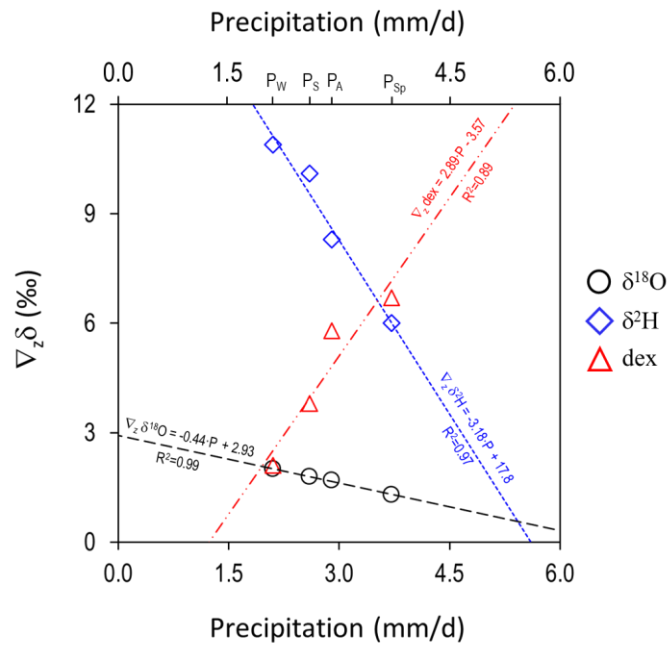
578

579 Fig. 6. Relationship between elevation and the mean isotopic content in precipitation and
 580 springs. (A) $\delta^{18}\text{O}$, (B) $\delta^2\text{H}$, and (C) \overline{dex} . Error bars indicate the standard deviation. Dashed lines
 581 indicate the local Isotopic Altitudinal Line (IAL) of precipitation.

582

583 The vertical gradients of the mean isotopic content in precipitation depend linearly on
 584 the mean seasonal precipitation (Fig. 7). In the case of $\delta^{18}\text{O}$ and $\delta^2\text{H}$, the higher the
 585 seasonal precipitation is, the lower the seasonal gradient is. In the case of \overline{dex} , the
 586 relationship is reversed, obtaining a higher $\nabla_z \overline{dex}$ value as seasonal precipitation

587 increases. In a seasonal framework, recycling moisture evaporated from the land surface
588 to atmosphere may increase dex of local precipitation. Soil evaporation is maximum
589 when atmospheric vapor pressure deficit ($\Delta e = e - e_{\text{sat}}$, e being the atmospheric water
590 pressure and e_{sat} the saturating water pressure at the air parcel temperature) is
591 maximum, if the soil contains water for evaporating. Therefore, to allow soil water to
592 evaporate, it is necessary to have enough (1) soil water content, which is higher in
593 spring and autumn since these are the rainiest seasons, and (2) atmospheric vapor
594 pressure deficits (Δe). Satisfying these two conditions, $\nabla_z dex$ is maximum when the
595 difference in dex (i.e., Δe) between the highest and the lowest points of the mountain
596 slope is maximum. Given that e_{sat} is an increasing function of temperature (Gonfiantini
597 et al., 2001), Δe will decrease as temperature declines. During the cold season, despite a
598 thermal difference existing between the highest and lowest points of the mountain, the
599 difference in Δe between these points is minimum. Additionally, the commented Δe
600 difference is minimum as well when there is no thermal difference along the mountain
601 slope, a situation that is favored by the cathabaltic winds in winter (Obleitner, 1994;
602 Gladich et al., 2011) but is also favored by the vertical atmosphere air mixing during the
603 typical summer local low pressure convective rainfall events.
604



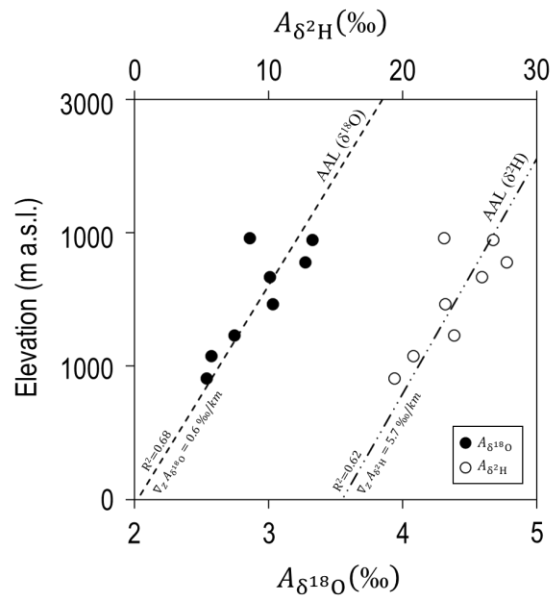
605

606 Fig. 7. Dependence of the vertical gradient of the mean isotopic content with respect to the
 607 mean seasonal precipitation. The subscripts Sp, S, A, and W stand for spring, summer, autumn
 608 and winter, respectively.

609

610 The amplitude of the seasonal variation in the isotopic content of precipitation $A_{\delta_{in}}$
 611 relates linearly to elevation (Fig. 8) to allow defining Amplitude Altitudinal Lines
 612 (AAL) for $\delta^{18}\text{O}$ and $\delta^2\text{H}$ with slopes (i.e., vertical gradients $\nabla_z A_{\delta^{18}\text{O}}$ and $\nabla_z A_{\delta^2\text{H}}$) of 0,6
 613 and 5,7 ‰/km, respectively. Similar vertical gradients have previously been reported in
 614 the central Pyrenees (Jóðar el al., 2016b) and the Bernese Alps (Jóðar el al., 2016a)
 615 (Table 4).

616



617

618 Fig. 8. Relationship between elevation and amplitude of the seasonal
 619 content ($\delta^{18}\text{O}$, $\delta^2\text{H}$) in precipitation. Dashed line and dashed-dotted line indicate the local
 620 Amplitude Altitudinal Lines (AALs) of precipitation for $\delta^{18}\text{O}$ and $\delta^2\text{H}$, respectively.

621

622 Table 4. Vertical gradients of mean isotopic water content and amplitude of the seasonal
 623 variation of the isotopic water content in precipitation.

	$Z_{\min} - Z_{\max}$	$\nabla_z \delta^{18}\text{O}$	$\nabla_z \delta^2\text{H}$	$\nabla_z dex$	$\nabla_z A_{\delta^{18}\text{O}}$	$\nabla_z A_{\delta^2\text{H}}$	Reference
Zone	(m a.s.l.)	(‰/km)	(‰/km)	(‰/km)	(‰/km)	(‰/km)	
Eastern Pyrenees (PCM ^a)	896-1936	-1,9	-15,2	4,7	0,6	6,1	This study
Central Pyrenees (PNOMP ^b)	772-2200	-2,2	-17,4	2,2	0,9	4,4	Jódar et al. (2016a)
Bernese Alps	874-2023	-3,0	-19,7	3,7	1,6	14,6	Jódar et al. (2016b)
Austrian Alps	580-2245	-1,9	-12,0	2,7	-	-	Froehlich et al. (2008)
Austrian Alps	469-1598	-1,3	-8,0	3,4	-	-	Froehlich et al. (2008)

Central (western flank)	Andes	2380-4250	-4,7	-42,5	2,2	-	-	Aravena et al. (1989)
Central (eastern flank)	Andes	2380-4250	-1,9	-14,3	1,1	-	-	Fiorella et al. (2015)
Central (eastern flank)	Andes	200-4080	-1,7	-11,7	2,0	-	-	Gonfiantini et al. (2001)
Western Carpathians		104-2008	-2,1	-	-	-	-	Holko et al. (2012)
Mount Cameroon		10-4050	-1,16	-11,4	1,4	-	-	Gonfiantini et al. (2001)

(a): Port del Comte Massif; (b): Ordesa and Monte Perdido National Park

624

625 The mean isotopic content of groundwater corresponding to local (perched) springs
626 shows a relationship with elevation dependence with a vertical gradient larger than that
627 of precipitation (Fig. 6), indicating the existence of aquifer recharge along the mountain
628 slope, a process also known as slope effect (Custodio and Jódar, 2016). Additionally,
629 the evolution of the isotopic content in the spring discharge shows a seasonal
630 dependence like precipitation but showing smaller amplitudes (Fig. B1 in Appendix B).
631 Even being lumped, the seasonal pattern of recharge is observed in the spring discharge,
632 indicating that MTT should not be longer than 5 or 6 years (DeWalle et al., 1997).

633

634 The isotopic altitudinal line (IAL, Fig. 6) allows estimation of the elevation of the
635 recharge zone (Z_R) corresponding to every spring by projecting their mean isotopic
636 content on IAL. Table 3 shows Z_R for all the springs, with their mean Z_R value ranging
637 between 1420 m a.s.l. (M-37) and 2136 m a.s.l. (M-17). With a known value for Z_R , it is
638 possible to calculate the amplitude of the variation in the isotopic content in
639 precipitation at the recharge zone elevation ($A_{\delta_{Z_R}}$) by projecting Z_R on the amplitude

640 altitudinal line (AAL, Fig. 8). Table 2 shows $A_{\delta_{ZR}}$ for every spring. Finally, if both $A_{\delta_{ZR}}$
641 (i.e., $A_{\delta_{in}}$ at the springs recharge zone) and $A_{\delta_{out}}$ are known, it is possible to obtain a
642 first analytical estimate of MTT through [Eq. 8]. Table 5 provides the MTT values
643 obtained for all the springs. As can be shown, the obtained MTT values range between
644 0,5 and 5 yr.

645

646

Table 5. MTT values estimated for the springs sampled

Spring	$\delta^{18}\text{O}$			$\delta^2\text{H}$		
	$\tau^a(\text{yr})$	$\tau^b(\text{yr})$	$\eta(-)$	$\tau^a(\text{yr})$	$\tau^b(\text{yr})$	$\eta(-)$
S-01	4,10	2,25	1,02	3,78	3,00	1,01
S-02	2,06	1,42	1,02	2,23	1,96	1,00
S-03	4,67	2,25	1,00	3,83	2,33	1,01
S-04	4,70	2,33	1,01	5,93	2,67	1,00
S-05	3,73	2,88	1,02	4,98	2,83	1,01
S-06	3,47	2,58	1,02	4,90	2,75	1,02
M-05	1,10	-	1,00	2,22	-	1,00
M-06	0,86	-	1,00	1,49	-	1,00
M-08	1,89	-	1,00	2,32	-	1,00
M-14	0,45	-	1,00	0,53	-	1,00
M-15	0,58	-	1,00	0,69	-	1,00
M-16	0,79	-	1,00	1,09	-	1,00
M-17	1,06	-	1,00	1,54	-	1,00
M-18	0,82	-	1,00	1,04	-	1,00
M-24	1,07	-	1,00	2,61	-	1,00
M-35	0,49	-	1,00	0,5	-	1,00
M-37	1,77	-	1,00	3,99	--	1,00

(a) Analytical MTT value obtained by [Eq. 8]. (b) Numerical MTT value
obtained by FlowPC.

647

648

649 **4.2 Aquifer recharge evaluation through HBV**

650 The HBV semi-distributed conceptual rainfall–runoff model has been used to simulate
 651 the observed groundwater discharge in every spring. The spring discharges were
 652 measured every fortnight between July 2013 and October 2015. This period has been
 653 used for calibrating the HBV parameters, which are shown in Table C4 (Appendix C).
 654 The efficiency parameter R_{eff} that describes the goodness of the model fit ranges
 655 between 0,55 (S-01) and 0,77 (S-05) (Table C5, Appendix C). The computed discharges
 656 resemble the observed discharges by reproducing their temporal evolution in all the
 657 springs (Fig. 3).

658

659 The results from the HBV model indicated that recharge is especially concentrated in
 660 the open areas (VZ_1) and meadow areas (VZ_2). The yearly average effective recharge
 661 ranges from 210 mm/yr (S-04) to 637 mm/yr (S-06) (Table 6). The aquifer infiltration
 662 capacity ξ (i.e., the ratio between Q_{Re} – the effective recharge of the aquifer, and P_{ZR} -
 663 precipitation at the spring recharge zone) ranges as the yearly average ranges from
 664 28,3% (S-03) to almost 62% (S-06) (Table 6).

665

666 Table 6. Mean annual precipitation P_{ZR} , mean aquifer recharge Q_R , seasonal distribution of
 667 recharge, infiltration capacity ξ .

Spring	P_{ZR}	Q_R	$\frac{Q_{Re\ Spring}}{Q_R}$	$\frac{Q_{Re\ Summer}}{Q_R}$	$\frac{Q_{Re\ Autumn}}{Q_R}$	$\frac{Q_{Re\ Winter}}{Q_R}$	ξ^a
	(mm/yr)	(mm/yr)	(%)	(%)	(%)	(%)	(%)
S-01	954	473	37,5%	15,0%	25,4%	22,1%	49,6%
S-02	1006	433	40,8%	12,3%	23,8%	23,1%	43,0%
S-03	793	227	38,1%	6,7%	27,2%	27,9%	28,6%

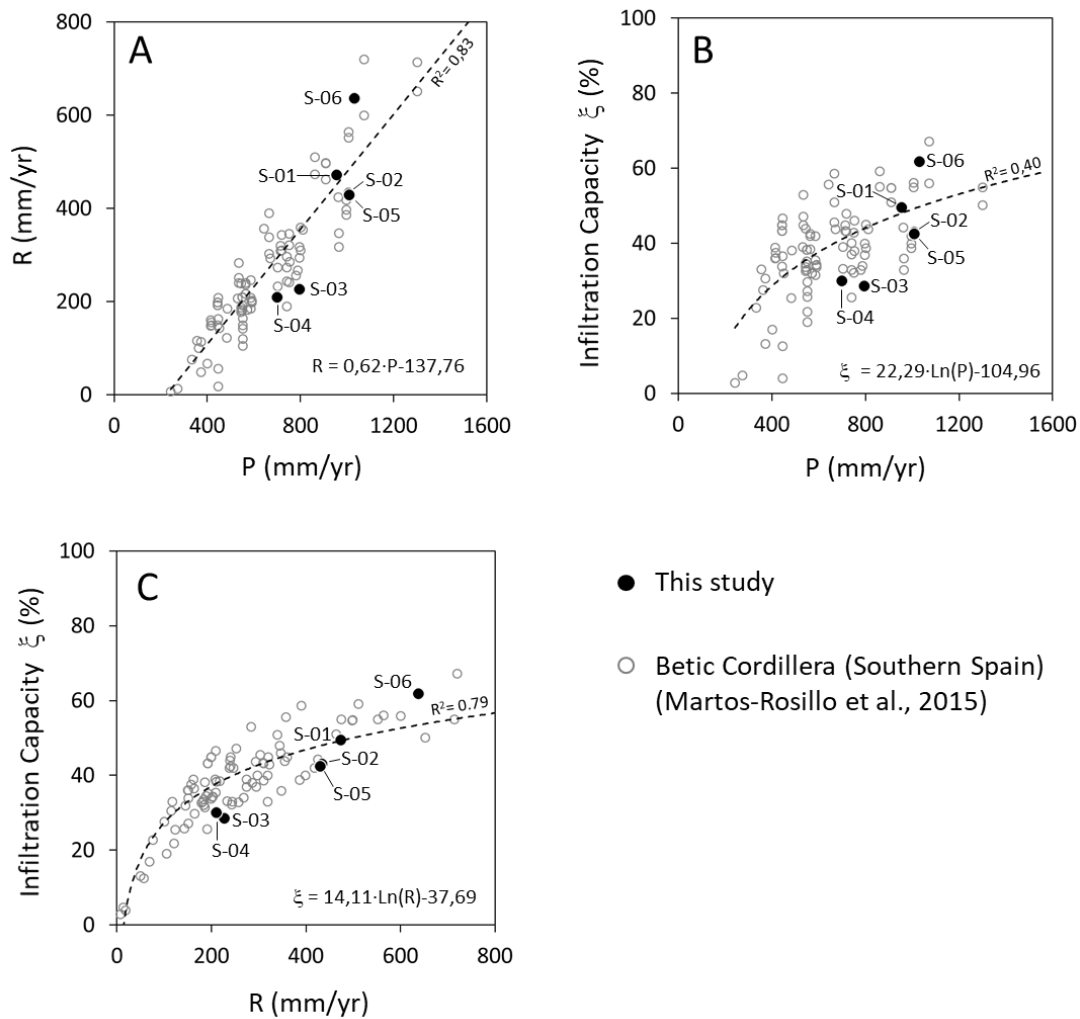
S-04	698	210	37,0%	10,2%	25,4%	27,4%	30,1%
S-05	1008	429	42,5%	14,3%	23,0%	20,2%	42,6%
S-06	1030	637	45,9%	8,9%	21,2%	24,0%	61,9%

(a) $\xi = Q_{R_e}/P_{ZR}$

668

669 Aquifer recharge follows a linear relationship similar to precipitation, as found by
670 Martos-Rosillo et al. (2015) for the mountain carbonate aquifers in the Betic Cordillera
671 (Southern Spain), where recharge is generally lower (Fig. 9A). In PCM, recharge is at a
672 maximum in spring, accounting for 40,3% of the total recharge, and this outcome is
673 explained by both rainfall and snow melt infiltration. Recharge is at a minimum (11,2%)
674 in summer, coinciding with the period of minimum seasonal precipitation.

675



676

677 Fig. 9. (A) Mean annual rainfall versus mean annual recharge, (B) Mean infiltration coefficient
 678 versus mean annual rainfall, and (C) Mean infiltration coefficient versus mean annual recharge.

679

680 The relationship between ξ and P (Fig. 9B) is not as clear as the relationship between ξ
 681 and R (Fig. 9C), indicating that precipitation is a necessary condition for aquifer
 682 recharge, but it is not enough. In this respect, the results of the application of the linear
 683 regression model between the variables Z_R , P_{ZR} , and VZ_1 , VZ_2 and VZ_3 , shows that the
 684 Z_R and is the most important predictor controlling the aquifer infiltration capacity ξ . In
 685 addition, VZ_1 (karren fields and sinkholes at the highest parts of the massif) and VZ_3
 686 (forest fields at the lowest of the massif) also play a role regarding ξ . These parameters

687 reflect the differences in both the karstification degree and the vegetation covering the
 688 epikarst system in the PCM.

689

690 Table 7. No standardized (λ) and standardized (β) regression coefficients associated with the
 691 explanatory variables used in the multiple regression method.

Explanatory Variable	λ	β
Intercept (λ_0)	-39,562	--
Z_R	0,047	0,823
P_{ZR}	-0,007	-0,054
VZ_1	6,034	0,133
VZ_2	4,018	0,072
VZ_3	258,518	0,122

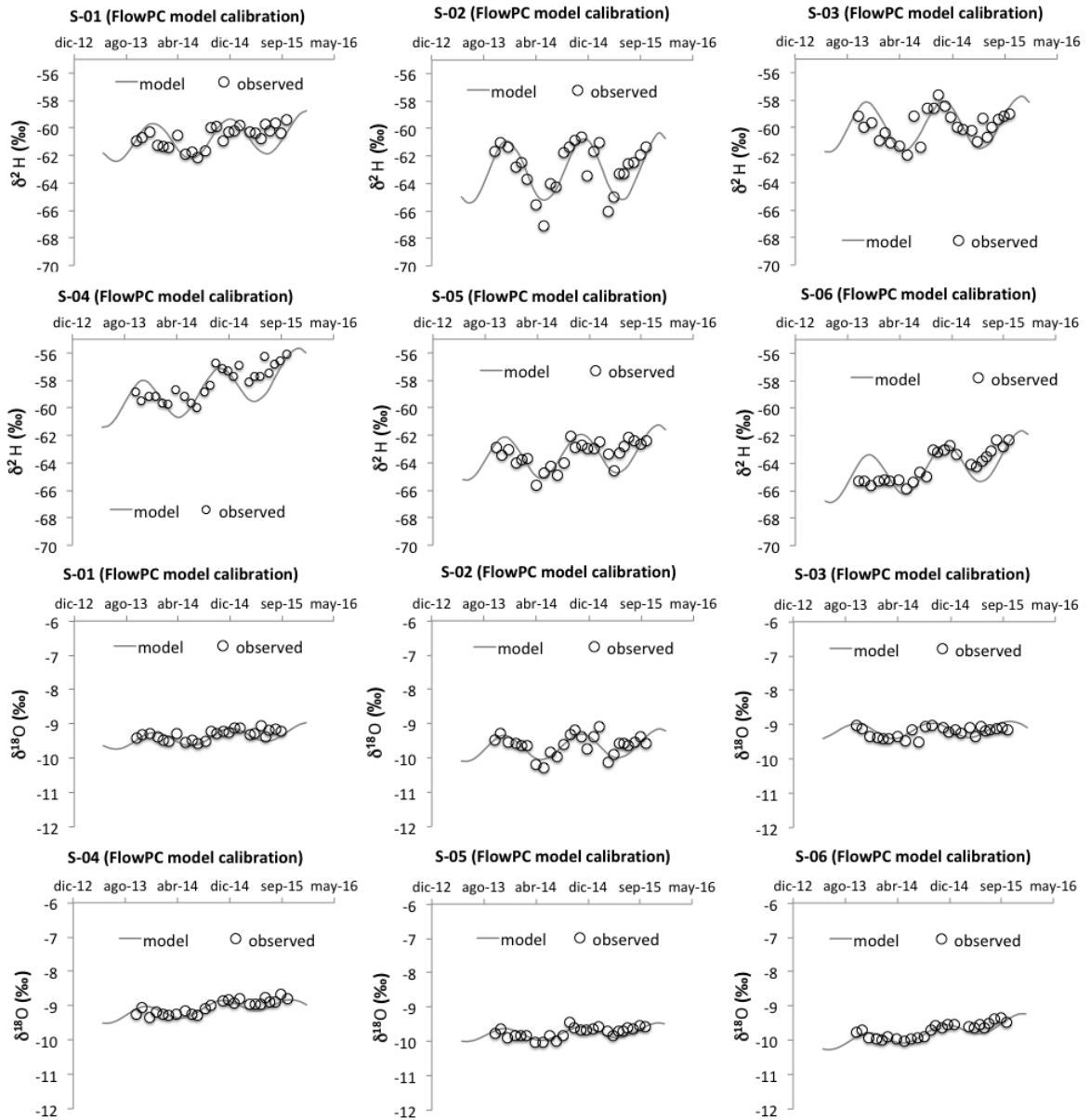
692

693

694 **4.3 Determination of spring discharge mean transit time**

695 To estimate the mean transit time of the spring discharge, the program FlowPC v3.2
 696 (Małoszewski and Zuber, 1996) has been used. According to the hydrogeological
 697 setting, it is assumed that the EPM flow model can describe the behavior of the aquifers
 698 discharging through the springs of PCM. The lumped model parameters (η and τ) have
 699 been calibrated (Table 5) by fitting the isotopic contents observed in the spring
 700 discharge from December 2013 to December 2015 (Fig. 10). The goodness of fit is
 701 defined in terms of RMSE, ranging between 0,02‰ (S-05) and 0,04‰ (S-02) for $\delta^{18}O$
 702 (Table D1, Appendix D), and between 0,17‰ (S-03) and 0,22‰ (S-04) for δ^2H (Table
 703 D2, Appendix D).

704



705

706 Fig. 10. Measured against simulated isotope content evolution with FlowPC and an EPM model.

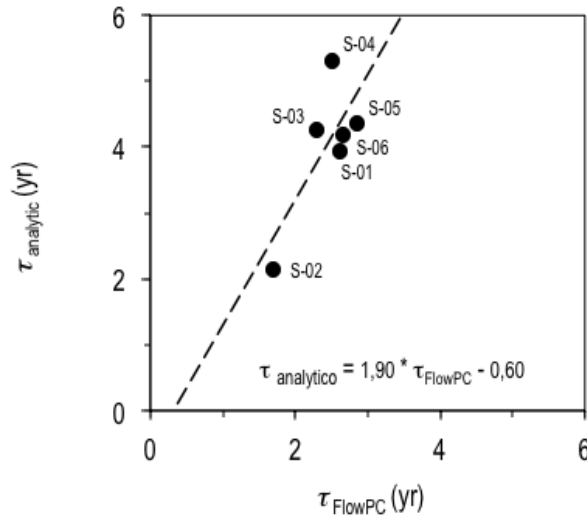
707 The gray line represents the best fit.

708

709 The estimated value of η is very close to 1 regardless of the spring, indicating that the
 710 corresponding aquifers behave as almost an exponential flow model in coherence with
 711 the behavior of a karst aquifer system discharging through a main spring. The estimated
 712 MTT with the applied methodology ranges between 1,69 yr (S-02) and 2,85 yr (S-05),

713 while in the case of the analytical approach MTT ranges between 2,14 yr (S-02) and
714 5,31 yr (S-04).

715



716

717 Fig. 11. Graph showing the MTT values estimated based on the lumped parameter model
718 FlowPC (Maloszewski, 1996) versus the MTT values estimated based on the analytical model
719 [Eq. 8] (Maloszewski et al., 1983)

720

721 The MTT values obtained by this numerical approach are 1,9 times shorter than the
722 MTT values analytically obtained through [Eq. 8] that compares the amplitude of the
723 seasonal isotopic content of recharge with the seasonal isotopic content in the spring
724 discharge [Fig 11]. In the numerical case, the monthly isotopic content in recharge is
725 weighted by the monthly volumetric recharge rate, whereas in the analytical case, the
726 isotopic content weighting coefficients for the monthly recharge are all equal to 1
727 because recharge is assumed constant (i.e., steady state) for the whole period covered by
728 the isotopic content time series. This assumption is worth keeping in mind when using
729 [Eq. 8] for estimating groundwater mean transit times. In other words, if aquifer
730 recharge shows a seasonal pattern, then the numerical approach should be used instead
731 of the analytical approach to estimate MTT. The transit time discrepancies between both

732 approaches may be critical when MTT is used as a vulnerability indicator for karst-
733 fissure aquifers (Malík et al, 2016). The results obtained suggest that the numerical
734 approach based explicitly on considering the recharge series in the LPM model provides
735 a more accurate evaluation of hydraulic dynamics throughout the system. This allows
736 better MTT estimations, similar of what concluded Vitvar et al. (1999) in pre-alpine
737 non-karst aquifers. The MTT values obtained in this work are consistent with the
738 conceptual model of the karst system. The aquifer presents specific zones with rapid
739 recharge through surficial karstic elements (e.g. swallow holes) and slow recharge
740 through meadows and forest.

741

742 In terms of MTT, the results obtained in this study are similar to those obtained in other
743 hydrological karst systems located in mountain zones: (1) In the case of the Ordesa and
744 Monte Perdido karst aquifer system (Central Pyrenees, Spain), which is the highest
745 calcareous massif in Western Europe, Lambán et al. (2015) and Jódar et al. (2016b)
746 estimated MMT for several springs. For each spring the authors fitted a sinusoidal
747 function [Eq. 1] to the measured tracer ($\delta^{18}\text{O}$ and $\delta^2\text{H}$) content time series
748 corresponding to rainfall entering the system as recharge and the spring discharge,
749 obtaining the amplitude of the seasonal variation of both the input and output system
750 tracer function ($A_{\delta_{\text{in}}}$ and $A_{\delta_{\text{out}}}$, respectively; Fig. 4). Besides, the authors assumed a
751 constant recharge rate along the year. This hypothesis allowed obtaining an analytical
752 solution to the convolution integral [Eq. 5] (Jódar et al., 2014) but also applying [Eq. 8]
753 to directly estimate MTT, that ranged between 1,12 and 4,48 yr.

754

755 (2) In the Wimbach high-alpine karst system (Berchtesgaden Alps) Einsiedl et al.
756 (2009) estimated MTT with FlowPC. To this end, they used as tracer input function the

757 time series of ^3H content in rainfall measured in a meteorological station close to the
758 study zone, and as system output the time series of ^3H content in groundwater discharge
759 for different springs and also at the outlet of the hydrological catchment. They obtained
760 MTT ranging between 4 and 5 yr for the considered springs, and 5 yr for the whole
761 hydrologic catchment. For the same catchment, Maloszewski et al. (1992) evaluated the
762 MTT by using monthly recharge time series instead of rainfall time series. The aquifer
763 recharge time series was obtained by applying a seasonal infiltration coefficient to the
764 observed monthly precipitation time series. With this approach they estimated a MTT of
765 4,15 yr. This value is close to that obtained by Einsiedl et al. (2009). Additionally,
766 Garvelmann et al. (2017) expanded the previous studies in the Berchtesgaden Alps for a
767 total of eight springs. For each spring they estimated MTT using two different methods;
768 (A) by numerically solving the convolution integral [Eq. 5], and (B) though [Eq. 8] by
769 previously conducting a sin-wave analysis [Eq. 1] to the input (i.e. rainfall) and output
770 tracer functions. The MTT obtained by both methods did not show large discrepancies
771 for the same spring. In terms of the obtained MTT the sampled springs were be
772 classified in two groups: a first group with relatively short MTTs (0,7 to 1,9 yr) and a
773 second group with longer MTTs (7,3 to 12,5 yr).

774

775 (3) In the Schneealpe massif Rank et al. (1992) used the environmental tracers to study
776 the karstic-fissured-porous aquifer system of Schneealpe, The aquifer system that is
777 drained by two principal springs is the main drinking water resource for Vienna
778 (Austria). It is composed of a fissured-porous aquifer with a high storage capacity that
779 partially feeds a karst aquifer conformed by a high- conductivity drainage channel
780 network. For each aquifer they estimated MTT by calibrating a LPM with a 8 years long
781 time series of environmental tracer data, using ^3H and $\delta^{18}\text{O}$ for the fissured-porous and

782 the karst aquifer, respectively. In the former case MTTs ranged between 2,5 and 4,5 yr,
783 whereas in the karst aquifer the estimated MTT was only 2 months. Maloszewski et al.
784 (2002) recalibrated both LPMs by refining and extending up to 20 years the length of
785 the observed time series of ^3H and $\delta^{18}\text{O}$ measurements. In the case of the fissured-
786 porous aquifer the obtained MTTs ranged between 14 and 26 yr, being significantly
787 larger than those obtained by Rank et al (1992). Nevertheless, in the case of the karst
788 aquifer the obtained MTTs were similar ranging between 1,2 and 1,5 months. The large
789 discrepancy between the MTT associated to the Fissured-Porous and karst aquifer
790 indicates that water enters the aquifer system at the surface and flows through it towards
791 the conductive drainage channels until reaching the springs. Nevertheless, the short
792 MTTs associated to the karst aquifer reveal a direct hydraulic connection between the
793 sinkholes at the surface and the drainage channel network.

794

795 (4) In the Wetterstein Mountains karst aquifer system Lauber and Goldscheider (2014)
796 used both artificial (uranine) and environmental tracers (^{18}O and ^2H) to investigate the
797 hydrological behavior of the system. Despite the low recovery of artificial tracer during
798 the tracer test, the fast tracer arrival observed in all the sampled springs, with peak times
799 between 1,8 and 3,2 days, indicates as in the previous case, the existence of well-
800 developed flow paths through thick (>1000 m) USZ. This result underlines the role that
801 may play the USZ conditioning the hydrologic response of the karst system. The
802 authors estimated the aquifer MTT with FlowPC by using as input tracer content that of
803 precipitation, and assuming a constant (without any seasonality) aquifer recharge rate.
804 The obtained MTT values ranged between 3 and 5 months, being significantly shorter
805 than those MTT presented above for the other karst systems.

806

807 The hydrological system MTT reflects the diversity of aquifer flow paths and
808 groundwater mixing from the recharge zone to the discharge point. Considering that the
809 different aquifers constituting the PCM show an exponential flow model (EM)
810 behavior, and provided that MTT (τ ; Table 5) and the aquifer mean recharge flow rate
811 (Q_R ; Table 6) are known, it is possible to estimate the aquifer storage (i.e., mixing)
812 volume by using [Eq. 7]. In Table 8, the stored dynamic volume ('mobile water volume
813 $-V_m$ '; Małoszewski and Zuber (2002); where: $V_m = Q_R \cdot \tau$) is associated with the
814 catchment areas (Fig. A1 of the Appendix A) discharging through the springs S-01 to S-
815 06. S-05 and S-02 play a major role in terms of both groundwater discharge and aquifer
816 storage. The springs S-05 and S-02 present a similar area and a similar discharge.
817 Nevertheless, from a geometrical point of view, they are different: S-05 is rounded in
818 shape whereas S-02 is elongated. Considering that aquifer recharge is produced mainly
819 in the highest parts of PCM, it is clear that the distance between the recharge and
820 discharge points is larger in the case of S-02. This difference is interesting if one
821 considers that the mean transit time of S-02 is shorter than the mean transit time of S-
822 05. The shorter transit time would indicate a higher development of the karst water
823 conducting features in the catchment area of S-02. The springs S-04 and S-06 denote
824 their perched character with the associated low discharge flow rates and groundwater
825 reserve volumes.

826

827 Table 8. Estimation of dynamic volume V_m stored in the aquifer for the springs analyzed

Spring	V_m (hm ³)
S-01	2,44 + 0,49
S-02	11,54 + 2,61
S-03	1,72 + 0,04

S-04	0,03 + 0,01
S-05	19,39 + 0,20
S-06	0,09 + 0,01

828

829 The few available groundwater level depth data from old water wells in the PCM
830 suggest the karst aquifer presents low regional hydraulic gradients in the phreatic zone
831 ranging between 1 - 2%. Nevertheless, while considering the expected mean phreatic
832 level above the horizontal plane from the spring levels (i.e., the groundwater that
833 contributes to each spring discharge), the 3D geological model evaluates the total
834 aquifer formation volume (V_{aq}) associated with the regional springs S-01, S-02, S-03
835 and S-05. Assuming V_{aq} as known, the mean aquifer interconnected porosity (ϕ) can
836 therefore be estimated as the ratio V_{GW}/V_{aq} . In the PCM, the average ϕ obtained is
837 3,1%. This result agrees with the value obtained for other carbonate aquifers of the
838 Betic Cordillera (Southern Iberian Peninsula) with an average value of 3% (Pulido-
839 Bosch et al., 2004; Martos- Rosillo et al., 2014).

840

841 This work is aimed to characterize the hydrological behavior of a high mountain karst
842 system with a overlaying thick UZS that plays a relevant role along with in the system
843 response. The applied approach allows accounting the effects of the extreme alpine
844 climate conditions on both the aquifer recharge rates and the isotopic composition of
845 recharge. The used approach provides a more reliable assessment of the hydrological
846 behavior of these alpine karst systems than the obtained applying the traditional
847 approaches found in the scarce bibliography. The methodology used in this work for
848 characterizing the hydrological behavior of PCM can be applied in many analogue high
849 mountain karst systems whose hydrologic behavior still remains unknown. In this sense,
850 Table 9 shows a brief summary of the available bibliography at the pan-European zone

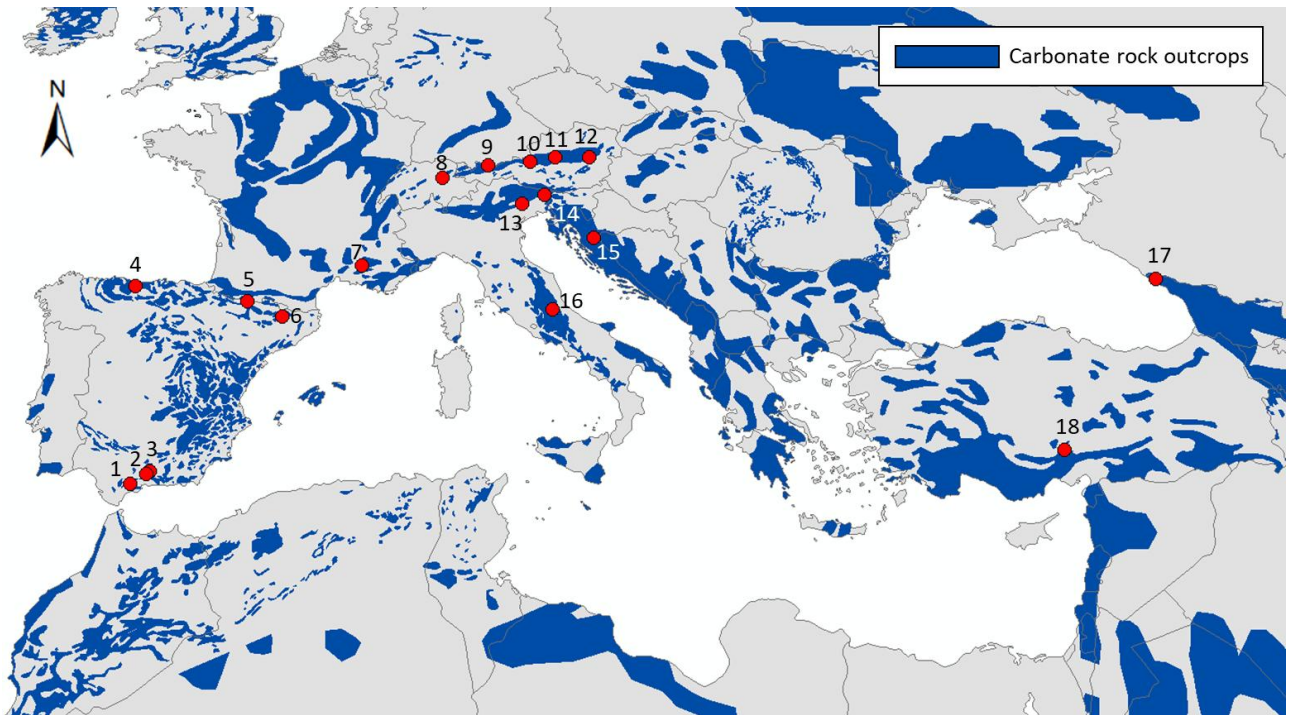
851 focused on high-mountain karst aquifers with a thick USZ in which this methodology
 852 could be tested (Fig. 12).

853

854 Table 9. Brief summary of published research studies of groundwater flow karst systems in
 855 mountain areas with thick USZ the pan-European zone.

Code	High mountain karst system	NSZ Thickness	Reference
1	Yunquera-Sierra de las Nieves	1000	Andreo et al. (2004); Pardo-Iguzquiza et al. (2015)
2	Alta Cadena	700	Mudarra and Andreo (2011)
3	Sierra Gorda	500	Mudarra and Andreo (2015)
4	Picos de Europa	1500	Ballesteros et al. (2015a); Ruiz and Poblete (2012)
5	Ordesa y Monte Perdido	1500	Lambán et al. (2015); Jódar et al. (2016b)
6	Port del Comte	1000	(This research)
7	Fontaine Vaucluse	800	Fleury et al. (2007)
8	Schlichenden Brünnen - Muotathal	1000	Jeannin (2001)
9	Wetterstein Mountains (Zugspitze)	1000	Lauber and Goldscheider (2014)
10	Wimbachtal catchment	1500	Maloszewski et al. (1992)
11	Totes Gebirge	1000	Laimer (2010)
12	Schneealpe Massif	900	Rank et al 1992; Maloszewski et al. (2002)
13	Cansiglio-Cavallo karst aquifer	800	Filippini et al. (2018)
14	Mount Kanin	2000	Zini et al. (2015); Turk et al. (2015)
15	Gacka	1000	Ozyurt et al. (2014)
16	Gran Sasso aquifer	1500	Falcone et al. (2008); Amuroso et al. (2013)
17	Arabika Massif	2500	Klimchouk (2009)
18	Aladaglar Mountains	2000	Ozyurt and Bayari (2008)

856



858

859 Fig. 12. Spatial distribution of carbonate rock outcrops at the pan-Mediterranean zone. Red
 860 points indicate the position of those high mountain karst aquifers zones with a thick (<500 m)
 861 NSZ referenced in the existing bibliography (map modified from the *World Map of Carbonate*
 862 *Rock Outcrops v.3.0*. Source: http://www.fos.auckland.ac.nz/our_research/karst). Numbers in
 863 bullets correspond to the codes shown in Table 9.

864

865 **4.4 Evaluation of results for groundwater management purposes**

866 MTT is a corner stone for groundwater management strategies, and many authors have
 867 used this variable as a proxy of vulnerability assessment in hydrogeological systems
 868 (Einsiedl et al., (2009) and Malik et al., (2016), among others). This work provides the
 869 first estimation of the MTT associated with most important springs discharging the
 870 PCM karst system. From the perspective of aquifer vulnerability, the intensive cattle
 871 grazing conducted in the PCM is the most threading activity to the groundwater
 872 resources stored in the underlying aquifer so far. The relatively large MTTs (2,25 yr)
 873 along with the exponential flow model describing the hydrologic behavior of PCM,

874 points to groundwater mixing as a natural attenuation/dilution process inside the aquifer
875 system. However, it must be taken in mind that the presence of unnoticed but likely
876 well-developed flow paths through the USZ and also the existence of karst conductive
877 features in the saturated zone of the PCM may favor fast contaminant migration from
878 the recharge areas to the groundwater discharge points of this aquifer system, but this is
879 investigation is out of the scope of this work.

880

881 From the perspective of water resources management the storage and dynamic volumes
882 associated with the PCM aquifer system are also valuable information obtained in this
883 study. In this line, it is worth to comment that the PCM aquifer system has an integrated
884 groundwater storage capacity (V_{GW}) of 35,2 hm³, and generates an overall mean annual
885 groundwater discharge of 15,35 hm³/yr, that represents 15% of the mean annual water
886 consumption in the city of Barcelona (Barcelona City Council, 2018). Moreover, the
887 average discharge of S-05, which is one of the main groundwater springs of the PCM
888 represents 7% of the mean annual water consumption of Barcelona city. This discharge
889 tributes to the Llobregat River Basin, which in turns provides critical water resources to
890 the Barcelona metropolitan area. It is important keeping these numbers in mind to
891 estimate the water resources availability given the increased frequency and severity of
892 the Mediterranean droughts reported by the experts (Hoerling et al., 2012; Vicente-
893 Serrano et al., 2014).

894

895 In the Pyrenean range, climate models forecast a precipitation decrease up to 14% with
896 respect to the observed mean precipitation and a temperature increase between 2 and 4
897 °C that will reduce the amount of solid precipitation and the corresponding snowmelt
898 runoff (López-Moreno et al., 2008, 2009). In addition, the duration of the snowpack will

899 be shorter, shifting the timing of the snowmelt (Adam et al., 2009). The PCM is in the
900 pre-Pyrenean zone to the South of the Pyrenean axial zone. Here, the elevation of the
901 mountains is lower, and the climate conditions are not so severe, accelerating the impact
902 of the forecast temperature increase on snow precipitation, snowmelt runoff generation
903 and the dynamics of the hydrological systems located in this area. Therefore, the
904 geographical and hydrogeological settings of the PCM, along with the groundwater
905 transit times calculated, make the PCM aquifer system an exceptional observatory for
906 anticipating and studying the climate change impact on southern Europe. In this line, it
907 would be extremely important to maintain the observation research program to fully
908 understand the hydrogeological behavior of this aquifer system.

909

910 **4.5 Future works in PCM**

911 This study is the first stage in the full hydrogeological characterization of this aquifer
912 system. The next step is to conduct the hydrogeochemical characterization of recharge
913 and groundwater springs discharge to complement the results obtained in this work by
914 focusing in relevant unsolved questions like (1) the role play by the epikarst zone in the
915 total transit time of groundwater and how this role is reflected in the hydrogeochemical
916 evolution of the springs discharge after important rainfall events and during low-flows
917 and (2) the use of artificial tracers and environmental isotopes (e.g. ^{34}S , ^{15}N) to
918 characterize not only the mean transit time (i.e. the first moment of the transit-time
919 distribution) but also to profile the groundwater transit-time distribution in terms of fast,
920 intermediate and slow groundwater flows. This investigation is crucial to evaluate the
921 aquifer vulnerability.

922 **5. Conclusions**

923 A distributed rainfall-runoff model and a lumped-parameter model have been combined
924 to estimate MTT in high-mountain karst systems with an overlying thick unsaturated
925 zone by using the stable isotopes of precipitation as environmental tracers. The
926 presented approach accounts for the effects of the alpine climate conditions on both the
927 aquifer recharge rates and the isotopic composition of recharge. The used approach
928 provides a more reliable assessment of mean transit time compared to traditional
929 methods for such alpine karst systems.

930

931 The approach presented in this work has been used to characterize the hydrological
932 behavior of the Port del Comte Massif, a high mountain karst aquifer with a 1000 m
933 thick unsaturated zone located in the southeastern part of the Pyrenees. The percentage
934 of precipitation that enters into the hydrogeological system as aquifer recharge reaches
935 61,9% (the highest studied spring in the area). This elevated infiltration capacity is
936 controlled by the presence of karren fields and sinkholes at the highest parts of Port del
937 Comte Massif, at elevations between 2050 and 2300 m a.s.l. The evolution of the
938 isotopic content in the sampled springs shows a sinusoidal pattern that reflects the
939 seasonal variation of the isotopic composition of recharge. This is consistent with the
940 relatively short groundwater transit times (2,25 yr) obtained for the hydrological system,
941 which is in agreement with its karstic nature of the aquifer system, and emphasizes the
942 high vulnerability of the aquifer system to variations in recharge.

943

944 The mean annual groundwater discharge and the mean water storage of the Port del
945 Comte Massif hydrogeological system represent 16 and 34% of the mean annual water
946 consumption in the city of Barcelona, underlying the important role as a strategic water

947 resource that the Port del Comte Massif may play for stakeholders and water resources
948 managers when facing the drought episodes that the Mediterranean region iteratively
949 suffers. Moreover, given the geographical position of the study zone, located to the
950 south of the Pyrenean axial zone, and the hydrogeological settings of the associated
951 karst aquifer system, the Port del Comte Massif is an exceptional watchtower for
952 anticipating the impact of climate change in Southern Europe.

953

954

955 **6. Acknowledgments**

956 This research was supported by Agencia Estatal de Investigación (AEI) from the
957 Spanish Government and the European Regional Development Fund (FEDER) from
958 EU, REMEDIATION (CGL2014-57215-C4-1-R), and PACE-ISOTEC (CGL2017-
959 87216-C4-1-R) projects, the PIRAGUA project (EFA210/16/ PIRAGUA) which is
960 funded by the European Union through the Interreg-POCTEFA territorial cooperation
961 program, the Catalan Government projects to support consolidated research groups
962 MAG (Mineralogia Aplicada, Geoquímica i Geomicrobiologia, 2017SGR-1733) from
963 Universitat de Barcelona (UB) and GREM (Grup de Recerca de Minería Sostenible)
964 from the Universitat Politècnica de Catalunya (UPC), and the Junta de Andalucía
965 research group RNM-308 (Hydrogeology Group). We also thank the Institut Cartogràfic
966 i Geològic de Catalunya (Hydrogeology and Geothermics Team) and CCiT from the
967 Universitat de Barcelona (UB) for their technical assistance, and especially Raul Carrey
968 from the MAiMA group for the help in the laboratory analyses. The Meteorological
969 Service of Catalonia (SMC) has kindly provided the meteorological data. The
970 constructive comments and interesting suggestions from four anonymous reviewers are
971 greatly appreciated since they have led to a substantial improvement of the final article

972

973 **7. References**

974 Adam, J.C., Hamlet, A.F., & Lettenmaier, D.P., 2009. Implications of global climate
975 change for snowmelt hydrology in the twenty-first century. *Hydrological
976 Processes: An International Journal*, 23(7), 962-972.
977 <https://doi.org/10.1002/hyp.7201>

978 Agencia Estatal de Meteorología de España (AEMET) and Instituto de Meteorologia –
979 Portugal (IMA). 2011. Iberian climate atlas. Air temperature and precipitation
980 (1971-2000).
981 [https://www.aemet.es/documentos/es/conocerlas/publicaciones/Atlas-
982 climatologico/Atlas.pdf](https://www.aemet.es/documentos/es/conocerlas/publicaciones/Atlas-climatologico/Atlas.pdf)

983 Allocca, V., De Vita, P., Manna, F., Nimmo, J.R. 2015. Groundwater recharge
984 assessment at local and episodic scale in a soil mantled perched karst aquifer in
985 southern Italy. *Journal of Hydrology*, 529 (2015) 843–853.
986 <https://doi.org/10.1016/j.jhydrol.2015.08.032>

987 Amin I.E., Campana, M.E. 1996. A general lumped parameter model for the
988 interpretation of tracer data and transit time calculation in hydrologic systems. *J
989 Hydrol*; 179 (1–4):1–21 [https://doi.org/10.1016/0022-1694\(95\)02880-3](https://doi.org/10.1016/0022-1694(95)02880-3)

990 Andreo, B., Linan, C., Carrasco, F., De Cisneros, C. J., Caballero, F., Mudry, J. 2004.
991 Influence of rainfall quantity on the isotopic composition (^{18}O and ^2H) of water
992 in mountainous areas. Application for groundwater research in the Yunquera-
993 Nieves karst aquifers (S Spain). *Applied Geochemistry*, 19(4), 561-574.
994 <https://doi.org/10.1016/j.apgeochem.2003.08.002>

995 Araguás-Araguás, L.J., Díaz-Teijeiro, M.F. 2005. Isotope composition of precipitation
996 and water vapour in the Iberian Peninsula. In “Isotopic Composition of

997 Precipitation in the Mediterranean Basin in Relation to Air Circulation Patterns
998 and Climate” (pp. 173-190). IAEA-TECDOC-1453.

999 Aravena, R., Peña, H., Grilli, A., Suzuki, O., Mordeckai, M., 1989. Evolución isotópica
1000 de las lluvias y origen de las masas de aire en el altiplano chileno. Isotope
1001 hydrology investigations in Latin America. IAEA-TECDOC-502. IAEA, Vienna,
1002 pp. 129–142.

1003 Bakalowicz, M. (2005). Karst groundwater: a challenge for new resources.
1004 Hydrogeology Journal, 13(1), 148-160. [https://doi.org/10.1007/s10040-004-0402-](https://doi.org/10.1007/s10040-004-0402-9)
1005 9

1006 Ballesteros, D., Jiménez-Sánchez, M., Giralt, S., García-Sansegundo, J., Meléndez-
1007 Asensio, M. 2015a. A multi-method approach for speleogenetic research on alpine
1008 karst caves. Torca La Texa shaft, Picos de Europa (Spain). *Geomorphology*, 247,
1009 35-54.

1010 Ballesteros, D., Arnauld Malard., A., Pierre-Yves Jeannin, P-Y., Jimenez-Sanchez M.,
1011 García-Sansegundo, J., Meléndez-Asensio, M., Sendra, G. 2015b. KARSYS
1012 hydrogeological 3D modeling of alpine karst aquifers developed in geologically
1013 complex areas: Picos de Europa National Park (Spain). *Environ Earth Sci.*
1014 Volume 74, Issue 12, pp 7699–7714. <https://doi.org/10.1007/s12665-015-4712-0>

1015 Barberá, J.A., Jódar, J., Custodio, E., González-Ramón, A., Jiménez-Gavilán, Vadillo,
1016 I., Pedrera, A., Martos-Rosillo, S., 2018a. Groundwater dynamics in a
1017 hydrologically-modified alpine watershed from an ancient managed recharge
1018 system (Sierra Nevada National Park, Southern Spain): insights from
1019 hydrogeochemical and isotopic information. *Science of the Total Environment*
1020 640–641, 874–893, <https://doi.org/10.1016/j.scitotenv.2018.05.305>

- 1021 Barberá, J. A., Mudarra, M., Andreo, B., De la Torre, B., 2018b. Regional-scale
1022 analysis of karst underground flow deduced from tracing experiments: examples
1023 from carbonate aquifers in Màlaga province, southern Spain. *Hydrogeology*
1024 *Journal*, 26(1), 23-40. <https://dx.doi.org/10.1007/s10040-017-1638-5>
- 1025 Barcelona City Council, 2018. Evolution of water consumption in the city of Barcelona.
1026 <http://www.bcn.cat/estadistica/angles/dades/economia/consum/evoconsum/coev04>
1027 [.htm](#) (last access 08/07/2018).
- 1028 Barnett, T.P., Adam, J.C., Lettenmaier, D.P., 2005. Potential impacts of a warming
1029 climate on water availability in snow-dominated regions. *Nature*, 438(7066),
1030 <https://dx.doi.org/10.1038/nature04141>
- 1031 Bergström, S., 1976. Development and Application of a Conceptual Runoff Model For
1032 Scandinavian Catchments, SMHI, Report No. RHO 7 (134 pp Norrköping).
- 1033 Braun, L.N., Renner, C.B., 1992. Application of a conceptual runoff model in different
1034 physiographic regions of Switzerland. *Hydrological Sciences Journal*, 37(3), 217-
1035 231. <https://doi.org/10.1080/02626669209492583>.
- 1036 Butscher C, Huggenberger P., 2007. Implications for karst hydrology from 3D
1037 geological modeling using the aquifer base gradient approach. *J Hydrol*; 342 (1–
1038 2):184–98. <https://doi.org/10.1016/j.jhydrol.2007.05.025>
- 1039 Celle-Jeanton, H., Travi, Y., Blavoux, B., 2001. Isotopic typology of the precipitation in
1040 the Western Mediterranean region at three different time scales. *Geophysical*
1041 *Research Letters*, Vol. 28, no. 7, pages 1215-1218
- 1042 Cervi, F., Marcaccio, M., Petronici, F., Borgatti, L., 2014. Hydrogeological
1043 characterization of peculiar Apenninic springs. *Proceedings of the International*
1044 *Association of Hydrological Sciences*, 364, 333-338.

1045 Chen, Z., 2017. Modeling a geologically complex karst aquifer system, Hochifen-
1046 Gottesacker, Alps. PhD. Thesis. Karlsruher Instituts für Technologie, Germany.
1047 <https://d-nb.info/1136660852/34>

1048 Chueca, J., Julián, A., López-Moreno, J.I., 2007. Recent evolution (1981–2005) of the
1049 Maladeta glaciers, Pyrenees, Spain: extent and volume losses and their relation
1050 with climatic and topographic factors. *Journal of glaciology*, 53(183), 547-557.
1051 <https://doi.org/10.3189/002214307784409342>

1052 Clark, I.D., Fritz, P. 1997. *Environmental isotopes in hydrogeology*. Lewis Publishers,
1053 New York.

1054 Coplen 2011. Guidelines and recommended terms for expression of stable-isotope-ratio
1055 and gas-ratio measurement results. *Rapid Commun. Mass Spectrom.* 2011, 25,
1056 2538–2560.

1057 CREAM, 2009. Land Cover Map of Catalonia (MCSC) 1:250,000. 4a edition (2009).
1058 <http://www.creaf.uab.es/mcsc/usa/index.htm>

1059 Custodio, E., Llamas, M.R. (Eds.), 1976. *Hidrología subterránea [Groundwater*
1060 *hydrology]*. 2 Vols: 1–2350. Ediciones Omega, Barcelona.

1061 Custodio, E., Jódar, J., 2016. Simple solutions for steady–state diffuse recharge
1062 evaluation in sloping homogeneous unconfined aquifers by means of atmospheric
1063 tracers. *J. Hydrol.* <http://dx.doi.org/10.1016/j.jhydrol.2016.06.035>

1064 De Jong, C., Lawler, D., Essery, R., 2009. Mountain hydroclimatology and snow
1065 seasonality and hydrological change in mountain environments. *Hydrological*
1066 *Processes* 23, 955–961. <https://doi.org/10.1002/hyp.7193>

1067 De Walle, D.R., Edwards, P.J., Swistock, B.R., Aravena, R., Drimmie, R.J., 1997.
1068 Seasonal isotope hydrology of three Appalachian forest catchments. *Hydrological*

1069 Processes, 11(15), 1895-1906. [https://doi.org/10.1002/\(SICI\)1099-](https://doi.org/10.1002/(SICI)1099-)
1070 1085(199712)11:15<1895::AID-HYP538>3.0.CO;2-#

1071 Einsiedl, F., 2005. Flow system dynamics and water storage of a fissured-porous karst
1072 aquifer characterized by artificial and environmental tracers. *J Hydrol* 312:312–
1073 321. <https://doi.org/10.1016/j.jhydrol.2005.03.031>

1074 Einsiedl, F., Maloszewski, P., Stichler, W., 2009. Multiple isotope approach to the
1075 determination of the natural attenuation potential of a high-alpine karst system.
1076 *Journal of Hydrology* 365 (2009) 113–121.
1077 <https://doi.org/10.1016/j.jhydrol.2008.11.042>

1078 Epting, J., M. Page, R., Auckenthaler, A., Huggenberger, P. 2018. Process-based
1079 monitoring and modeling of Karst springs – Linking intrinsic to specific
1080 vulnerability. *Sci. Total Environ.* 625, 403-415-
1081 <https://doi.org/10.1016/j.scitotenv.2017.12.272>

1082 Falcone, R.A., Falgiani, A., Parisse, B., Petitta, M., Spizzico, M., Tallini, M. 2008.
1083 Chemical and isotopic ($\delta^{18}\text{O}\%$, $\delta^2\text{H}\%$, $\delta^{13}\text{C}\%$, ^{222}Rn) multi-tracing for
1084 groundwater conceptual model of carbonate aquifer (Gran Sasso INFN
1085 underground laboratory–central Italy). *Journal of hydrology*, 357(3-4), 368-388.

1086 Farlin, J., Maloszewski, P., 2013. On the use of spring baseflow recession for a more
1087 accurate parameterization of aquifer transit time distribution functions. *Hydrology*
1088 *and Earth System Sciences*, 17(5), 1825-1831. <https://doi.org/10.5194/hess-17->
1089 1825-2013

1090 Fiorella, R.P., Poulsen, C.J., Pillco Zolá, R.S., Barnes, J.B., Tabor, C.R., Ehlers, T.A.,
1091 2015. Spatiotemporal variability of modern precipitation $\delta^{18}\text{O}$ in the central Andes
1092 and implications for paleoclimate and paleoaltimetry estimates. *Journal of*

1093 Geophysical Research: Atmospheres, 120(10), 4630-4656.
1094 <https://dx.doi.org/10.1002/2014JD022893>

1095 Fleury, P., Plagnes, V., Bakalowicz, M. 2007. Modelling of the functioning of karst
1096 aquifers with a reservoir model: Application to Fontaine de Vaucluse (South of
1097 France). Journal of Hydrology 345, 38– 49.
1098 <https://doi.org/10.1016/j.jhydrol.2007.07.014>

1099 Filippini, M., Squarzone, G., De Waele, J., Fiorucci, A., Vigna, B., Grillo, B., Riva, A.,
1100 Rossetti, S., Zini, L., Casagrande, G., Stumpp, C., Gargini, A. 2018.
1101 Differentiated spring behavior under changing hydrological conditions in an
1102 alpine karst aquifer. Journal of Hydrology, 556, 572-584.
1103 <https://doi.org/10.1016/j.jhydrol.2017.11.040>

1104 Freixes, A., 2014. Els aqüífers càrstics dels Pirineus de Catalunya. Interès estratègic i
1105 sostenibilitat [The karstic aquifers of the Catalanian Pyrenees. Strategic interest
1106 and sustainability]. PhD. Thesis. Universitat de Barcelona.
1107 <http://hdl.handle.net/2445/65187>

1108 Froehlich, K., Gibson, J.J., Aggarwal, P., 2001. Deuterium excess in precipitation and
1109 its climatological significance. In Study of environmental change using isotope
1110 techniques (Vol. 13, pp. 54-66). IAEA.

1111 Froehlich, K., Kralik, M., Papesch, W., Rank, D., Scheifinger, H., Stichler, W., 2008.
1112 Deuterium excess in precipitation of Alpine regions—moisture recycling. Isotopes
1113 in Environmental and Health Studies, 44(1), 61-70.
1114 <https://doi.org/10.1080/10256010801887208>

1115 García-Ruiz, J.M., López-Moreno, J.I., Vicente-Serrano, S.M., Lasanta-Martínez, T.,
1116 Beguería, S., 2011. Mediterranean water resources in a global change scenario.

1117 Earth-Science Reviews, 105(3-4), 121-139.
1118 <https://doi.org/10.1016/j.earscirev.2011.01.006>

1119 Garvelmann, J., Warscher, M., Leonhardt, G., Franz, H., Lotz, A., Kunstman, H. 2017.
1120 Quantification and characterization of the dynamics of spring and stream water
1121 systems in the Berchtesgaden Alps with a long-term stable isotope dataset.
1122 *Environ Earth Sci* 76:766 <https://doi.org/10.1007/s12665-017-7107-6>

1123 Giorgi, F., Lionello, P., 2008. Climate change projections for the Mediterranean region.
1124 *Global and planetary change*, 63(2-3), 90-104.
1125 <https://doi.org/10.1016/j.gloplacha.2007.09.005>

1126 Gladich, I., Gallai, I., Giajotti, D. B., & Stel, F. 2011. On the diurnal cycle of deep
1127 moist convection in the southern side of the Alps analysed through cloud-to-
1128 ground lightning activity. *Atmospheric Research*, 100(4), 371-376.
1129 <https://doi.org/10.1016/j.atmosres.2010.08.026>

1130 Goldscheider, N., 2005. Fold structure and underground drainage pattern in the alpine
1131 karst system Hochifen-Gottesacker. *Eclogae Geologicae Helvetiae*, 98(1), 1-17.
1132 <https://doi.org/10.1007/s00015-005-1143-z>

1133 Goldscheider N, Drew D (eds) (2007) *Methods in Karst Hydrogeology*. International
1134 Contributions to Hydrogeology 26, International Association of Hydrogeologists,
1135 Taylor & Francis, London, 264 pp. ISBN 978-0-415-42873-6

1136 Goldscheider, N., Meiman, J., Pronk, M., Smart, C., 2008. Tracer tests in karst
1137 hydrogeology and speleology. *International Journal of Speleology*, 37(1), 3.
1138 <http://dx.doi.org/10.5038/1827-806X.37.1.3>

1139 Goldscheider, N., 2011. *Alpine Hydrogeologie [Alpine hydrogeology]*. *Grundwasser*
1140 16:1–1. <https://doi.org/10.1007/s00767-010-0157-2>

1141 Gonfiantini, R., Roche, M.A., Olivry, J.C., Fontes, J.C., Zuppi, G.M., 2001. The altitude
1142 effect on the isotopic composition of tropical rains. *Chemical Geology*, 181(1-4),
1143 147-167. [https://doi.org/10.1016/S0009-2541\(01\)00279-0](https://doi.org/10.1016/S0009-2541(01)00279-0)

1144 Gremaud, V., Goldscheider, N., Savoy, L., Favre, G., Masson, H., 2009. Geological
1145 structure, recharge processes and underground drainage of a glacierised karst
1146 aquifer system, Tsanfleuron-Sanetsch, Swiss Alps. *Hydrogeol. J.* 17, 1833–1848.
1147 <https://doi.org/10.1007/s10040-009-0485-4>

1148 Grunewald, K., Scheithauer, J., 2010. Europe's southernmost glaciers: response and
1149 adaptation to climate change. *Journal of glaciology*, 56(195), 129-142.
1150 <https://doi.org/10.3189/002214310791190947>

1151 Hernández-Mora, N., del Moral Ituarte, L., La-Roca, F., La Calle, A., Schmidt, G.,
1152 2014. Interbasin water transfers in Spain: Interregional conflicts and governance
1153 responses. In *Globalized Water* (pp. 175-194). Springer, Dordrecht. ISBN 978-94-
1154 007-7322-6. https://doi.org/10.1007/978-94-007-7323-3_13

1155 Hargreaves, G.H. and Samani, Z.A. 1982. Estimating potential evapotranspiration.
1156 *Journal of Irrigation and Drainage Engineering*, 108, 223-230

1157 Hoerling, M., Eischeid, J., Perlwitz, J., Quan, X., Zhang, T., Pegion, P., 2012. On the
1158 increased frequency of Mediterranean drought. *Journal of Climate*, 25(6), 2146-
1159 2161. <https://doi.org/10.1175/JCLI-D-11-00296.1>

1160 Holko, L., Dóša, M., Michalko, J., Šanda, M. 2012. Isotopes of oxygen-18 and
1161 deuterium in precipitation in Slovakia. *Journal of Hydrology and*
1162 *Hydromechanics*, 60(4), 265-276. <https://doi.org/10.2478/v10098-012-0023-2>

1163 Hood, J.L., Hayashi, M., 2010. Assessing the application of a laser rangefinder for
1164 determining snow depth in inaccessible alpine terrain. *Hydrology and Earth*
1165 *System Sciences*, 14(6), 901. <http://dx.doi.org/10.5194/hess-14-901-2010>

1166 Hottelet, Ch., Braun, L.N., Leibundgut, Ch., Rieg, A., 1993. Simulation of Snowpack
1167 and Discharge in an Alpine Karst Basin. IAHS Publication No. 218, pp. 249–260
1168 ICGC, 2007. Mapa geològic comarcal de Catalunya 1:50 000. Full Alt Urgell
1169 (BDGC50M). [http://www.icgc.cat/ca/Administracio-i-
1170 empresa/Descarregues/Cartografia-geologica-i-geotematica/Cartografia-
1171 geologica/Mapa-geologic-comarcal-de-Catalunya-1-50.000/Mapa-geologic-
1172 comarcal-de-Catalunya-1-50.000](http://www.icgc.cat/ca/Administracio-i-empresa/Descarregues/Cartografia-geologica-i-geotematica/Cartografia-geologica/Mapa-geologic-comarcal-de-Catalunya-1-50.000/Mapa-geologic-comarcal-de-Catalunya-1-50.000)

1173 Jeelani, G., Shah, R.A., Deshpande, R.D., Fryar, A.E., Perrin, J., Mukherjee, A., 2017.
1174 Distinguishing and estimating recharge to karst springs in snow and glacier
1175 dominated mountainous basins of the western Himalaya, India. Journal of
1176 hydrology, 550, 239-252. <https://doi.org/10.1016/j.jhydrol.2017.05.001>

1177 Jeannin, P-Y. 2001. Modeling flow in phreatic and epiphreatic karst conduits in the
1178 Hölloch cave (Muotatal, Switzerland). Water Resources Research. Vol. 37, No. 2,
1179 pp 191-200. <https://doi.org/10.1029/2000WR900257>

1180 Jiménez-Martínez, J. y Custodio, E., 2008. El exceso de deuterio en la lluvia y en la
1181 recarga a los acuíferos en el área circum-mediterránea y en la costa mediterránea
1182 española. Boletín Geológico y Minero, 119 (1): 21-32.

1183 Jódar, J., Lambán, L.J., Medina, A., Custodio, E., 2014. Exact analytical solution of the
1184 convolution integral for classical hydrogeological lumped-parameter models and
1185 typical input tracer functions in natural gradient systems. J. Hydrol. 519, 3275–
1186 3289. <http://dx.doi.org/10.1016/j.jhydrol.2014.10.027>.

1187 Jódar, J., Custodio, E., Liotta, M., Lambán, L.J., Herrera, C., Martos-Rosillo, S.,
1188 Sapriza, G., Rigo, T., 2016a. Correlation of the seasonal isotopic amplitude of
1189 precipitation with annual evaporation and altitude in alpine regions. Sci. Total
1190 Environ., 550: 27-37. <https://dx.doi.org/10.1016/j.scitotenv.2015.12.034>

1191 Jódar, J., Custodio, E., Lambán, L.J., Martos-Rosillo, S., Herrera-Lameli, C., Sapriza-
1192 Azuri, G., 2016b. Vertical variation in the amplitude of the seasonal isotopic
1193 content of rainfall as a tool to jointly estimate the groundwater recharge zone and
1194 transit times in the Ordesa and Monte Perdido National Park aquifer system,
1195 north-eastern Spain. *Sci. Total Environ.* 573, 505–517.
1196 <https://dx.doi.org/10.1016/j.scitotenv.2016.08.117>

1197 Jódar, J., Cabrera, J.A., Martos-Rosillo, S., Ruiz-Constan, A., Gonzalez-Ramón, A.,
1198 Lambán, L.J., Herrera, C., Custodio, E., 2017. Groundwater discharge in high-
1199 mountain watersheds: a valuable resource for downstream semi-arid zones. The
1200 case of the Bérchules River in Sierra Nevada (Southern Spain). *Science of The*
1201 *Total Environment*, <https://doi.org/10.1016/j.scitotenv.2017.03.190>

1202 Jódar, J., Carpintero, E., Martos-Rosillo, S., Ruiz-Constán, A., Marín-Lechado, C.,
1203 Cabrera-Arrabal, J.A., Navarrete-Mazariego, E., González-Ramón , A., Lambán,
1204 L.J., Herrera, C., González-Dugo, M.P. 2018. Combination of lumped
1205 hydrological and remote-sensing models to evaluate water resources in a semi-
1206 arid high altitude ungauged watershed of Sierra Nevada (Southern Spain). *Sci.*
1207 *Total Environ.*, 625: 285-300. [https://doi-](https://doi-org.recursos.biblioteca.upc.edu/10.1016/j.scitotenv.2017.12.300)
1208 [org.recursos.biblioteca.upc.edu/10.1016/j.scitotenv.2017.12.300](https://doi-org.recursos.biblioteca.upc.edu/10.1016/j.scitotenv.2017.12.300)

1209 Katsuyama, M., Tani, M., Nishimoto, S., 2010. Connection between streamwater mean
1210 residence time and bedrock groundwater recharge/discharge dynamics in
1211 weathered granite catchments. *Hydrological Processes*, 24(16), 2287-2299.
1212 <https://doi.org/10.1002/hyp.7741>

1213 Kazakis, N., Chalikakis, K., Mazzilli, M., Ollivier, C., Manakos, A., Voudouris, K.,
1214 2018. Management and research strategies of karst aquifers in Greece: Literature
1215 overview and exemplification based on hydrodynamic modelling and

1216 vulnerability assessment of a strategic karst aquifer. *Sci. Total Environ.*, 643:
1217 592–609. <https://doi.org/10.1016/j.scitotenv.2018.06.184>

1218 Klimchouk, A. Samokhin, G.V., Kasian, Y.M. 2009. The deepest cave in the world in
1219 the arabika massif (western caucasus) and its hydrogeological and
1220 paleogeographic significance. 2009 ICS Proceedings. 15th International Congress
1221 of Speleology

1222 Konz, M., Seibert, J., 2010. On the value of glacier mass balances for hydrological
1223 model calibration. *Journal of hydrology*, 385(1-4), 238-246.
1224 <https://doi.org/10.1016/j.jhydrol.2010.02.025>

1225 Kurylyk, B.L., Hayashi, M., 2017. Inferring hydraulic properties of alpine aquifers from
1226 the propagation of diurnal snowmelt signals. *Water Resources Research*.
1227 <https://doi.org/10.1002/2016WR019651>

1228 Laimer, H.J. 2010. Neue Ergebnisse zur Karsthydrogeologie des westlichen Toten
1229 Gebirges (Österreich). (New karst hydrogeological research in the western Totes
1230 Gebirge, Austria). *Grundwasser*. Volume 15, Issue 2, pp 113–122

1231 Lambán, L.J., Jódar, J., Custodio, E., Soler, A., Sapriza, G. and Soto, R., 2015. Isotopic
1232 and hydrogeochemical characterization of high-altitude karst aquifers in complex
1233 geological settings. The Ordesa and Monte Perdido National Park (Northern
1234 Spain) case study. *Sci. Total Environ.*, 506–507: pp 466–479,
1235 <https://doi.org/10.1016/j.scitotenv.2014.11.030>

1236 Lauber, U., Kotyla, P., Morche, D., Goldscheider, N., 2014. Hydrogeology of an Alpine
1237 rockfall aquifer system and its role in flood attenuation and maintaining baseflow.
1238 *Hydrology and Earth System Sciences*, 18(11), 4437.
1239 <http://dx.doi.org/10.5194/hess-18-4437-2014>

1240 Lauber, U., Goldscheider, N., 2014. Use of artificial and natural tracers to assess
1241 groundwater transit-time distribution and flow systems in a high-alpine karst
1242 system (Wetterstein Mountains, Germany). *Hydrogeology Journal*, 22(8), 1807-
1243 1824. <http://dx.doi.org/10.1007/s10040-014-1173-6>

1244 Liu, Z., Tian, L., Yao, T., & Yu, W. 2008. Seasonal deuterium excess in Nagqu
1245 precipitation: influence of moisture transport and recycling in the middle of
1246 Tibetan Plateau. *Environmental Geology*, 55(7), 1501-1506.
1247 <http://dx.doi.org/10.1007/s00254-007-1100-4>

1248 López-Moreno, J.I., García-Ruiz, J.M., 2004. Influence of snow accumulation and
1249 snowmelt on streamflow in the central Spanish Pyrenees/Influence de
1250 l'accumulation et de la fonte de la neige sur les écoulements dans les Pyrénées
1251 centrales espagnoles. *Hydrological Sciences Journal*, 49(5).
1252 <https://doi.org/10.1623/hysj.49.5.787.55135>

1253 López-Moreno, J. I., Goyette, S., Beniston, M., 2008. Climate change prediction over
1254 complex areas: spatial variability of uncertainties and predictions over the
1255 Pyrenees from a set of regional climate models. *International Journal of*
1256 *Climatology*, 28(11), 1535-1550. <https://doi.org/10.1002/joc.1645>

1257 López-Moreno, J.I., Revuelto, J., Rico, I., Chueca-Cía, J., Julián, A., Serreta, A.,
1258 Serrano, E., Vicente-Serrano, S.M., Azorin-Molina, C., Alonso-González, E.,
1259 García-Ruiz, J.M., 2016. Thinning of the Monte Perdido Glacier in the Spanish
1260 Pyrenees since 1981. *The Cryosphere*, 10(2), 681-694. [https://doi.org/10.5194/tc-](https://doi.org/10.5194/tc-10-681-2016)
1261 [10-681-2016](https://doi.org/10.5194/tc-10-681-2016)

1262 Mađrala, M., Wąsik, M., Małoszewski, P., 2017. Interpretation of environmental tracer
1263 data for conceptual understanding of groundwater flow: an application for
1264 fractured aquifer systems in the Kłodzko Basin, Sudetes, Poland. *Isotopes in*

1265 environmental and health studies, 53(5), 466-483.
1266 <https://dx.doi.org/10.1080/10256016.2017.1330268>

1267 Malard, A., Jeannin, P.Y., Vouillamoz, J. et al 2015. An integrated approach for
1268 catchment delineation and conduit-network modeling in karst aquifers: application
1269 to a site in the Swiss tabular Jura. *Hydrogeol J* 23: 1 1341–1357.
1270 <https://doi.org/10.1007/s10040-015-1287-5>

1271 Malard, A., Sinreich, M., Jeannin, P.Y., 2016. A novel approach for estimating karst
1272 groundwater recharge in mountainous regions and its application in Switzerland.
1273 *Hydrological Processes*, 30(13), 2153-2166. <https://doi.org/10.1002/hyp.10765>

1274 Malík, P., Svasta, J., Michalko, J., Gregor, M., 2016. Indicative mean transit time
1275 estimation from $\delta^{18}\text{O}$ values as groundwater vulnerability indicator in karst-
1276 fissure aquifers. *Environmental Earth Sciences*. 75. [10.1007/s12665-016-5791-2](https://doi.org/10.1007/s12665-016-5791-2).

1277 Małoszewski, P., Rauert, W., Stichler, W., Herrmann, A., 1983. Application of flow
1278 models in an alpine catchment area using tritium and deuterium data. *Journal of*
1279 *Hydrology*, 66: 319–330. [http://dx.doi.org/10.1016/0022-1694\(83\)90193-2](http://dx.doi.org/10.1016/0022-1694(83)90193-2)

1280 Maloszewski, P., Rauert, W., trimborn, P., Herrmann, A., Rau, R. 1992. Isotope
1281 hydrological study of mean transit times in an alpine basin (Wimbachtal,
1282 Germany). *Journal of Hydrology*, 140: 343-360. [https://doi.org/10.1016/0022-](https://doi.org/10.1016/0022-1694(92)90247-S)
1283 [1694\(92\)90247-S](https://doi.org/10.1016/0022-1694(92)90247-S)

1284 Małoszewski, P., Zuber, A., 1996. Lumped parameter models for the interpretation of
1285 environmental tracer data. *Manual on mathematical models in isotope hydrology*.
1286 IAEA-TECDOC 910. Vienna (Austria): IAEA; 1996

1287 Małoszewski, P., Zuber, A., 2002. *Manual on lumped parameter models used for the*
1288 *interpretation of environmental tracer data in groundwaters (IAEA-UIAGS/CD--*
1289 *02-00131). International Atomic Energy Agency (IAEA)*

1290 (https://inis.iaea.org/search/search.aspx?orig_q=RN:33037906, last access
1291 12/04/2018)

1292 Marti, R., Gascoin, S., Houet, T., Ribière, O., Laffly, D., Condom, T., Monnier, S.,
1293 Schmutz, M., Camerlynck, C., Tihay, J.P., Soubeyroux, J.M., 2015. Evolution of
1294 Ossoue Glacier (French Pyrenees) since the end of the Little Ice Age. The
1295 Cryosphere, 9(5), 1773-1795. <http://dx.doi.org/10.5194/tc-9-1773-2015>.

1296 Martos-Rosillo, S., Marín-Lechado, C., Pedrera, A., Vadillo, I., Motyka, J., Molina,
1297 J.L., Ortiz, P., Martín-Ramírez, J.M., 2014. Methodology to evaluate the renewal
1298 period of carbonate aquifers: a key tool for their management in arid and semiarid
1299 regions, with the example of Becerrero aquifer, Spain. Hydrogeology Journal,
1300 22(3), 679-689. <http://dx.doi.org/10.1007/s10040-013-1086-9>

1301 Martos-Rosillo, S., González-Ramón, A., Jiménez-Gavilán, P., Andreo, B., Durán, J.J.,
1302 Mancera, E., 2015. Review on groundwater recharge in carbonate aquifers from
1303 SW Mediterranean (Betic Cordillera, S Spain). Environ Earth Sci. 74: 7571.
1304 <https://doi.org/10.1007/s12665-015-4673-3>

1305 Merz, R., Blöschl, G., 2004. Regionalisation of catchment model parameters. Journal of
1306 hydrology, 287(1-4), 95-123. <http://dx.doi.org/10.1016/j.jhydrol.2003.09.028>

1307 Milano, M., Ruelland, D., Fernandez, S., Dezetter, A., Fabre, J., Servat, E., Fritsch,
1308 J.M., Ardoin-Bardin, S., Thivet, G., 2013. Current state of Mediterranean water
1309 resources and future trends under climatic and anthropogenic changes.
1310 Hydrological Sciences Journal, 58(3), 498-518.
1311 <http://dx.doi.org/10.1080/02626667.2013.774458>

1312 Molina, A., Melgarejo, J., 2016. Water policy in Spain: seeking a balance between
1313 transfers, desalination and wastewater reuse. International Journal of Water

1314 Resources Development, 32(5), 781-798.
1315 <http://dx.doi.org/10.1080/07900627.2015.1077103>

1316 Mook, W.G., De Vries, J.J., 2000. Volume I, Introduction: theory methods review.
1317 Environmental Isotopes in the Hydrological Cycle—Principles and Applications,
1318 International Hydrological Programme (IHP-V). Technical Documents in
1319 Hydrology (IAEA/UNESCO) No, 39 vol. 1 ([http://www-](http://www-naweb.iaea.org/napc/ih/IHS_publication.html)
1320 [naweb.iaea.org/napc/ih/IHS_publication.html](http://www-naweb.iaea.org/napc/ih/IHS_publication.html), last access 12/04/2018).

1321 Mudarra, M., Andreo, B. 2011. Relative importance of the saturated and the unsaturated
1322 zones in the hydrogeological functioning of karst aquifers: The case of Alta
1323 Cadena (Southern Spain). Journal of Hydrology 397, 263–280.
1324 <https://doi.org/10.1016/j.jhydrol.2010.12.005>

1325 Mudarra, M., Andreo, B., Marín, A.I., Vadillo, I., Barberá, J.A., 2014. Combined use of
1326 natural and artificial tracers to determine the hydrogeological functioning of a
1327 karst aquifer: the Villanueva del Rosario system (Andalusia, southern Spain).
1328 Hydrogeology journal, 22(5), 1027-1039. [http://dx.doi.org/10.1007/s10040-014-](http://dx.doi.org/10.1007/s10040-014-1117-1)
1329 [1117-1](http://dx.doi.org/10.1007/s10040-014-1117-1)

1330 Mudarra, M., Andreo, B., 2015. Role of the Soil-Epikarst-Unsaturated Zone in the
1331 Hydrogeological Functioning of Karst Aquifers. The Case of the Sierra Gorda de
1332 Villanueva del Trabuco Aquifer (Southern Spain). Hydrogeological and
1333 Environmental Investigations in Karst Systems. (ed. Andreo, B., Carrasco, F.,
1334 Durán, J.J., Jiménez, P., LaMoreaux.) Series: Environmental Earth Sciences.
1335 Springer. 638 pp.

1336 Nimon, K.F., Oswald, F.L., 2013. Understanding the results of multiple linear
1337 regression: Beyond standardized regression coefficients. Organizational Research
1338 Methods, 16(4), 650-674.

- 1339 Nogués-Bravo, D., Araújo, M.B., Lasanta, T., López-Moreno, J.I., 2008. Climate
1340 change in Mediterranean mountains during the 21st century. *AMBIO: A Journal*
1341 *of the Human Environment*, 37(4), 280-285. [https://doi.org/10.1579/0044-](https://doi.org/10.1579/0044-7447(2008)37[280:CCIMMD]2.0.CO;2)
1342 [7447\(2008\)37\[280:CCIMMD\]2.0.CO;2](https://doi.org/10.1579/0044-7447(2008)37[280:CCIMMD]2.0.CO;2)
- 1343 Obleitner, F., 1994. Climatological features of glacier and valley winds at the
1344 Hintereisferner (Ötztal Alps, Austria). *Theoretical and Applied Climatology*,
1345 49(4), 225-239. <https://doi.org/10.1007/BF00867462>
- 1346 Ozyurt, N.N., Bayari, C.S. 2008. Temporal variation of chemical and isotopic signals in
1347 major discharges of an alpine karst aquifer in Turkey: implications with respect to
1348 response of karst aquifers to recharge. *Hydrogeology Journal* 16: 297–309.
1349 <http://dx.doi.org/10.1007/s10040-007-0217-6>
- 1350 Ozyurt, N.N., Lutz, H.O., Hunjak, T., Mance, D., Roller-Lutz, Z. 2014. Characterization
1351 of the Gacka River basin karst aquifer (Croatia): Hydrochemistry, stable isotopes
1352 and tritium-based mean residence times. *Sci. Total Environ.* 87 245–254.
1353 <http://dx.doi.org/10.1016/j.scitotenv.2014.04.018>
- 1354 Pardo-Igúzquiza, E., Durán, J.J., Luque-Espinar, J.A., Robledo-Ardila, P.A., Martos-
1355 Rosillo, S., Guardiola-Albert, C., Pedrera, A. 2015. Karst massif susceptibility
1356 from rock matrix, fracture and conduit porosities: a case study of the Sierra de las
1357 Nieves (Málaga, Spain). *Environ Earth Sci.* 74:7583–7592.
1358 <http://dx.doi.org/10.1007/s12665-015-4545-x>
- 1359 Peel, M.C., Finlayson, B.L., McMahon, T.A., 2007. Updated world map of the Köppen–
1360 Geiger climate classification. *Hydrol. Earth Syst. Sci.* 11, 1633–1644.
1361 <http://dx.doi.org/10.5194/hess-11-1633-2007>
- 1362 Poage, M.A., Chamberlain, C.P., 2001. Empirical relationships between elevation and
1363 the stable isotope composition of precipitation and surface waters: considerations

1364 for studies of paleoelevation change. *Am. J. Science* 301 (1), 1–15.
1365 <http://dx.doi.org/10.2475/ajs.301.1.1>

1366 René, P., 2013. *Glaciers des Pyrénées: le réchauffement climatique en images*. Éd.
1367 Cairn.

1368 Ribalaygua, J., Pino, M.R., Pórtoles, J., Roldán, E., Gaitán, E., Chinarro, D., Torres, L.,
1369 2013. Climate change scenarios for temperature and precipitation in Aragón
1370 (Spain). *Science of the Total Environment*, 463, 1015-1030.
1371 <https://doi.org/10.1016/j.scitotenv.2013.06.089>

1372 Rodgers, P., Soulsby, C., Waldron, S., 2005. Stable isotope tracers as diagnostic tools in
1373 upscaling flow path understanding and residence time estimates in a mountainous
1374 mesoscale catchment. *Hydrol Process* 19(11):2291–2307.
1375 <http://dx.doi.org/10.1002/hyp.5677>

1376 Ruiz-Constán, A., Marín-Lechado, C., Martos-Rosillo, S., Fernández-Leyva, C., García-
1377 Lobón, J. L., Pedrera, A., López-Geta, J.A., Hernández-Bravo, J.A., Rodríguez-
1378 Hernández, L., 2015. Methodological Procedure for Evaluating Storage Reserves
1379 in Carbonate Aquifers Subjected to Groundwater Mining: The Solana Aquifer
1380 (Alicante, SE Spain). In *Hydrogeological and Environmental Investigations in
1381 Karst Systems* (pp. 255-262). Springer, Berlin, Heidelberg.
1382 http://dx.doi.org/10.1007/978-3-642-17435-3_28

1383 Sánchez-Murillo, R., Brooks, E.S., Elliot, W.J., Boll, J., 2015. Isotope hydrology and
1384 baseflow geochemistry in natural and human-altered watersheds in the Inland
1385 Pacific Northwest, USA. *Isotopes in environmental and health studies*, 51(2), 231-
1386 254. <http://dx.doi.org/10.1080/10256016.2015.1008468>

1387 Schotterer, U., Froehlich, K., Stichler, W., Trimborn, P., 1993. Temporal variation of
1388 ^{18}O and deuterium excess in precipitation, river and spring waters in Alpine

1389 regions of Switzerland. In *Isotope Techniques in the study of Past and Current*
1390 *Environmental Changes in the Hydrosphere and the Atmosphere*. Edited by
1391 IAEA. Proceedings series, ISSN 0074-1884, STI/PUB/908, ISBN 92-0-103293-5
1392 (https://inis.iaea.org/search/search.aspx?orig_q=RN:25027909, last access
1393 12/04/2018).

1394 Seibert, J., 2005. *HBV Light Version 2. User's Manual*. Uppsala University, Dept. of
1395 Earth Science, Hydrology, Uppsala, Sweden.

1396 Seibert, J., Vis, M.J.P, 2012. Teaching hydrological modelling with a user-friendly
1397 catchment-runoff-model software package, *Hydrol. Earth Syst. Sci.*, 16(9), 3315–
1398 3325. <http://dx.doi.org/10.5194/hess-16-3315-2012>, 102012

1399 Seibert, J., Jenicek, M., Huss, M., Ewen, T., 2015. Snow and ice in the hydrosphere. In
1400 *Snow and Ice-Related Hazards, Risks and Disasters* (pp. 99-137). ISBN: 978-0-
1401 12-394849-6. <https://doi.org/10.1016/B978-0-12-394849-6.00004-4>

1402 Solder, J.E., Stolp, B.J., Heilweil, V.M., Susong, D.D., 2016. Characterization of mean
1403 transit time at large springs in the Upper Colorado River Basin, USA: a tool for
1404 assessing groundwater discharge vulnerability. *Hydrogeology Journal*, Volume
1405 24, Issue 8, pp 2017–2033, <https://doi.org/10.1007/s10040-016-1440-9>

1406 Staudinger, M., Stoelzle, M., Seeger, S., Seibert, J., Weiler, M., Stahl, K., 2017.
1407 Catchment water storage variation with elevation. *Hydrological Processes*, 31(11),
1408 2000-2015. <https://doi.org/10.1002/hyp.11158>

1409 Turnadge, C., Smerdon, B.D. 2014. A review of methods for modelling environmental
1410 tracers in groundwater: advantages of tracer concentration simulation. *Journal of*
1411 *Hydrology*, 519, 3674-3689. <https://doi.org/10.1016/j.jhydrol.2014.10.056>

1412 Turk, J., Malard, A., Jeannin, P.-Y., Petric M., Gabrovšek, F., Ravbar, N., Vouillamoz,
1413 J., Slabe, T., Sordet, V., 2015. Hydrogeological characterization of groundwater

1414 storage and drainage in an alpine karst aquifer (the Kanin massif, Julian Alps).
1415 Hydrological Processes 29(8), 1986-1998. <https://doi.org/10.1002/hyp.10313>

1416 Uhlenbrook, S., Seibert, J.A.N., Leibundgut, C., Rodhe, A., 1999. Prediction
1417 uncertainty of conceptual rainfall-runoff models caused by problems in
1418 identifying model parameters and structure. Hydrological Sciences Journal, 44(5),
1419 779-797. <https://doi.org/10.1080/02626669909492273>

1420 Vergés, J. 1999. Estudi geològic del vessant sud del Pirineu oriental i central. Evolució
1421 cinemàtica en 3D. PhD Thesis. University of Barcelona (UB), Faculty of
1422 Geology, 180 pp.

1423 Vicente-Serrano, S.M., Lopez-Moreno, J.I., Beguería, S., Lorenzo-Lacruz, J., Sanchez-
1424 Lorenzo, A., García-Ruiz, J.M., Azorin-Molina, C., Morán-Tejeda, E., Revuelto,
1425 J., Trigo, R., Coelho, F., Espejo, F., 2014. Evidence of increasing drought severity
1426 caused by temperature rise in southern Europe. Environmental Research Letters,
1427 9(4), 044001. <https://doi.org/10.1088/1748-9326/9/4/044001>

1428 Vitvar, T., Gurtz, O., Lang, H. 1999. Application of GIS-based distributed hydrological
1429 modelling for estimation of water residence times in the small Swiss pre-alpine
1430 catchment Rietholzbach. Integrated Methods in Catchment Hydrology—Tracer.
1431 Remote Sensing and New Hydrometric Techniques (Proceedings of IUGG 99
1432 Symposium HS4, Birmingham, July 1999). IAHS Publ. no. 258, 1999

1433 Viville, D., Ladouche, B. and Bariac, T., 2006. Isotope hydrological study of mean
1434 transit time in the granitic Strengbach catchment (Vosges Massif, France).
1435 Application of the FlowPC model with modified input function. Hydrol. Process.
1436 20, 1737–1751. <https://doi.org/10.1002/hyp.5950>

1437 Viviroli, D., Weingartner, R., 2004. The hydrological significance of mountains: from
1438 regional to global scale. *Hydrology and Earth System Sciences* 8, 1016–1029.
1439 <https://doi.org/10.5194/hess-8-1017-2004>

1440 Viviroli, D., Dürr, H.H., Messerli, B., Meybeck, M., Weingartner, R., 2007. Mountains
1441 of the world— water towers for humanity: typology, mapping and global
1442 significance. *Water Resources Research* 43 (7), W07447.
1443 <https://doi.org/10.1029/2006WR005653>

1444 Wassenaar, L. I., Ahmad, M., Aggarwal, P., van Duren, M., Pölsenstein, L., Araguas,
1445 L., & Kurttas, T. 2012. Worldwide proficiency test for routine analysis of $\delta^2\text{H}$
1446 and $\delta^{18}\text{O}$ in water by isotope-ratio mass spectrometry and laser absorption
1447 spectroscopy. *Rapid Communications in Mass Spectrometry*, 26(15), 1641-1648.
1448 <https://doi.org/10.1002/rcm.6270>

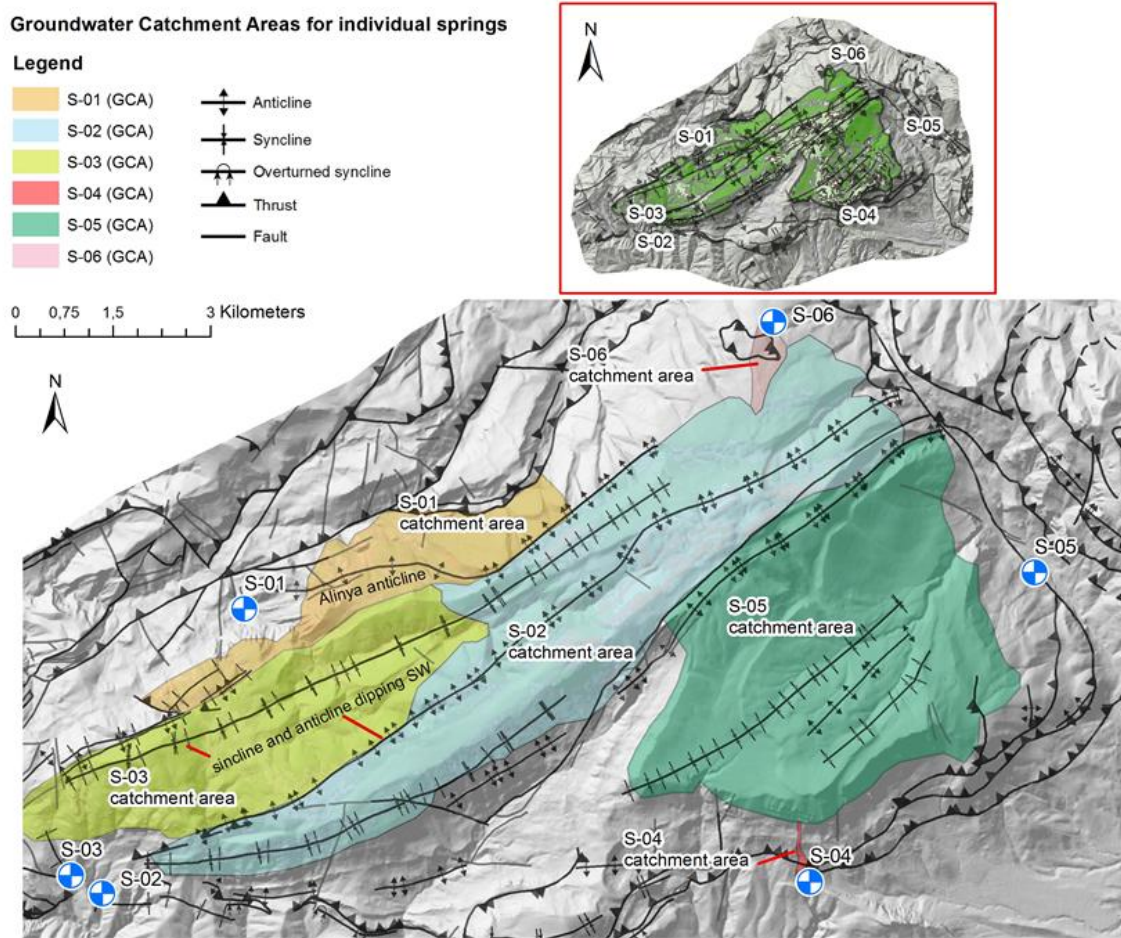
1449 Wetzel, K., 2004. On the hydrogeology of the Partnach area in the Wetterstein
1450 Mountains (Bavarian Alps). *Erdkunde* 58:172–186.
1451 <http://www.jstor.org/stable/25647659>

1452 Zini, L., Casagrande, G., Calligaris, C., Cucchi, F., Manca, P., Treu, F., Zavagno, E.,
1453 Biolchi, S. 2015. The Karst Hydrostructure of the Mount Canin (Julian Alps, Italy
1454 and Slovenia). *Hydrogeological and Environmental Investigations in Karst*
1455 *Systems*. (ed. Andreo, B., Carrasco, F., Durán, J.J., Jiménez, P., LaMoreaux.)
1456 Series: *Environmental Earth Sciences*. Springer. 638 pp.
1457 <https://doi.org/10.1007/978-3-642-17435-3>

1458

1459 **Appendix A: Groundwater catchment areas for the springs S-01 to S-06.**

1460



1461

1462 Fig. A1. Groundwater catchment areas for the springs S-01 to S-06.

1463

1464 Table A1. Distribution of geographical and elevation zones considered into the HBV semi-
 1465 distributed rainfall-runoff model into the groundwater catchment zones. The areas of the
 1466 different vegetation zones (VZs) are provided, considering the three different elevation zones
 1467 into which every GWC is divided.

GWC		Elevation Zones			Vegetation Zone Areas			Percentage Areas		
Index	Associated Spring	Z_{min} (m a.s.l.)	Z_{max} (m a.s.l.)	EZ_{ij}^a (ha)	VZ_1^b (ha)	VZ_2^c (ha)	VZ_3^d (ha)	VZ_1/EZ_{ij} (%)	VZ_2/EZ_{ij} (%)	VZ_3/EZ_{ij} (%)
1	S-01	1334	1600	204,0	41,8	56,8	105,5	20,5	27,8	51,7
		1601	1851	219,1	19,0	67,7	132,4	8,7	30,9	60,4
		1851	2141	122,8	4,8	6,8	111,1	3,9	5,5	90,5
2	S-02	1122	1543	106,9	8,2	26,0	72,7	7,7	24,3	68,0

		1544	1965	756,5	32,2	210,3	514,0	4,3	27,8	67,9
		1966	2385	1389,5	183,8	443,5	762,2	13,2	31,9	54,9
3	S-03	1201	1443	102,3	1,7	36,9	63,7	1,7	36,1	62,3
		1444	1686	561,2	19,5	178,9	362,8	3,5	31,9	64,6
		1687	1927	522,6	12,6	119,4	390,6	2,4	22,8	74,7
4	S-04	1468	1710	9,1	0,1	2,8	6,2	1,1	30,8	68,1
		1711	1847	0,9	0,1	0,5	0,3	11,1	55,6	33,3
		1848	1875	0,1	0,0	0,1	0,0	0,0	100,0	0,0
5	S-05	1421	1663	234,3	8,1	24,4	201,8	3,5	10,4	86,1
		1664	1973	635,5	45,4	126,0	464,1	7,1	19,8	73,0
		1974	2348	1278,4	215,5	495,0	568,0	16,9	38,7	44,4
6	S-06	1838	1926	11,9	0,7	0,7	10,5	5,9	5,9	88,2
		1927	2014	20,7	0,1	1,8	18,8	0,5	8,7	90,8
		2015	2101	13,4	0,0	2,3	11,2	0,0	17,2	83,6

(a) For a given elevation zone EZ_{ij} the subscripts “i” (from 1 to 6) and “j” refer to the corresponding groundwater catchment zone and elevation zone number, respectively; (b) VZ_1 corresponds to open areas; (c) VZ_2 corresponds to mountain meadows; (d) VZ_3 corresponds to forest zones

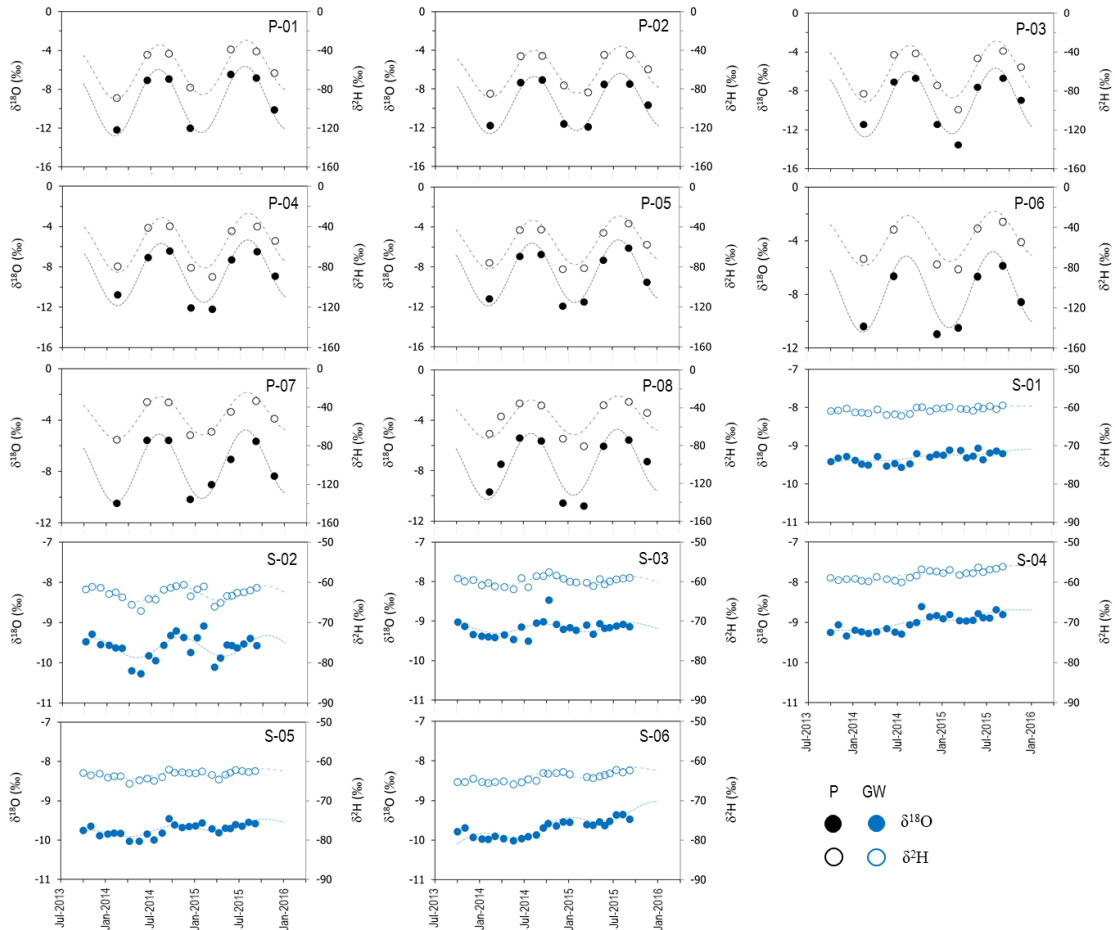
1468

1469

1470

1471 **Appendix B: Sinusoidal functions fitting the measuring the isotopic content**
 1472 **($\delta^{18}\text{O}$ and $\delta^2\text{H}$) variation in precipitation and spring discharges.**

1473



1474

1475 Fig. B1. Isotopic content of precipitation (P; black symbols) and spring discharge (GW; blue
 1476 symbols). $\delta^{18}\text{O}$ and $\delta^2\text{H}$ are indicated by solid and empty symbols, respectively. The dashed lines
 1477 indicate the fitted sinusoidal function [Eq.1]. The identification codes correspond to those in
 1478 Table 1.

1479

1480 **Appendix C: HBV hydrological modeling**

1481 Table C1. List of abbreviations for the vegetation zone parameters of HBV (Seibert, 2005)

Parameter	Units	Valid range	Description
TT	°C	(-inf,inf)	Threshold temperature to produce accumulation of precipitation as snow. Melt of snow starts if temperatures are above TT calculated with a simple degree-day (degree-Δt in case of a non-daily time step) method
CFMAX	mm/Δt/°C	[0,inf)	Degree-Δt factor - CFMAX varies normally between 1.5 and 4 mm oC-1 day-1 (in Sweden), with lower values for forested areas. As approximation the values 2 and 3.5 can be used for CFMAX in forested and open landscape respectively.
SFCF	-	[0,inf)	Snowfall correction factor
CFR	-	[0,inf)	Refreezing coefficient
CWH	-	[0,inf)	Water holding capacity, according to: refreezing meltwater = CFR·CFMAX(TT-T)'
FC	mm	(0,inf)	Maximum soil moisture storage
LP	-	[0,1)	Soil moisture value above which AET reaches PET
BETA	-		Parameter that determines the relative contribution to runoff from rain or snowmelt

1482

1483 Table C2. List of abbreviations for the catchment parameters of HBV (Seibert, 2005)

Parameter	Units	Valid range	Description
PERC	mm/Δt	[0,inf)	Threshold parameter
UZL	mm	[0,inf)	Threshold parameter
K0	1/Δt	[0,1)	Storage (or recession) coefficient 0
K1	1/Δt	[0,1)	Storage (or recession) coefficient 1
K2	1/Δt	[0,1)	Storage (or recession) coefficient 2
MAXBAS	Δt	[1,100]	Length of triangular weighting function

1484

1485 Table C3. Objective functions for the calibration of the HBV hydrologic model, where Q_{obs_i}
 1486 and Q_{sim_i} are the measured and computed of spring discharge values, respectively, $\overline{Q_{obs}}$ is the
 1487 arithmetic mean of the observed spring discharge values, and $\overline{Q_{sim}}$ is the arithmetic mean of the
 1488 computed spring discharge values.

Objective function	Observations
$R_{eff} = 1 - \frac{\sum_{i=1}^N (Q_{sim_i} - Q_{obs_i})^2}{\sum_{i=1}^N (Q_{obs_i} - \overline{Q_{obs}})^2}$	$R_{eff} = 1$ means perfect fit $R_{eff} = 0$, indicates that the model fits the observed data no better than a horizontal line through $\overline{Q_{obs}}$ $R_{eff} < 0$ means very poor fit
$R^2 = \frac{(\sum_{i=1}^N (Q_{obs_i} - \overline{Q_{obs}}) * (Q_{sim_i} - \overline{Q_{sim}}))^2}{\sum_{i=1}^N (Q_{obs_i} - \overline{Q_{obs}})^2 * \sum_{i=1}^N (Q_{sim_i} - \overline{Q_{sim}})^2}$	R^2 is the determination coefficient. The higher the R^2 value the better the model performance

1489

1490

1491 Table C4. Calibrated values of the parameters in the HBV-light model

Catchment Parameters	Units	S-01	S-02	S-03	S-04	S-05	S-06
Snow Routine (VZ ₁)							
TT	°C	-0,2	-4,52	-1,6	-1,1	-1	-1,1
CFMAX	mm/d/°C	1,9	2,4	2	1,7	2,8	1,2
SFCF	-	1	2,38	0,5	1	1,2	1,5
CFR	-	1	2,5	0,7	0,5	0,6	0,6
CWH	-	0,5	2	2	1	0,8	0,8
Snow Routine (VZ ₂)							
TT	°C	-0,2	-4,39	-1,6	-0,5	-3	-0,46
CFMAX	mm/d/°C	1,9	1	2	1,6	1	2,1
SFCF	-	1	2,6	0,7	1	1,2	1,16
CFR	-	1	2,5	0,7	0,3	1	1
CWH	-	1	2	1	1	0,2	0,2
Snow Routine (VZ ₃)							

TT	°C	4	6	6	0	5,5	6,5
CFMAX	mm/d/°C	1,5	1	1,5	1,5	1	4
SFCF	-	0,001	0,001	0,001	0,01	0,001	0,001
CFR	-	0,7	1	0,7	0,2	0,4	0,4
CWH	-	2	2	3	1	1	1
Soil Moisture Routine							
(VZ ₁)							
FC	mm	95	75	80	75	50	80
LP	-	0,07	0,01	0,02	0,02	0,01	0,01
BETA	-	0,60	0,40	1,54	1,70	0,30	2,5
Soil Moisture Routine							
(VZ ₂)							
FC	mm	180	120	150	125	139	150
LP	-	0,07	0,01	0,06	0,01	0,01	0,01
BETA	-	0,60	2,20	3,90	3,45	1,80	2,7
Soil Moisture Routine							
(VZ ₃)							
FC	mm	750	550	490	750	660	700
LP	-	0,00	0,01	0,01	0,01	0,01	0,01
BETA	-	6,00	3,00	5,70	6,00	3,50	4,00
Response Routine							
PERC	mm/d	5	20,0	2,2	1,1	25,0	1,7
UZL	mm	100	80	100	110	100	100
K0	1/d	0,20	0,50	0,20	0,20	0,20	0,40
K1	1/d	0,07	0,11	0,13	0,17	0,20	0,20
K2	1/d	0,01	0,02	0,04	0,04	0,05	0,05
Routing Routine							
MAXBAS	d	1,7	6,2	2	2,45	4,3	4,22

1492

1493

1494

1495

1496

Table C5. Goodness of the result of the HBV calibrations for each spring model

HBV model	$R_{\text{eff}} (-)$	$R^2 (-)$
S-01	0,55	0,55
S-02	0,66	0,67
S-03	0,73	0,78
S-04	0,57	0,73
S-05	0,77	0,80
S-06	0,62	0,66

1497

1498

1499 **Appendix D: FlowPC modeling**

1500 Table D1. Fitted parameters of the exponential-piston flow model (EPM) for the estimated
 1501 mean transit times (τ) with FlowPC model and $\delta^{18}\text{O}$ data

Parameters	S-01	S-02	S-03	S-04	S-05	S-06
β (%) ^a	0	0	0	0	0	0
δ_{β} (‰) ^b	0	0	0	0	0	0
η (-) ^c	1,02	1,02	1,00	1,01	1,02	1,02
τ (yr)	2,25	1,42	2,25	2,33	2,88	2,58
RMSE (%)	0,03	0,04	0,03	0,03	0,02	0,03

(a) A constant discharge component as a fraction (usually older) of the total spring volumetric discharge flow rate. (b) Constant isotopic content of β . (c) η is the ratio of the total volume to the volume with exponential distribution transit time (TTD). $\eta = 1$ means the Exponential model (EM) and $\eta > 1$ for Exponential-piston flow model (EPM)

1502

1503

1504 Table D2. Fitted parameters of the exponential-piston flow model (EPM) for the estimated
 1505 mean transit times (τ) with FlowPC model and $\delta^2\text{H}$ data

Parameters	S-01	S-02	S-03	S-04	S-05	S-06
β (%) ^a	0	0	0	0	0	0
δ_{β} (‰) ^b	0	0	0	0	0	0
η (-) ^c	1,01	1,00	1,01	1,00	1,01	1,02
τ (yr)	3,00	1,92	2,33	2,67	2,83	2,75
RMSE (%)	0,19	0,21	0,17	0,22	0,18	0,20

(a) A constant discharge component as a fraction (usually older) of the total spring volumetric discharge flow rate. (b) Constant isotopic content of β . (c) η is the ratio of the total volume to the volume with exponential distribution transit time (TTD). $\eta = 1$ means the Exponential model (EM) and $\eta > 1$ for Exponential-piston flow model (EPM)

1506

Supplementary material for on-line publication only

[Click here to download Supplementary material for on-line publication only: Supplementary materials.pdf](#)